Regional and Cellular Localization of TASK-3 Potassium Channel RNA and Protein in the Rat Brain

Inaugural-Dissertation
to obtain the academic degree
Doctor rerum naturalium (Dr. rer. nat.)

submitted to the Department of Biology, Chemistry and Pharmacy
of the Freie Universität Berlin

by

CHRISTIANE MARINC

from Biedenkopf

2011

The present work was carried out under the supervision of Prof. Dr. Rüdiger W. Veh in the period of November 2007 to March 2011 at the Institute of Integrative Neuroanatomy, Charité - University Medicine, Berlin.

Gutachter:

1. 1^{st} reviewer: Prof. Dr. Rüdiger W. Veh
   Charité - Universitätsmedizin, Berlin

2. 2^{nd} reviewer: Prof. Dr. Hans-Joachim Pflüger
   Freie Universität, Berlin

Date of defence: 31.05.2011

Dedicated to my parents and my grandparents

Abbreviations

3	oculomotor nucleus
3V	third ventricle
4	trochlear nucleus
4V	fourth ventricle
6	abducens nucleus
5-HT	5-hydroxy tryptamine
6HisTR	N-terminal six histidine tail, C-terminal thioredoxin
7	facial nucleus
7n	facial nerve
10	dorsal nucleus of the vagus nerve
12	hypoglossal nucleus
aca	anterior commissure, anterior
AChE	acetylcholine esterase
Acs7	accessory facial nucleus
Amb	ambiguus nucleus
AT1a	angiotensine receptor 1a
Aq	cerebral aqueduct
BCA	bicinchoninic acid
BCIP	5-bromo-4-chloro-3-indolyl-phosphat
BSA	bovine serum albumin
BST	bed nucleus of the stria terminalis
CA	catecholamines
cDNA	complementary DNA
CG	central gray
CGNs	cerebellar granule cells
ChAT	choline acetyl tranferase
CNS	central nervous system
cp	cerebral peduncle
CPu	caudate putamen
Cy2	cyanine dye, max. adsorption/excitation 492 nm
Cy3	cyanine dye, max. adsorption/excitation 550 nm
DAB	3,3-diaminobenzidine tetrahydrochloride
DBH	dopamine-β-hydroxylase
Dk	nucleus of Darkschewitsch
dNTP	desoxynucleotide triphosphate
DOPA	di-ortho-hydroxy-phenylalanine
DR	dorsal raphe
DTT	dithiothreitol
ec	external capsule

EDTA	ethylene diamine tetraacetic acid
ELISA	ezyme-linked immunosorbent assay
EtOH	ethanol
EW	Edinger-Westphal nucleus
EWB	ELISA wash buffer
Fl	forelimb area of the cortex
fr	fornix
GABA	gamma aminobutyric acid
GPCR	G protein-coupled receptors
GP	globus pallidus
GST	gluthatione-S-transferase
Hb	hemoglobine
HDC	histidine decarboxylase
ic	internal capsule
ICC	immunocytochemistry
ICj	islands of Calleja
IgG	immunglobuline G
IgM	immunglobuline M
IMLF	interstitial nucleus medial longitudinal fasciculus
IPTG	isopropyl-D-thiogalactosid
ISH	*in situ* hybridization
K_{2P}	tandem pore-domain potassium channels
kDa	kilo Dalton
K_{ir}	inward rectifier potassium channels
K_v	voltage-sensitive potassium channels
LB medium	Lauria Bertani medium
LB-A medium	Lauria Bertani medium containing ampicilline
LC	locus coeruleus
LHb	lateral habenula
lo	lateral olfactory tract
M1-M4	transmembrane segments 1 to 4
Me	medial amygdaloid nucleus
Me5	mesencephalic trigeminal nucleus
MG	medial geniculate nucleus
MHb	medial habenula
ml	medial lemniscus
mlf	medial longitudinal fasciculus
MnR	median raphe
Mo5	motor trigeminal nucleus
mp	mammillary peduncle
NBM	basal nucleus of Meynert
NBT	*p*-nitro blue tetrazolium chloride
NGS	normal goat serum
NHS	normal horse serum
Ni-NTA	nickel-nitrilotriacetic acid
opt	optic tract
Par	parietal cortex

P1-P2	pore-forming region 1 and 2
PBS	phosphate buffered saline
PBS-A	PBS containing bovine serum albumin
PCR	polymerase chain reaction
PDTg	posterodorsal tegmental nucleus
PIP_2	phosphatidylinositol 4,5-bisphosphate
PKC	proteine kinase C
PMSF	phenyl methane sulfonyl fluoride
PMV	premammillary ventral nucleus
PP	phosphate buffer
py	pyramidal tract
pyx	pyramidal decussation
rAmb	retroambiguus nucleus
RPC	red nucleus parvocellular
RN	red nucleus
SA	sodium azide
scp	superior cerebellar peduncle
SDS-PAGE	sodium dodecyl sulfate polyacrylamide gel electrophoresis
SNc	substantia nigra pars compacta
SNR	substantia nigra pars reticulata
sol	solitary tract
sp5	spinal trigeminal tract
Sp5C	spinal trigeminal nucleus
SSRI	selctive serotonin reuptake inhibitor
STh	subthalamic nucleus
str	superior thalamic radiation
TASK	TWIK-related acid-sensitive K^+ channel
TBS	tris buffered saline
TH	tyrosine hydroxylase
THIK	tandem pore-domain halothane-inhibited K^+ channel
TM	tuberomammillary nucleus
TMD	dorsal tuberomammillary nucleus
TMV	ventral tuberomammillary nucleus
TREK	TWIK-related K^+ channel
TRESK	TWIK-related spinal cord K^+ channel
TWIK	weakly inward rectifying K^+ channel
tz	trapezoide body
VAChT	vesicular acetylcholine transporter
VDB	nucleus vertical limb diagonal band
VP	ventral pallidum
VTA	ventral tegmental area
VTg	ventral tegmental nucleus

Abstract

Members of the K_2P channel family (two pore-domain K^+ channels) have gained particular attention, because as background channels they can control the membrane potential of excitable cells. Considering their manifold modulation by physicochemical and pharmacological stimuli, they provide a potential target to influence cellular activity.

TASK-3 is the K_2P channel that shows the widest distribution throughout the brain. One of the most striking properties of TASK channels is their sensitivity to variations in extracellular pH. Special interest in TASK-3 channels arises from their responsiveness to a range of pharmacological agents. An interesting characteristic is their activation by volatile anesthetics and inhibition by local anesthetics. Furthermore, TASK-3 channels are inhibited by several neurotransmitters such as serotonin and noradrenaline. Inasmuch, TASK-3 might be a promising target for pharmacological intervention. A detailed analysis of the distribution of the channel can help to gain insight into its biological function, which is the requirement for any therapeutic use.

Therefore, a monospecific anti-TASK-3 antibody was prepared and used to study the distribution of the TASK-3 protein in the rat brain. Polyclonal anti-TASK-3 antibodies were raised in rabbits, freed from cross reactivities and affinity purified to gain a monospecific antibody. Detailed characterization of the antibody by ELISA and western blot analyses showed that the antibody specifically recognized the recombinant as well as the native TASK-3 protein.

TASK-3 demonstrated a widespread but not ubiquitous distribution throughout the rat brain. Immunoreactive neurons were found in all areas examined, from the forebrain to the spinal cord. Very strong TASK-3 expression was detected in serotoninergic dorsal raphe neurons, noradrenergic locus coeruleus neurons, cholinergic neurons in the basal nucleus of Meynert and the striatum and all motoneurons. Considerable expression was also found in histaminergic tuberomammillary neurons. In the dopaminergic system strong TASK-3 expression was found in some neurons of the VTA, whereas neurons of the substantia nigra compacta were only weakly labeled. Results were confirmed by *in situ* hybridization with TASK-3 specific riboprobes and immunofluorescence double-labeling experiments with appropriate marker enzymes.

Monoaminergic and cholinergic neurons are supposed to be affected in many neuropsychiatric disorders. Strong and differential expression of TASK-3 in these neurons suggests that channel expression may be affected under several pathological conditions. Furthermore, pharmacological modulation of TASK-3 channels may help to restore cellular excitability of lesioned cells or compensate for dysregulations of monoaminergic and cholinergic systems.

Zusammenfassung

Die Kanäle der K_{2P}-Familie (Zwei-Porendomänen Kaliumkanäle) haben in den letzten Jahren besondere Aufmerksamkeit erhalten, da sie als Hintergrundkanäle das Membranpotential erregbarer Zellen kontrollieren können. Aufgrund ihrer vielfältigen Modulation durch physikalische, chemische und pharmakologische Reize bieten sie ein mögliches Ziel um die Erregbarkeit von Zellen zu beeinflussen.
TASK-3 zeigt unter allen K_{2P}-Kanälen die weiteste Verbreitung im Gehirn. Eine der auffälligsten Eigenschaften der TASK-Kanäle ist ihre Sensitivität gegenüber Veränderungen des extrazelluären pH-Wertes. Das besondere Interesse an TASK-3-Kanälen beruht auch auf ihrer Empfindlichkeit gegenüber einer Reihe an pharmakologischen Wirkstoffen. Eine interessante Eigenschaft ist die Hemmung des Kanals durch Lokalanästhetika sowie ihre Aktivierung durch Inhalationsanästhetika. Des weiteren werden TASK-3 Kanäle durch eine Reihe an Neurotransmittern gehemmt, darunter Serotonin und Noradrenalin. Aufgrund dieser Charakteristika bieten TASK-3-Kanäle ein vielversprechendes Ziel für eine mögliche pharmakologische Intervention. Eine detaillierte Untersuchung der Verteilung des Kanals im Gehirn könnte dabei helfen, seine spezifischen Funktionen besser zu verstehen und damit die Voraussetzungen für eine therapeutische Nutzung der Kanalmodulation zu schaffen.
Aus diesem Grund wurde ein monospezifischer anti-TASK-3 Antikörper hergestellt und dazu genutzt die Verteilung des TASK-3 Proteins im Gehirn der Ratte zu untersuchen. Polyklonale anti-TASK-3 Antikörper wurden durch die Immunisierung von Kaninchen gewonnen, von Kreuzreaktivitäten befreit und Affinitätsaufgereinigt um einen monospezifischen Antikörper zu erhalten. Eine detaillierte Charakterisierung des Antikörpers in Western Blot und ELISA Analysen zeigte, dass der Antikörper nur das rekombinante sowie das native TASK-3 Protein erkennt.
Immunzytochemische Experimente zeigten eine weite, aber nicht ubiquitäre, Verbreitung des Kanalproteins im Gehirn. Immunreaktive Neurone wurden in allen untersuchten Arealen, vom Vorderhirn bis in das Rückenmark, beobachtet. Eine besonders starke Expression wurde in serotonergen Neuronen der Dorsalen Raphe, noradrenergen Neuronen des Locus coeruleus sowie cholinergen Neuronen im Nucleus Basalis Meynert und Striatum sowie in allen Motoneuronen beobachtet. Außerdem zeigten histaminerge Neurone des Nucleus tuberomammillaris eine deutliche Immunreaktivität. Neuronen des dopaminergen System wiesen Intensitätsunterschiede in der Immunreaktivität auf. Eine starke TASK-3 Expression wurde in einzelnen Neuronen der VTA beobachtet, wohingegen Neurone der Substantia nigra compacta nur sehr schwach positiv waren. Alle Ergebnisse wurden durch den Nachweis von TASK-3 mRNA mit Hilfe TASK-3-spezifischer Ribosonden und über eine Immunfluoreszenz-Doppelmarkierung mit Antikörpern gegen entsprechende Markerenzyme bestätigt.
Vielen neuropsychatrischen Erkrankungen liegen Störungen oder Dysregulationen monoaminerger oder cholinerger Systeme zugrunde. Die starke und differenzierte Expression von TASK-3 in Neuronen dieser Systeme könnte darauf hindeuten, dass eine veränderte Kanalexpression oder Funktion eine Rolle bei der Entstehung verschiedener pathologischer Zustände spielt. Außerdem könnte möglicherweise über eine pharmakologische Modulation von TASK-3 Kanälen die Erregbarkeit geschädigter Zellen wieder hergestellt oder eine Dysregulationen monoaminerger und cholinerger Systeme kompensiert werden.

Table of Contents

1 Introduction

1.1 Ion channels

Ion channels are formed by a large family of proteins, which span the membrane of a cell and allow efflux and influx of ions into cells or cell organelles. Although the passage of ions through these channels is a passive transport along an existing electrochemical gradient, they are much more than only holes; they are ion specific pores that enable the selective passage of ions through a membrane. Most channels are named by their specificity, differentiating for example sodium-, calcium-, chloride-, or potassium channels. Other channels show minor selectivity such as the transient receptor potential (TRP) channels that allow the passage of many small cations including Na^+, K^+, Mg^{2+}, and Ca^{2+}. Another example are the ligand-gated cationic (e.g. nicotinic acetylcholine receptor) and anionic (e.g. glutamate receptor) channels.
Ion channels gain their selectivity by a specific selectivity filter motif assembling a defined pore structure. Furthermore, many chemical and physical aspects regulate their conductivity and open probability. Another ion channel classification is based on their gating mechanisms. The opening of voltage-gated channels depends on the membrane potential. Another class of ion channels only opens by binding certain molecules; they are called ligand-gated ion channels. In addition, there are several other physical and chemical stimuli that promote opening and closing of ion channels. Channels can be activated or inactivated by cyclic nucleotides or various other second messengers or they can be sensitive to stretches of the membrane (mechanosensitive), to light or to changes in temperature, pH and oxygen tension.

1.1.1 Potassium channels

As designated by their name, potassium channels allow the specific passage of potassium ions through membranes. The first potassium channel gene was isolated from *Drosophila* in 1987 and was named Shaker after a motion disorder in fruit flies [Papazian et al., 1987]. Affected flies show an atypical behavior and shake their legs under ether anesthesia. These effects are caused by a mutation in a gene encoding for a presynaptic potassium channel. A lack of the underlying potassium currents leads to a delayed repolarization and increased transmitter release. Since then, more than 80 K^+ channel genes have been cloned based on their homology to Shaker [Chandy and Gutman, 1993]. They comprise the biggest family of ion channels and are expressed in nearly all excitable and non-excitable cells. The sheer number of potassium channels indicates their wide distribution and diversity as well as their importance for cellular integrity and function.
All K^+ channels share some common structural features. A functional channel is formed by pore-forming subunits, called α-subunits. Some channels associate with additional auxiliary subunits called

β-subunits that can change inactivation kinetics or regulation and pharmacology. Furthermore, K^+ channels can associate with scaffold or adapter proteins. These are proteins that lack intrinsic enzymatic properties but can facilitate protein-protein interaction and localization of proteins or protein complexes to specific compartments of the cell. One example is the adaptor protein 14-3-3 that promotes the trafficking of TASK-1 and TASK-3 channels to the membrane [Rajan et al., 2002]. Two or four α-subunits have to assemble to form a functional pore region (selectivity filter) consisting of four pore-lining P-loops and at least two transmembrane segments flanking those loops. The selectivity filter is formed by a conserved motif of five residues, TXG[YF]E, in the P-loop of each subunit. Point mutations in the K^+ signature sequence abolish K^+ selectivity [Henginbotham et al. 1994].
The general role of K^+ channels is to bring the membrane potential closer to the potassium equilibrium potential and away from the firing threshold. In this regard, they help to set, stabilize and regain the resting membrane potential and terminate periods of action. The opening mechanism of a K^+ channel determines its function in the regulation of cell excitability. In addition, K^+ channels serve various roles in non-excitable cells. In epithelial cells, K^+ channels enable the excretion of K^+ ions into secreted fluids and therefore are important in K^+ homeostasis. Furthermore, by stabilizing the membrane potential they help to maintain the driving force for the electrogenic transport of Na^+ and Cl^- [Heitzmann and Warth, 2008]. In the CNS, glial K^+ channels help to maintain normal function by transporting excessively released K^+ ions away from active neurons. Based on their function and structure, all potassium channels are grouped into three protein families.
Voltage-sensitive potassium (K_v) channels open as a result of a decrease of the membrane potential (depolarization). Hence, they help to terminate an action potential, repolarize the cell, and restore the resting membrane potential. They are composed of four α-subunits, each consisting of one pore-forming domain and six transmembrane segments (1P/6TM). The α-subunits are often associated with various β-subunits that can modulate the physiological function of the channel. This class of potassium channels also comprises the Ca^{2+}-dependent K^+ channels that have an additional transmembrane helix [Yellen, 2002].
The second family comprises the inward rectifier channels, called K_{ir} channels. The term inward rectifier describes their tendency to allow the entry of K^+ ions under hyperpolarization, while K^+ efflux is blocked at depolarization. Depolarization causes K_{ir} channel closure, because of a voltage-dependent block by Mg^{2+} ions or polyamines from the intracellular side. These channels help to stabilize the membrane potential. If other influences cause the cell to depolarize they close and do not further counteract a change of the membrane potential. K_{ir} channels are regulated by a number of intracellular factors. They share the tetrameric arrangement with the K_v channels, but their subunit composition is much more simple with only two transmembrane segments and one pore-domain. Sometimes they are associated with auxiliary subunits. The K_{ATP} channel is made up of four Kir6 subunits and four sulfonylurea receptor subunits, forming a special ATP-sensitive channel [Hibino et al., 2010].
The third class of potassium channels is named after their special structural composition. These so-called K_{2P} channels, or tandem-pore-domain channels, have subunits composed of four transmembrane segments and two pore-domains (4TM/2P, see Fig. 1.1). Therefore, only two subunits need to associate to form the K^+ selectivity filter consisting of four pore-lining P-loops. These channels are background channels and contribute to the resting membrane potential of many neurons and regulate

their excitability. They show a high degree of regulation by variable factors.

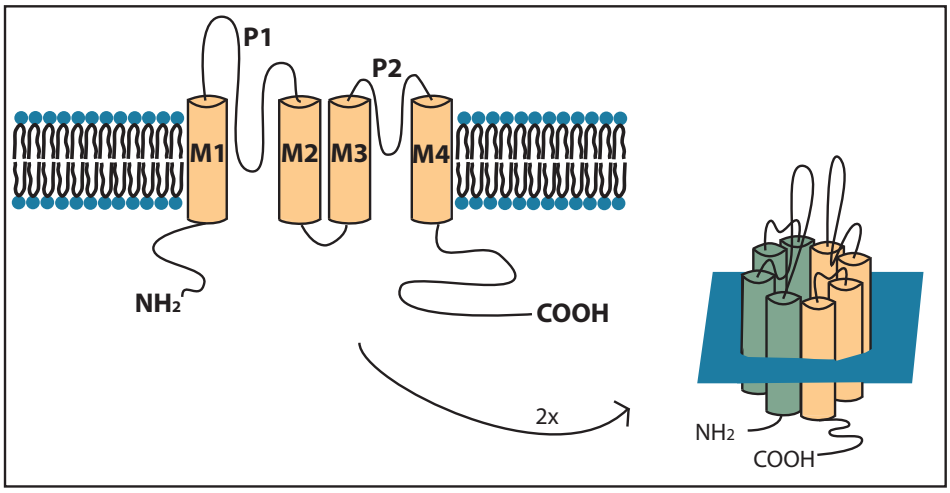

Figure 1.1 – Structure of K_{2P} channels. The subunits of K_{2P} channels are composed of four transmembrane segments (M1-M4) and two pore-domains (P1 and P2). Furthermore, all K_{2P} channels share an extended loop between M1 and P1, a short amino-terminal and a longer carboxy-terminal sequence both on the cytoplasmatic side. Two subunits need to associate to form a functional channel with the K^+ selectivity filter.

1.1.2 K_{2P} channels

The resting membrane potential is determined by the equilibrium potential of the permeant ions and their conductances. Long before the discovery of the K_{2P} channel family the importance of potassium currents for the negative resting membrane potential has been described. At rest the membrane is far more permeable to potassium ions than to Na^+ or Ca^{2+} ions. Potassium currents provide the dominant background conductance driving the membrane potential towards the K^+ equilibrium potential (-96 mV under physiological K^+ concentration and temperature). This is the well-accepted basic principle of the negative resting membrane potential of excitable and non-excitable cells. Nevertheless, the molecular basis underlying these resting or background currents was unclear until recently. It was discussed that leakage currents through voltage-gated K^+ channels that even flow following channel blockade might underlie the high resting K^+ conductance. In the late nineties tandem pore-domain K^+ channels were identified as the main carriers for these 'leak' or background conductances. Their discovery provided new insights into basic principles of cellular excitability and the modulation of membrane properties and membrane potential.

The first cloned channel with two pore-domains was TOK-1, which was isolated from *Saccharomyces cervisiae* in 1995 [Ketchum et al., 1995]. This channel differs from other K_{2P} channels in having eight transmembrane domains. The first channel with the 4TM/ 2P structure was TWIK-1 (tandem of pore in a weak inward rectifier), thus can be regarded as the founding-member of the K_{2P} family [Lesage et al., 1996]. Like TOK-1 it was discovered by computer searches for K^+ channel motifs in

global databases. Members of the K_{2P} channel family were described as background channels, because they share some important criteria; they show baseline activity at resting membrane potential and their gating is voltage- and time-independent [Lesage and Lazdunski, 2000]. Furthermore, background or 'leak' channels show Goldmann-Hodgkin-Katz or open rectification, meaning that ion currents flow more easily from the side of higher permeant ion concentration [Duprat et al., 1997]. Therefore, at physiological conditions of higher intracellular K^+ concentration they pass outward currents. These channels enable the transport of K^+ ions along a wide range of membrane potentials. Thus, they play a key role in setting the resting membrane potential and modulating cellular excitability, but also influencing action potential duration. Most of the K_{2P} channels differ from these criteria in that they are for example weakly voltage-dependent or show weak rectification or inactivation kinetics; but so far channels of this family fit the criteria for leak channels best.
Nevertheless, K_{2P} channels provide more than only unregulated leakage K^+ currents. They are subject to modulation by numerous factors, showing sensitivity to various physico-chemical factors including temperature, pH, oxygen tension or stretch. In addition, the channels are modulated by neurotransmitters, anesthetics or bioactive lipids [Lesage and Lazdunski, 2000, Goldstein et al., 2001, Patel and Honoré, 2001].
The 15 members of the K_{2P} channel family found in mammals and their relationship can be seen in the dendrogram of Fig. 1.2. Currently, there are three widely used nomenclatures for this family. One was given by the Human Genome Organization. The channel name comprises the suffix KCNK and an additional number for each gene. The problem is that the numbers were given in the order of discovery of the channels. Hence, they do not provide any classification by structure or sequence. Another classification implicates similarities in sequences and functional resemblance. This nomenclature utilizes acronyms that are based on the channels main physical and chemical characteristics. For example KCNK9, the channel examined in this work, is a member of the TASK family, which is an acronym for TWIK-related acid-sensitive K^+ channel. The third nomenclature was introduced by the International Union of Pharmacology in an attempt to formulate a more rational classification [Gutman et al., 2003]. This nomenclature uses the numbers from the 'KCNK' numbering but with the prefix K_{2P} (e.g K_{2P}9.1 for TASK-3).

1.1.3 The TASK family

The TASK family of K_{2P} channels received their name from their strong sensitivity to variations in extracellular pH (TWIK-related acid-sensitive K^+ -channel). The first member that was later called TASK-1, was isolated from human kidney in 1997 [Duprat et al., 1997]. This channel fitted the criteria of a leak channel better than any other channel discovered so far. At asymetric K^+ concentrations TASK-1 channels show a weakly rectifying current-voltage relationship as predicted by the constant field equation (Goldmann-Hodgkin-Katz [GHK] rectification). Furthermore, they open instantaneously without inactivation (time-independent) and are voltage-independent. Surprisingly, this channel was activated by elevation in extracellular K^+ [Duprat et al., 1997]. It was suggested that this dependence on K^+ is based on the stabilizing effect of K^+ ions on the open pore conformation [Niemeyer et al., 2006]. The main feature of TASK-1 is its inhibition by extracellular acidification; it has a pK of 7.3 and a Hill coefficient of 1.6 [Duprat et al., 1997]. Protonation of a histidine residue

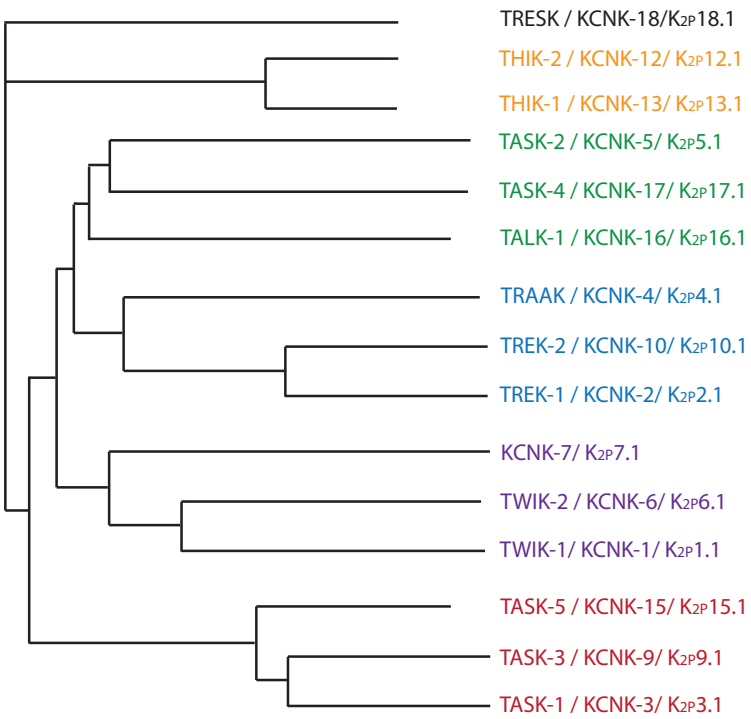

Figure 1.2 – Dendrogram of the subfamily of K_{2P} channels. In humans 14 members of the K_{2P} channel family have been identified. They are grouped into five subfamilies based on sequence homologies (THIK, TWIK, TREK, TASK, TALK). For each channel all three commonly used names are indicated. The first one is an acronyme based on salient physiological and pharmacological properties. The second was given by the Human Genome Organization and comprises the suffix KCNK and a number that reflects the order of discovery. The third names are derived from the KCNK numbering and were given by the International Union of Pharmacology.

(H98) near the selectivity filter confers this pH-sensitivity [Morton et al., 2003].
TASK-3 was first described in a study using a DNA-fragment of the pore and C-terminal region of TASK-1 to screen rat cardiac and cerebellum cDNA libraries [Kim et al., 2000]. Screening of the cerebellum library revealed a positive clone that contained a partial sequence of a new K_{2P} channel with a high sequence similarity to TASK-1. The full sequence was obtained by a rescreen of the cerebellum library with a specific fragment. The new channel shared 54% amino acid identity with TASK-1. Furthermore, it shared strong sensitivity to changes in extracellular pH with the formerly described members of the TASK family, TASK-1 and TASK-2. Thus, Kim and his colleagues called the new channel TASK-3. Shortly later, Rajan and colleagues reported from the cloning and expression of a novel human K_{2P} channel, TASK-3 [Rajan et al., 2000].
TASK-3 and TASK-1 are the only members along the K_{2P} channels that were found to form heterodimers [Czirják and Enyedi, 2002b]. This heterodimers show characteristics of both channels, for example intermediate pH-sensitivity and insensitivity to ruthenium red, a typical feature of TASK-1. Heteromers are functionally expressed in motoneurons (hypoglossal motoneurons [Berg et al., 2004] and facial motoneurons [Larkman and Perkins, 2005]), in cerebellar granule cells [Kang et al., 2004], in dorsal lateral geniculate thalamocortical relay neurons [Meuth et al., 2006] and in hippocampal CA1 neurons [Torborg et al., 2006].
The third member of the TASK family is TASK-5. It was grouped into this subfamily because of sequence and functional similarities with TASK-1 and TASK-3 [Vega-Saenz de Miera et al., 2001]. TASK-5 shares 51% sequence homology with TASK-3 [Kim and Gnatenco, 2001]. Although there is no prove for a functional expression, TASK-5 mRNA is abundantly expressed in many tissues. In the brain it shows an especially strong expression in areas associated with the auditory system [Karschin et al., 2001].
Despite their names, TASK-2 [Reyes et al., 1998] and TASK-4 [Decher et al., 2001] have only little homology with the other TASK members, hence they do not belong to this subfamily. Now they are grouped into the TALK family with which they share their sensitivity to pH-changes in the alkaline range.

A closer look at TASK-3 In *Rattus norvegicus* the TASK-3 gene comprises 1191 bp located at chromosome 7 (7q34), encoding a channel protein of 396 amino acids. In the nomenclature of the Human Genome Organization TASK-3 was given the name KCNK9 (K_{2P}9.1). The channel shares all typical features of the K_{2P} family. All subunits consist of four transmembrane segments (M1-M4), two pore-forming regions (P1 and P_2) containing the conserved TXG(YIF)G consensus motif for potassium channels, a large extracellular loop between M1 and P1 and an extended C-terminal sequence (see Fig. 1.1). The C-terminus includes two protein kinase C phosphorylation sites, two casein kinase phosphorylation sites and a cAMP-dependent protein kinase phosphorylation site [Rajan et al., 2000]. At symmetrical 140 mM K^+ concentrations, the channel exposes a weak inward-rectification that is more pronounced when extracellular divalent cations are omitted [Rajan et al., 2000]. The single channel conductance is 27 pS at -60 mV and 17 pS at +60mV [Kim et al., 2000]. According to its name, TASK-3 is very sensitive to changes in extracellular pH; changing the pH from 7.2 to 6.4 and 6.0 resulted in a decrease of TASK-3 currents of 74% and 96%, respectively. The histidine residue at

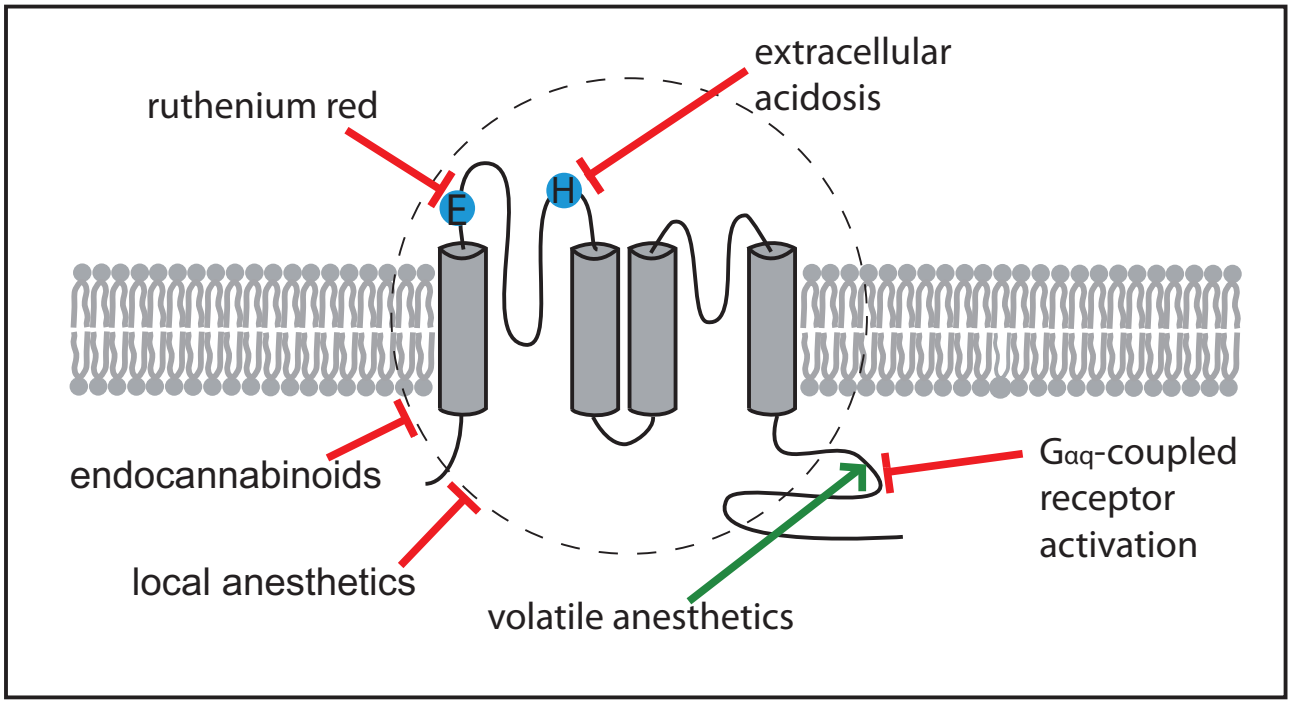

Figure 1.3 – Regulation of TASK-3 channels. TASK-3 channel activity can be influenced by several physical and chemical stimuli. TASK-3 is inhibited by external acidification, the effect is mediated by protonation of a histidine residue at position 98 of the first extracellular loop. A glutamate at position 70 is important for sensitivity to ruthenium red. Furthermore, TASK-3 is inhibited by endocannabinoids (anandamide, methanandamide), local anesthetics (lidocaine, bupivacaine) and as a result of Gαq-coupled receptor activation. In contrast, channels are activated by volatile anesthetics (halothane, isoflurane). Figure modified from [Enyedi and Czirják, 2010]

position 98 is part of the pH-sensor [Kim et al., 2000, Rajan et al., 2000]. With a pK value of 6.7 and a Hill coefficient of 1.82 to 2, TASK-3 is slightly less sensitive to acidification than TASK-1 [Kim et al., 2000]. Furthermore, TASK-1 and TASK-3 can be distinguished by their sensitivity to ruthenium red, zinc and anandamide. Ruthenium red blocks TASK-3 at concentrations not affecting TASK-1 [Czirják and Enyedi, 2003]. In contrast, zinc [Kim et al., 2000] and anandamide [Maingret et al., 2001] are more effective in blocking TASK-1 channels. Although inconsistent results may suggest species-dependent differences in the pharmacological sensitivity of both channels [Bayliss et al., 2003].
Due to its phosphorylation domains, TASK-3 is subject to a wide range of modulatory influences. In addition to a current decrease by external acidification and ruthenium red, anandamide and zinc, TASK-3 is blocked by barium and quinidine [Kim et al., 2000]. Furthermore, the channel is inhibited by local anesthetics such as lidocaine and bupivacaine. In contrast, TASK-3 is activated by volatile anesthetics, for example halothane and isoflurane [Patel et al., 1999, Patel and Honoré, 2001, Meadows and Randall, 2001, Talley and Bayliss, 2002]. Another important feature of TASK-3 and also TASK-1 channels is their inhibition following activation of G protein-coupled receptors (see below). Fig. Fig. 1.3 provides an overview of the multifaceted regulation of TASK-3 channels.

Distribution of TASK-3 Rajan et al. [2000] detected strong TASK-3 mRNA levels only in the brain. In contrast, Kim et al. [2000] also found minor levels in several other tissues, including lung, stomach, kidney, liver, colon, spleen, testis and skeletal muscle by using RT-PCR analyses. The localization of TASK-3 mRNA was analyzed in detail in two *in situ* hybridization studies (see table 3.1), in-

dicating a widespread distribution of the channel throughout the rat brain [Karschin et al., 2001, Talley et al., 2001]. Less comprehensive data are available on the localization of the channel protein. Using an antibody purified in their laboratory, Berg and colleagues found strong TASK-3 expression in cholinergic striatal interneurons [Berg et al., 2004, Berg and Bayliss, 2007]. Furthermore, they mentioned strong immunoreactivity of neurons of the locus coeruleus, the anterodorsal thalamic nucleus and the dorsal raphe [Berg et al., 2004]. TASK-3 immunoreactivity was also found in a subset of cortical neurons and in neurons of the dentate gyrus and the CA1 region of the hippocampus [Callahan et al., 2004, Torborg et al., 2006]. Finally, TASK-3 channel expression has been found in the molecular layer, the granule cell layer and in Purkinje cells of the cerebellum [Rusznak et al., 2004]. Furthermore, TASK-3 is also expressed in several other cell types including adrenal glomerulosa cells [Czirják and Enyedi, 2002b, Lotshaw, 2006, Brenner and O'Shaughnessy, 2008], carotid body glomus cells [Yamamoto et al., 2002, Tan et al., 2007] and T-lymphocytes.

Biological functions of TASK-3 According to their widespread distribution, TASK-3 channels have been implicated in several processes including a role in the pathomechanisms of cancer, Parkinson's disease, and epilepsy. TASK channels are involved in the control of breathing and under hypoxic conditions. TASK-1 as well as TASK-3 mRNA are strongly expressed in carotid body glomus cells [Yamamoto et al., 2002]. These cells depolarize in response to hypoxia, metabolic acidosis and elevation of external K^+ concentrations, leading to a stimulation of respiration. The depolarization is at least partially mediated by the inhibition of a K^+ background channel whose pharmacological profile resembles that of TASK channels [Buckler et al., 2000]. Recently, pharmacological and single-cells analyses revealed that the major part of the oxygen-sensitive background K^+ current is carried by TASK-1/TASK-3 heterodimeric channels [Kim et al., 2009]. The exact mechanism of the hypoxia-induced TASK channel inhibition is still elusive, but it is likely that effects are mediated by the inhibition of oxidative phosphorylation and ATP-production [Buckler, 2007]. However, a potential role of TASK channels in the control of central respiratory chemosensitivity is still a matter of debate. In TASK-1 and TASK-3 single knockout mice as well as in double-knockout mice the pH-sensitivity of chemoreceptive raphe neurons is lost, but central respiratory chemosensitivity is maintained [Mulkey et al., 2007].
Cohesive to their inhibition by pH-reduction and O_2-deprivation, TASK-1 and TASK-3 may play a neuroprotective role during stroke development by limiting tissue damage during cerebral ischemia [Meuth et al., 2009].

According to its strong expression in rat adrenal glomerulosa cells [Czirják and Enyedi, 2002b], TASK-3 is assigned a role in the regulation of aldosterone secretion. A high plasma K^+ concentration stimulates aldosterone secretion and this mechanism depends on a high background potassium conductance of adrenal glomerulosa cells. In rat glomerulosa cells, TASK-3 is probably the most important background channel [Czirják and Enyedi, 2002b]. In addition, deletion of TASK-1 and TASK-3 (TASK-1/TASK-3 double-knock-out) in mice causes primary hyperaldosteronism, suggesting TASK channels as a potential target in the future therapy of this disease [Davies et al., 2008].

Furthermore, TASK-3 is involved in mechanisms related to cell death and apoptosis. This is not surprising, as cell excitability is a critical determinant of neuronal survival [Pettmann and Henderson, 1998] and background channels like TASK-3 are important in setting the resting membrane potential. Meuth et al. [2008b] suggested that the switch between cell death and cell survival in autoimmune CNS inflammation is at least partly mediated by the regulated expression of TASK-1 and TASK-3 proteins. The authors further predicted a (therapeutically relevant) role in T-cell-mediated autoimmune disorders, as application of TASK channel blockers led to a reduction in cytokine production and proliferation of T-cells [Meuth et al., 2008a]. TASK-3 may also have protective effects during cellular stress by inhibiting the activation of intracellular apoptosis pathways [Liu et al., 2005]. In contrast, TASK-3 as well as TASK-1 and TASK-1/TASK-3 heterodimers may be involved in the K^+-dependent programmed cell death of cerebellar granule cells during development of the cerebellum [Lauritzen et al., 2003].

Moreover, TASK-3 has a role in cell proliferation and a dysregulation of its expression may be implicated in tumorigenesis. Strong TASK-3 expression has been found in melanoma cells [Pocsai et al., 2006]. Additionally, the TASK-3 gene is amplified in 10% of breast cancers and overexpressed in breast, lung, colon and metastatic prostate cancer [Mu et al., 2003]. Overexpression of TASK-3 in special C8 cells transformed with oncogenes enhanced tumorogenesis and confered hypoxia-resistance [Mu et al., 2003]. A following study showed that TASK-3 overexpression confers a growth advantage and partial resistance to apoptosis to mouse embryonic fibroblast cells [Pei et al., 2003]. Supposedly, TASK-3 overexpression provides an advantage in the poorly oxygenated areas of solid tumors [Mu et al., 2003]. This is supported by the fact that TASK-3 is responsible for oxygen-sensing in a human lung cancer cell line and mediates the physiological effects of hypoxia [Hartness et al., 2001].

Regulation of TASK channels by G protein-coupled receptors Many K_{2P} channels are regulated by different G protein-coupled receptor (GPCR) pathways. This has been shown for the TREK, TRESK and TASK subfamilies. The effects following activation of Gαq proteins are the best-studied pathways so far. TASK-3 as well as TASK-1 is strongly inhibited following activation of Gαq-coupled receptors. TASK-1 in cerebellar granule neurons and TASK-1 and TASK-3 in thalamocortical relay neurons are inhibited following activation of muscarinic M3 receptors by the application of muscarine or acetylcholine [Millar et al., 2000, Meuth et al., 2003]. In cerebellar granule cells TASK channels are also inhibited by the action of glutamate on group I Gαq-coupled metabotropic glutamate receptors [Chemin et al., 2003]. Moreover, TASK-3 channels in motoneurons are regulated by the action of several neurotransmitters. TASK-1 is inhibited by a number of neurotransmitters such as serotonin, glutamate, thyrotropine-releasing hormone, and noradrenaline in respiratory neurons [Bayliss et al., 2001] and also in hypoglossal motoneurons [Talley et al., 2000]. In dorsal vagal neurons excitatory effects of 5-HT are mediated by the inhibition of TASK-1/TASK-3 heterodimers [Hopwood and Trapp, 2005]. GPCR-mediated inhibition has also been identified in other tissues. In adrenal glomerulosa cells, TASK-1 and TASK-3 are inhibited by the stimulation of angiotensin II type I receptors (AT1a) [Czirják et al., 2000, Czirják and Enyedi, 2002b].
There are three competing hypotheses on how the inhibition of TASK channels is mediated by GPCR

activation. The first hypothesis suggests an involvement of the PKC pathway and is supported by the fact that TASK channels contain a consensus site for PKC phosphorylation [Kim et al., 2000, Rajan et al., 2000]. TASK-1 and TASK-3 are inhibited following activation of PKC [Lopes et al., 2000, Besana et al., 2004, Vega-Saenz de Miera et al., 2001, Veale et al., 2007]. However, activators of PKC (e.g. phorbol 12-myristate 13-acetate [PMA]) failed to inhibit TASK-1 [Duprat et al., 1997, Czirják et al., 2001] or TASK-3 [Kim et al., 2000, Chemin et al., 2003].
Another hypothesis is that depletion of PIP_2 (Phosphatidylinositol 4,5-bisphosphate) from the membranes following PLC activation leads to TASK inhibition. Other K_{2P} channels are activated by PIP_2 and data suggesting that PIP_2 may be essential for normal TASK channel function [Chemin et al., 2003, Lopes et al., 2005]. Furthermore, wortmannin, preventing the re-synthesis of PIP_2, slows the recovery of K_{2P} channels following GPCR mediated inhibition [Czirják and Enyedi, 2002b, Lopes et al., 2005]. Controversially, inhibition of TASK-1 and TASK-3 via activation of GPCRs also occurred in mutant cell lines with very low PIP_2 levels. Moreover, TASK-3 expressed in HEK-cells was also inhibited by a mutant form of a constitutively active Gαq protein that is deficient in PLC activation, arguing that TASK channel inhibition does not require PLC [Chen et al., 2006].
This leads to the third hypotheses that Gαq proteins directly regulate TASK channels. Gαq proteins associate with TASK channels and inhibit them directly in excised membrane patches [Chen et al., 2006]. Probably, these mechanisms act together to confer the effects. Furthermore, mechanisms of inhibition could depend on the cell type, the channels involved, and many other factors.
In any way, the inhibition of TASK-3 by activation of GPCRs provides a way for neurotransmitters to mediate their action on cellular excitability.

1.2 The monoaminergic and cholinergic system of the brain

Neurotransmitters are biochemical substances that serve to transport information from one neuron to the other. There are two main possibilities for the transport of neurotransmitters to their target cells, the synaptic transmission (wiring transmission) and the diffusion through the extracellular space or cerebrospinal fluid (volume transmission, [Agnati et al., 2010]). At synapses neurotransmitters are released from vesicles that fuse to the presynaptic membrane. Released transmitters act on the postsynaptic neuron by diffusing through the synaptic cleft and binding to receptors in the postsynaptic membrane. Extrasynaptic communication can be carried by neurotransmitters that are released at synapses, but reach extrasynaptic receptors via diffusion. Furthermore, neurotransmitters can be released asynaptically from soma, dendrites or axons and act as short- or long-distance signals by migrating in the extracellular space. Neurotransmitters can also be released from non-neuronal cells, in the first instance astrocytes, oligodendrocytes, microglia or ependymal cells. There are four groups of neurotransmitters, including neuropeptides (e.g. endorphines, substanz P, somatostatin), amino acids (like GABA, glycine, glutamate), the gaseous transmitters nitric oxide, hydrogen sulfate and carbon monoxide, and the widely distributed group of biogenic amines.

One of the most important aminergic neurotransmitters is acetylcholine (ACh). ACh transfers excitation from the nerve to the muscle at the neuromuscular junction, but it is also involved in cog-

nitive processes in the cerebral cortex. Another important group of monoaminergic neurotransmitters are the catecholamines (CA) including dopamine, adrenaline and noradrenaline, and the indolamines serotonin (5-HT) and melatonin. They are produced by their respective neurons via an enzymatic alteration of the aromatic amino acids tyrosine (CA) or tryptophan (5-HT and melatonin). Furthermore, the monoamine histamine has to be mentioned, which is a biogenic amine of histidine. In addition, several other biogenic amines can act as neurotransmitters, such as octopamine, agmatine, spermine and taurin.
Monoamines have been found in nearly all animal phyla [Parent, 1984], arguing for an important role in the control of basic physiological processes. In the central nervous system of vertebrates monoamines modulate many processes associated with the regulation of autonomic functions and motor activity [Haxhiu et al., 2001].

The cholinergic system of the brain was described in detail by Mesulam et al. [1983]. They investigated the organization of cholinergic pathways ascending from the basal forebrain and upper brainstem to the cerebral cortex, the amygdala, the hippocampus, the olfactory bulb, and the thalamus in detail with the help of an anti-choline acetyltransferase antibody. Based on connectivity patterns six cholinergic cell groups (Ch1-Ch6) can be differentiated. Cells of Ch1 and Ch2 are located in the medial septal nucleus and vertical limb nucleus of the diagonal band. They provide the major input to the hippocampus. The Ch3 group contains neurons in the lateral portion of the horizontal limb of the diagonal band that project to the olfactory bulb. Ch4 includes neurons of the basal nucleus and the diagonal band nuclei that provide the major input to the amygdala and the cerebral cortex. At least there are the Ch5 and Ch6 groups, comprising mostly neurons located in the pedunculopontine nucleus and the laterodorsal gray of the periventricular area; these neurons innervate the thalamus [Mesulam et al., 1983].
The other important neurotransmitter system was carefully studied by Dahlstroem and Fuxe, who described a system of neurons located mainly in the brain stem and containing either a catecholamine (noradrenaline or dopamine) or 5-HT [Dahlstroem and Fuxe, 1964, Fuxe, 1965]. Most monoaminergic neurons are located in the brainstem nuclei and the hypothalamus. Serotoninergic neurons are found nearly exclusively in the brainstem raphe nuclei. Noradrenaline is also produced by groups of neurons of the brainstem, mainly the locus coeruleus. Histaminergic neurons are restricted to the tuberomammillary nucleus in the hypothalamus. Most dopaminergic neurons are localized in the mesencephalic substantia nigra and the adjacent ventral tegmental area, but there are also groups of dopaminergic neurons scattered throughout the CNS. These comprise neurons in the periaqueductal grey (A11), hypothalamic cell groups (A12, A14, A15), neurons in the zona incerta of the ventral thalamus (A13) and dopaminergic neurons in the olfactory bulb (A16).
One way to identify monoaminergic neurons is the immunocytochemical detection of key enzymes of their synthesis. All catecholaminergic neurons can be stained with an anti-tyrosine hydroxylase antibody. This enzyme catalyzes the first step in the catecholamine synthesis, the conversion of tyrosine to di-ortho-hydroxy-phenylalanine (DOPA), the direct precursor of dopamine. A specific marker for noradrenergic neurons is dopamine-β-hydroxylase, the key enzyme catalyzing the hydroxylation of dopamine to noradrenaline. Histaminergic neurons can be visualized by immunocytochemical labeling

of histidine decarboxylase, the enzyme forming histamine from the amino acid histidine. Another possibility to identify monoaminergic neurons is the use of antibodies against specific transporters. One example is the serotonin transporter that provides the passage of serotonin from the synaptic space into the presynaptic neuron and can be detected immunocytochemically. Anti-5-HT antibodies are also a useful tool for the visualization of serotoninergic neurons. These antibodies do not recognize 5-HT directly, but recognize a β-carboline derivative of 5-HT formed by the formaldehyde fixation. For the detection of cholinergic neurons and fibers, an antibody directed against its vesicular transporter is available (anti-vAChT). This transporter facilitates the uptake of acetylcholine into synaptic vesicles. There are also commercial antibodies against choline acetyltransferase, the enzyme forming ACh by linking acetyl groups from acetyl-CoA to choline.

Dysregulations of monoaminergic and cholinergic systems underlie many clinically relevant conditions. Therefore, a modulation of these systems could be beneficial in the treatment of many diseases. Serotonin is implicated in the regulation of many brain functions. One of the best-known and clinically important roles is its influence on mood. Elevated serotonin levels can lead to euphoria and hallucinations, whereas depressive moods presumably are caused by its deprivation [Lucki, 1998]. Accordingly, selective serotonin re-uptake inhibitors (SSRIs) have become an important tool in the therapy of mood disorders.
Dopamine is associated with disorders such as Parkinson's disease and schizophrenia [Carlsson, 1988]. Dopamine receptor agonists help to ease the symptoms of Parkinson's disease [Gárdián and Vécsei, 2010], while receptor antagonists are used in the treatment of hallucinations occurring in schizophrenia [Creese et al., 1976]. A number of studies suggest an implication of noradrenaline in the mediation and modulation of stress responses and anxiety [Lader, 1974, Itoi and Sugimoto, 2010]. Consequently, the profit of noradrenaline receptor antagonists in the treatment of panic and post-traumatic-stress disorders is under investigation.
Histamine is best known for its role in allergic reactions. Nevertheless, it also participates in the regulation of many higher brain functions. Histaminergic neurons of the posterior hypothalamus play a critical role in cortical activation and arousal mechanisms [Schwartz et al., 1991] and in this context especially in the regulation of the sleep-wake-cycle. Damage of histaminergic neurons or pathways leads to sleep disorders like insomnia, whereas classical antihistamines (H1 histamine receptor antagonists) produce sleep.
Beside the monoamines, the cholinergic system is involved in many brain functions, and dysregulation of this system underlies several pathological conditions. Acetylcholine has been implicated in cognitive processing, arousal and attention [Karczmar, 1993]. In addition, it has been shown that ACh is important in memory formation and learning. Hence, reduced levels of ACh by a loss of cholinergic neurons are thought to be implicated in the memory loss associated with Alzheimer's disease [Martorana et al., 2010].

1.3 Intention of my work

Since their discovery about fifteen years ago a growing interest in the members of the family of K_{2P} channels has emerged. K_{2P} channels are expressed in the entire human body. As background channels they can control the membrane potential of excitable cells and their activity can be influenced by a wide range of pharmacological agents. This makes them a promising target for potential therapeutic intervention of disorders associated with the CNS. An interesting member of this family is TASK-3. In the brain, this channel shows the widest distribution of all K_{2P} channels.
Like the other K_{2P} channels, TASK-3 is regulated by several pharmacological mediators, including anesthetics, endocannabinoids and neurotransmitters. The pharmacological modulation of TASK-3 channels may provide a target to influence cellular excitability. Whereas the inhibition of TASK channels could depolarizes the cell, their activation could lead to hyperpolarization and decreased cellular activity and responsiveness. Any potential therapeutic use of TASK-3 channel modulation requires the knowledge of the specific cellular function of the channel. An investigation of the channel's function also could help to elucidate its contribution to the action of pharmacological agents such as anesthetics. This could help to understand the mechanisms of their effects. The specific distribution of a channel can give hints to its function.
Antibodies provide a useful tool to study the distribution of a protein and today, thousands of antibodies are commercially available. Unfortunately, many of these antibodies are insufficiently characterized and the data provided to proof their specificity are often not comprehensive. In the worst case, an antibody is not specific and stains other proteins.
The present work, therefore, aimed to
(i) raise a polyclonal anti-TASK-3 antibody in rabbits and purify it to obtain a monospecific antibody
(ii) characterize the antibody by applying several tests to confirm its specificity and
(iii) use the purified, monospecific anti-TASK-3 antibody to study the regional and cellular distribution of the TASK-3 channel protein in the rat brain.

2 Materials and Methods

2.1 General Materials

2.1.1 Chemicals

1,4-dithiotreitol	Sigma-Aldrich (Steinheim)
2,2'-azino-bis-[3-ethylbenzthiazoline-6-sulfonic acid] (ABTS)	Roth (Karlsruhe)
3,3-diaminobenzidine tetrahydrochloride (DAB)	Sigma-Aldrich (Steinheim)
5,5-diethylbarbituric acid sodium salt	Sigma-Aldrich (Steinheim)
5-bromo-4-chloro-3-indolyl-phosphat (BCIP)	Sigma-Aldrich (Steinheim)
β-mercaptoethanol	Sigma-Aldrich (Steinheim)
acetic acid	Merck (Darmstadt)
acrylamide, 30%	Roth (Karlsruhe)
agarose GTQ	Roth (Karlsruhe)
ammonium nickel sulfate, 3%	Fluka (Buchs, Schweiz)
ammonium persulfate (APS)	Sigma-Aldrich (Steinheim)
ampicillin	Roth (Karlsruhe)
bicinchoninic acid-dinatrium (BCA)	Sigma-Aldrich (Steinheim)
biotinyl-thyramide	made in our lab
bisacrylamide, 2%	Roth (Karlsruhe)
bovine serum albumin (BSA)	Sigma-Aldrich (Steinheim)
bromophenol blue	Roth (Karlsruhe)
calcium chloride ($CaCl_2$)	Sigma-Aldrich (Steinheim)
Complete Protease Inhibitor Cocktail	Roche Applied Science (Mannheim)
coomassie blue, Roti© Blue (5x)	Roth (Karlsruhe)
copper(II) sulfate ($CuSO_2x5H_2O$)	Merck (Darmstadt)
cresylviolet acetate	Sigma-Aldrich (Steinheim)
dextran	Sigma-Aldrich (Steinheim)
dextran sulphate	Fluka (Schweiz)
Entellan	Merck (Darmstadt)
ethidiumbromide solution, 1%	Roth (Karlsruhe)
ethylene diamine tetraacetic acid (EDTA)	Roth (Karlsruhe)
formaldehyde, 37%	Merck (Darmstadt)
formamide	Fluka (Buchs, Schweiz)
gelatine	Merck (Darmstadt)
Gel Code Blue Stain Reagent	Pierce Biotechnology (Rockford, USA)
glycine	Merck (Darmstadt)
glycerine	Merck (Darmstadt)
hydrogen peroxide (H_2O_2)	Sigma-Aldrich (Steinheim)

Heparin-sodium-2500-ratiopharm	Ratiopharm (Ulm)
hepes sodium salt	Roth (Karlsruhe)
imidazole	Sigma-Aldrich (Steinheim)
isopropyl-β-D-thiogalactopyranoside (IPTG)	Sigma-Aldrich (Steinheim)
ketamine	CuraMED Pharma (Karlsruhe)
LB agar	Invitrogen (Karlsruhe)
loading dye (6x)	Fermentas (St. Leon-Rot)
lysozyme	Serva, Böhringer (Heidelberg)
magnesium chloride ($MgCl_2$)	Merck (Darmstadt)
maleic acid ($C_4H_4O_4$)	Sigma-Aldrich (Steinheim)
methyl green zinc chloride double salt	Merck (Darmstadt)
paraformaldehyde	Sigma-Aldrich (Steinheim)
phenylhydrazine	Merck (Darmstadt)
picrid acid	Merck (Darmstadt)
phenyl methan sulfonyl fluoride (PMSF)	Roth (Karlsruhe)
p-nitro blue tetrazolium chloride (NBT)	Sigma-Aldrich (Steinheim)
polyvinylpyrrolidone	Serva, Böhringer (Heidelberg)
Ponceau-S red	Sigma-Aldrich (Steinheim)
potassium chromosulftate-12-hydrate	Merck (Darmstadt)
p-phenylene diamine ($C_6H_4(NH_2)_2$)	Sigma-Aldrich (Steinheim)
RNase free water	Roth (Karlsruhe)
Rompun©, 2%	BayerVital (Leverkusen)
sodium azide (NaN_3)	Sigma-Aldrich (Steinheim)
sodium borohydrid ($NaBH_4$)	Sigma-Aldrich (Steinheim)
sodium carbonate (Na_2CO_3)	Merck (Darmstadt)
sodium citrate ($C_6H_5Na_3O_7$)	Merck (Darmstadt)
sodium chloride (NaCl)	Sigma-Aldrich (Steinheim)
sodium dodecyl sulfate (SDS)	Böhringer (Mannheim)
sodium hydrogen carbonate ($NaHCO_2$)	Merck (Darmstadt)
sodium hydrogen phosphate (NaH_2PO_4)	Sigma-Aldrich (Steinheim)
sodium hydroxid (NaOH)	Merck (Darmstadt)
sodium-tartrate-dihydrate ($C_4H_8Na_2O_8$)	Merck (Darmstadt)
sucrose	Sigma-Aldrich (Steinheim)
tetramethyl ethylenediamine (TEMED)	Roth (Karlsruhe)
thimerosal	Sigma-Aldrich (Steinheim)
tissue tec	Jung (Nussloch)
tris(hydroxy mehtyl)aminomethan (Tris)	Sigma-Aldrich (Steinheim)
Triton-X-100	Serva, Böhringer (Heidelberg)
tryptone	Sigma-Aldrich (Steinheim)
X-gal	Roche Applied Science (Mannheim)
xylole	J.T. Baker (Deventer, Netherlands)
xylencyanol FF	Merck (Darmstadt)
yeast extract	Sigma-Aldrich (Steinheim)

2.1.2 Antibodies, proteins, enzymes

2x Rapid Ligation Buffer	Promega (Mannheim)
ABC-Elite kit, Vectastain	Vector (Burlington, USA)
Advantage Taq 2 Polymerase	Clontech (Hamburg)
AlexaFluor 488 anti-guinea pig antibody	Vector (Burlington, USA)
AlexaFluor 594 anti-rabbit antibody	Vector (Burlington, USA)
alkaline phosphatase goat anti-rabbit IgG	Vector (Burlington,USA)
anti-FLUOS-AP	Roche Applied Science (Mannheim)
biotinylated goat anti-guinea pig antibody	Vector (Burlington, USA)
biotinylated goat anti-rabbit antibody	Vector (Burlington, USA)
biotinylated horse anti-goat antibody	Vector (Burlington, USA)
biotinylated horse anti-mouse antibody	Vector (Burlington, USA)
bovine hemoglobine	Sigma-Aldrich (Steinheim)
*Cfr*42I	Fermentas (St. Leon-Roth)
Cy2- and Cy3 antibodies	Jackson Immuno Research (West Grove, USA)
DNA-marker λ-*Eco*47I	Fermentas (St. Leon-Rot)
Dual color protein standard	Bio-Rad (USA)
FLUOS, from Fluorescein Labeling Kit	Roche Applied Science (Mannheim)
goat anti-5-HT antibody	DAKO (Glostrup, Denmark)
goat anti-TASK-3 antibody	Santa Cruz (Santa Cruz, USA)
goat anti-vesicular acetylcholine transporter (anti-VAChT) antibody	Chemicon (Temecula, USA)
guinea pig anti-histamine decarboxylase (anti-HDC) antibody	Acris (Bad Nauheim)
low-fat milk powder	Saliter (Obergünzburg)
Low Molecular Weight Marker	Amersham Bioscience (Freiburg)
mouse anti-digoxigenine antibody	Jackson Immuno Research (West Grove, USA)
mouse anti-dopamine-β-hydroxylase (anti-DBH) antibody	Chemicon (Temecula, USA)
mouse anti-tyrosine hydroxylase (anti-TH) antibody	Chemicon (Temecula, USA)
normal goat serum (NGS)	PAN-Systems (Aidenbach)
normal horse serum (NHS)	PAN-Systems (Aidenbach)
*Not*I	Fermentas (St. Leon-Roth)
peroxidase goat anti-rabbit IgG (P-GaR)	Vector (Burlington, USA)
*Pst*I	Fermentas (St. Leon-Roth)
Precision Plus protein standard, unstained	Bio-Rad (USA)
rabbit anti-GST antibody	Chemicon (Temecula, USA)
rabbit anti-HisTag antibody	MoBiTec (Göttingen)
rabbit IgG	Sigma-Aldrich (Steinheim)
rat liver extract	MP Biomedicals (Solon, USA)
RNase A	Quiagen (Hilden)
*Sph*I	Fermentas (St. Leon-Roth)
T4 DNA ligase	Promega (Mannheim)

vector pET32b(+)	Novagene (Madison, USA)
vector pGEM-T	Promega (Mannheim)
vector pGEX-4T-1	Amersham Bioscience (Freiburg)

2.1.3 Equipment and auxiliary materials

autoclave	Holzner (Nussloch)
automatic fraction collector	Abimed (Langenfeld)
centrifuge, Labofuge 400 R	Heraeus (Hanau)
centrifuge 5417 C	Eppendorf (Hamburg)
cryostat, Frigocut 2800	Reichert-Jung (Nussloch)
dialysis tube	Roth (Karlsruhe)
Dig RNA labeling kit	Roche Diagnostics (Mannheim)
electroelution system Biotrap	Schleicher&Schüll (Dassel)
electrophoretic chamber, Protean© II xi Cell	Bio-Rad (München)
ELISA microtiterplate, Falcon 3912	Becton Dickinson (Franklin Lakes, USA)
ELISA reader, HT II	Anthos (Wals, Austria)
filter, 0.2 μm, 0.45 μm, 1.2 μm	Schleicher&Schüll (Dassel)
gluthation-Sepharose 4B	Pharmacia Biotech (Freiburg)
heating cabinet, Kelvitron©	Heraeus (Hanau)
HiTrap DEAE FF sepharose columns	GE Healthcare (Uppsala, Sweden)
HiLoad 16/60 Superdex 75 column	Pharmacia Biotech (Freiburg)
HiLoad 16/60 Superdex 200 column	Pharmacia Biotech (Freiburg)
Homogenisator, UW70	Bandelin electronic (Berlin)
incubator	Heraeus (Hanau)
laboratory balance, BP 4100	Sartorius (Göttingen)
magnetic stirrer	Ika Labortechnik (Staufen)
microsyringe, Exmire	Ito Corporation (Fuji, Japan)
Milli-Q academic integral system	Millipore (Schwalbach)
minishaker, KMS1	Ika Labortechnik (Staufen)
nickel-nitrilotriacetic acid (NTA) matrix	Quiagen (Netherlands)
nitrocellulose membranes	Bio-Rad (München)
PCR Mastercycler	Eppendorf (Hamburg)
peristaltic pump, Gilson© Minipuls 3	Abimed (Langenfeld)
petri dishes	Roth (Karlsruhe)
pH meter, 761 Calimatic Knick	Elscolab (Netherlands)
photometer, Gilson© 112 UV/VIS Detector	Abidmed (Langenfeld)
photometer, ultrospec III	Pharmacia LKB (Cambridge, England)
pipettes und tips	Eppendorf (Hamburg)
Power Pac 200	Bio-Rad (München)
QIAfilter Plasmid Midi Kit	Qiagen (Hilden)
QIAprep Spin Miniprep Kit	Qiagen (Hilden)
QIAquick Gel Extraction Kit	Qiagen (Hilden)
precison scale, MC 1	Sartorius (Göttingen)
reaction vessels, FALCON©	Eppendorf (Hamburg)
recorder	Geitmann Messtechnik (Menden)
shaker, KS 250 basic	Ika Labortechnik (Staufen)

SP-sepharose 66% suspension, fast flow	Pharmacia Biotech (Freiburg)
thermomixer comfort	Eppendorf (Hamburg)
Trans-Blot SD Semidry Transfer Cell	Bio-Rad (München)
ultracentrifuge, J2-HS	Beckman (Krefeld)
UV-Transilluminator (312 nm)	INTAS (Göttingen)
water bath, DC10	HAAKE (Karlsruhe)

2.2 Expression and purification of recombinant proteins

Recombinant proteins are synthesized using specialized *E.coli* strains, which after transformation with an appropriate expression vector express the protein of interest. After growth of the culture and lysis of the cells the corresponding protein was separated from the supernatant and purified. Two different expression vectors were used in this work. The first is the vector pET32b(+) from Novagen. This is a vector for the expression of peptide sequences fused to thioredoxin. Furthermore, this vector contains a short open reading frame for a histidine-tag. The resulting thioredoxin fusion protein has an N-terminal tail of six histidine molecules (6HisTR), which could be used for purification by affinity chromatography. As a second vector, the vector pGEX-4T-1 from Amersham Bioscience was utilized. This vector carries the gene encoding for gluthatione-S-transferase (GST). In the resulting fusion protein GST is bound to the N-terminal end of the respective TASK protein fragment. GST fusion proteins are purified by using the high affinity of GST to its substrate gluthatione.
C-terminal fragments of the cDNA of TASK-1 (GenBank-Acc.No.: NM_033376, nucleotides: 854-1336, amino acids: 251-411), TASK-3 (GenBank-Acc.No.: NM_053405, nucleotides: 967-1188, amino acids: 323-396) and TASK-5 (GenBank-Acc.No.: NM_ 130813, nucleotides: 951-1034, amino acids: 290-318) were amplified by PCR and cloned in frame into the bacterial expression vectors pGEX-4T-1 and pET32b(+). TASK1-, TASK-3- and TASK-5-pET32b(+) as well as TASK1-, TASK-3- and TASK-5-pGEX-4T-1 plasmid-DNA was provided by Dr. Christian Derst and Dr. Regina Preisig-Müller.

2.2.1 Overexpression of proteins

2 μl of plasmid DNA each were added to 100 μl *E.coli* BL21DE3 competent cells, incubated on ice for 30 min and plated on LB-agar plates (10 g NaCl, 10 g tryptone, 5 g yeast extract, 20 g agar in 1 l H_2O, pH 7) containing 100 μg/ml ampicillin. Plates were incubated over night at 37 °C. The next day colonies were picked with a sterile tooth pick and carried over to a 50 ml LB medium containing 100 μg/ml ampicillin. Cultures were growing over night on a shaker at 37 °C, then the proliferated cells were transferred into 500 ml LB culture medium (containing 100 μg/ml ampicillin). When the culture has reached an OD_{600} of 0.5-1, Isopropyl-β-D-thiogalactosid (IPTG; ad 1 mM) was added and the culture was incubated under shaking for another 4 h to induce protein expression. Finally, cultures were chilled on ice and centrifuged at 5000xg for 5 min at 4 °C.
To control protein expression probes were taken from the overnight culture, before IPTG addition and before harvesting and checked by SDS-PAGE and western blot analyses.

2.2.2 Purification of 6HisTR fusion proteins

The purification of 6HisTR fusion proteins was carried out under denaturing conditions with the help of a Ni^{2+}-NTA-chromatography. The NTA matrix is pre-charged with Ni^{2+} ions, which are bound to a nitrilotriacetic acid (NTA) moiety. The fusion proteins bind with their histidine tag to the Ni^{2+} ions and can then be eluted from the matrix with a buffer containing a high concentration of imidazole or with an acidic buffer. Pellets were resuspended in lysisbuffer (8 M urea pH 8, 0.1 M NaH_2PO_4, 0.01 M Tris-HCl) added with phenyl methane sulfonyl fluoride (PMSF; ad 1 mM) and Triton-X-100 (ad 0.2%)

and sonicated (5x10 sec). Subsequently, the suspension was centrifuged for 5 min at 10,000xg and the supernatant was used for further protein extraction. 2 ml of NTA-matrix were equilibrated with lysis buffer and either applied to a column and loaded with the supernatant or the matrix was mixed with the supernatant and after shaking at 4 °C over night applied to a column (BATCH variant). Proteins were eluted from the matrix with an acidic buffer (8 M urea pH 4.5, 0.1 M NaH_2PO_4, 0.01 M Tris-HCl) or a buffer containing imidazole (8 M urea pH 8, 0.1 M NaH_2PO_4, 0.01 M Tris-HCl, 250 mM imidazole). Seven 2-ml fractions were taken and fractions as well as aliquots from pellet, supernatant, flow and wash were checked by SDS-PAGE. Finally, fractions were pooled, boiled up with about 1.5 ml of 6 x Laemmli buffer (6% SDS, 15% β-mercaptoethanol, 10% glycerine, 0.005% bromophenol blue in 187.5 mM Tris-HCl pH 6.8) and dialyzed against phosphate buffered saline (PBS; 8 g NaCl, 0.2 g KCl, 2.8 g NaH_2PO_4 and 0.4 g NaOH in 1 l H_2O, pH 6.8).
To further purify and analyze the TASK-3-6HisTR protein, the pre-purified protein was applied to a superdex 75 column for gelfiltration. This column acts as a molecular sieve, separating proteins depending on their molecular weight. Probes were dialyzed against PBS and loaded on the column. The protein concentration (extinction at 280 nm) of the outflow was measured and documented by a coupled photometer and reader and 2-ml fractions were collected. Fractions of each peak of the reader curve were checked in an ELISA (see page 25). Additionally, the pre-purified protein was processed in a preparative gel electrophoresis (see page 20).

2.2.3 Purification of GST fusion proteins

In contrast to the purification of 6HisTR proteins, GST fusion proteins were purified under native conditions. Pellets were resuspended in 20 ml STE (10 mM Tris pH 8, 150 mM NaCl, 1 mM EDTA), again pelleted and then resuspended in 10 ml STE containing 100 μg/ml lysozyme. Following 15 min of incubation on ice, 5 mM dithiothreitol (DTT), PMSF ad 1 mM and 1% Triton-X-100 were added. The suspension was shaken for 30 min, then centrifuged at 10,000xg for 5 min. 2 ml gluthatione-sepharose were equilibrated with PBS and mixed with the supernatant under shaking over night at 4 °C. The matrix was applied to the column and washed, then bound proteins were eluted from the matrix with a buffer containing reduced gluthatione (75 mM Hepes pH 7.4, 10 mM gluthatione, 5 mM DTT, 150 mM NaCl) in seven 2-ml fractions. The purification was checked by SDS-PAGE. This procedure failed to extract TASK-1-GST from the pellet. Therefore, the pellet was applied to a maxi-gel and the protein was purified by electroelution (see page 20).

2.2.4 Preparative gel electrophoresis

This method was applied to gain proteins of a higher purity. This was especially important for TASK-3-6HisTR, because this protein was used for the affinity-purification. About 2 mg of protein were loaded on a maxi SDS-gel (16x16 cm), electrophoretically separated and stained with coomassie-blue (45% ethanol, 45% A.bidest, 10% acetic acid, 1 g/ml coomassie blue) until the dominant band was faintly visible. The band was cut of the gel with a scalpel, crushed within a small amount of Biotrap-buffer (25 mM Tris, 192 mM glycine, 0.025% SDS) and transferred into the electro elution chamber. The proteins were eluted from the gel over night at 200 mV and dialyzed against PBS. Finally, the protein concentration was determined in a BCA test (see page 21).

	separation gel	stacking gel
bidest H_2O	49.9 ml	5.6 ml
1.5 M Tris-HCl pH 8.8, 0.4% SDS	43.8 ml	
0.5 M Tris-HCl pH 6.8, 0.4% SDS		2.5 ml
acrylamide, 30%	58.0 ml	1.35 ml
bisacrylamide, 2%	26.2 ml	0.5 ml
APS, 10%	87.5 μl	50 μl
TEMED	87.5 μl	10 μl

2.2.5 BCA test

The BCA test is based on the Biuret reaction. In an alkaline solution proteins build up complexes with Cu^{2+}, Cu^{2+} is reduced to Cu^{+}, which forms a violet complex with BCA (bicinchoninic acid). The optimal dilutions of the protein solutions were each determined in a preliminary test.
40 μl of each sample and the BSA-standard-solutions (0 μg/ml, 50 μg/ml, 100 μg/ml or 200 μg/ml in PBS) were mixed with 400 μl BCA (1.7% Na_2CO_3, 0.16% Na_2-tartrate-dihydrate, 0.4 % NaOH, 0.95% $NaHCO_2$ in H_2O, pH 11.25, complemented with 200 μl 4% $CuSO_2x5H_2O$ per 10 ml) and incubated for 30 min at 60 °C. Chilled samples were transferred into a hard plastic microtiter plate and the extinction at 550 nm was meassured. The protein concentration of the samples was calculated from the standard values.

2.2.6 SDS-polyacrylamide gel electrophoresis

The sodium dodecyl sulfate-polyacrylamide gel electrophoresis (SDS-PAGE) is a method for the separation of proteins. The gels were 9x6 cm in length. 12% gels were used for the detection of recombinant proteins, for the separation of membrane fractions 10% gels. Probes were boiled with 2xLaemmli buffer (62.5 mM Tris-HCl pH 6.8, 2% SDS, 5% β-mercaptoethanol, 10% glycerine, 0.05% bromophenole blue) for 3 min at 96 °C, and following chilling and centrifugation loaded to the gel with a microsyringe. The applied potential was 100 V until the samples had passed the separation gel. After about 30 min the potential was raised to 150 V for another 60-70 min. For the direct detection of proteins the gel was washed in A. dest. (3x10 min) and stained with a solution based on coomassie-blue (bluestain reagent). Once all bands of the co-applied marker were visible the staining procedure was stopped by the substitution of the staining reagent with H_2O. Gels were washed and photographed for documentation.

	separation gel	12% stacking gel	10% stacking gel
bidest H_2O	1.0 ml	1150 μl	1.3 ml
1.5 M Tris-HCl pH 8.8, 0.4% SDS	1.25 ml		1.25 ml
0.5 M Tris-HCl pH 6.8, 0.4% SDS		500 μl	
acrylamide, 30 %	2.0 ml	250 μl	1.65 ml
bisacrylamide, 2%	0.75 ml	100 μl	750 μl
APS, 10%	50 μl	20 μl	50 μl
TEMED	6.25 μl	2.6 μl	6.2 μl

2.3 Production and purification of antibodies

2.3.1 Raising of TASK-3 antibodies in rabbits

The purified TASK-3-GST protein was send to Pineda (Antikörper-Service, Berlin) who immunized two 5-month-old New Zealand rabbits with either 90 or 180 μg of the fusion protein (Harlow and Lane, 1988). At least two booster immunizations were performed to increase the immune reaction. The first blood samples were taken from the rabbit ear before immunization and beginning with day 35 weekly. After 12 weeks the animals were exsanguinated and the blood as well as the weekly samples were coagulated over night at 4 °C, followed by centrifugation at 2500xg and decomplementation for 1 h at 56 °C. Samples were stored at -80 °C until further processing.
The weekly samples were tested in an ELISA (see page 25) to control the process of immunization. Plates were coated with the TASK-3-6HisTR fusion protein or the carrier protein GST and incubated with the decomplemented serum samples.

2.3.2 Removal of unspecific cross reactivities

In a first step the serum was freed from cross-reactive antibodies against extracellular matrix and house-keeping proteins. The serum was treated with 50 mg/ml aceton-treated rat liver powder. Following 20 min of incubation under shaking, the solution was centrifuged and the supernatant was filtered through a sterile syringe.

2.3.3 Removal of IgMs

The IgMs were removed from the crude serum via a separation on a superdex 200 column. The column functions as a molecular sieve, separating the serum components by their molecular weight. The big IgMs are less retained by the matrix, thus can pass the column faster than the smaller IgGs. By pooling the corresponding (later) fractions the IgMs could be excluded from the serum.
The superdex column was equilibrated with degased PBS and loaded with 5 ml of the pre-absorbed serum. The outflow was collected in fractions of 2 ml and the extinction at 280 nm of each fraction was determined by an attached photometer and documented continuously via a pen recorder. Subsequently, fractions were tested in an ELISA (see page 25) and those with the highest activity against the antigen

(TASK-3-GST) were pooled. The serum pool was made up to 25 ml with 10% normal goat serum (NGS; dilution of 1:5 in regard to the crude serum) and stored at -20 °C until further purification.

2.3.4 Removal of cross reactivity against the carrier protein

To remove cross reactivities against the GST-fusion part, autoclaved and fixated bacterial pellets from *E.coli* BL21DE3 overexpressing the GST protein were generated and used for absorption. Cells were cultured over night at 37 °C and pelleted (see page 19). Bacterial pellets were resuspended in PBS. One half of the sample was autoclaved at 121 °C for 60 min, the other half was treated with 0.5% formaldehyde for 60 min at 37 °C under shaking. Subsequently, both parts were mixed, washed three times in PBS, pelleted and stored at -4 °C until use. The amount of bacterial pellet required for removal of anti-GST-activity was determined in a pilot experiment. Absorption with 4 mg pellet per 100 μl serum was chosen; the suspension was incubated for 30 min at RT while softly shaking. Afterwards, the serum was made up to 50 ml with 10% NGS in PBS (1:25 in regard to crude serum) and centrifuged for 15 min at 4000xg.

2.3.5 Removal of cross reactivities against paralogous proteins

Antibodies against paralogous proteins were removed from the serum by adsorption to nitrocellulose membranes bearing the corresponding protein. The immune activity against various proteins of the TASK family and other related proteins was identified in an ELISA. Beside the closely related TASK-1 and TASK-5, C-terminal fragments of THIK-1 and THIK-2 [Theilig et al., 2008] were tested. The two proteins showing the highest activity were used for the following adsorption. The adsorption was carried out in two steps with two different proteins, TASK-1-GST and TASK-5-6HisTR. The use of a GST fusion protein removes remaining activity against the carrier protein.
Four nitrocellulose membranes à 6x8 cm were equilibrated in PBS and incubated with the corresponding protein over night at 4 °C. The amount of protein best for the adsorption was determined in a preliminary test. The following incubation and all other incubations were carried out on a shaker. Coated membranes were washed in PBS, incubated with 5% NGS for 1 h to block free binding sides and then incubated with the serum (25 ml per membrane, serum dilution 1:50 in regard to the crude serum). Incubation was carried out for 4.5 h at RT or over night at 4 °C. The serum was first incubated on membranes bearing TASK-1-GST, the resulting supernatant was incubated on membranes bearing TASK-5-6HisTR.

2.3.6 Affinity purification

For the affinity-purification 6x8 cm nitrocellulose membranes were incubated with the TASK-3-6HisTR fusion protein. Coating of the membranes and the following incubation with the serum pool were carried out as described above (section 2.3.5). The protein amounts that give the best rates of yield of eluted antibody were determined in a pilot experiment (between 2-5 μg/ml). Membranes were incubated with the pre-purified serum for 4.5 h at RT or over night at 4 °C. Subsequently, they were washed in PBS and treated with the elution buffer (200 mM glycerine, 150 mM NaCl, 1 mg/ml bovine

serum albumin, pH 2.5) for 30 min (10 ml/membrane). The eluate was dialyzed against 50 mM phosphate buffer (pH 6) over night.

2.3.7 Concentrating antibody solution

To get a more concentrated antibody solution self-prepared SP-sepharose columns (matrix volume 1 ml) were used. SP-sepharose is a strong cation-exchanger with sulfopropyl groups that are negatively charged at a pH $\geq$ 2. The dialyzed eluate from the affinity purification was loaded on the column with the help of a peristaltic pump at a velocity of about 7 ml/h at 4 °C. As a function of their isoelectric point, the antibodies carry a positive charge at pH 6 (pH of the loading buffer), and can interact via electrostatic forces with the negatively charged column matrix. After washing the column with 20 mM phosphate buffer (PP) the bound antibodies were eluted from the matrix with a basic sodium carbonate buffer (200 mM $NaHCO_3$, pH 9.5). Twenty 200-μl fractions were eluted and tested in an ELISA. Those with the highest activity against the antigen were pooled and dialyzed against PBS. Finally, 0.1% sodium azide was added and the antibody was aliquoted and stored frozen at -80 °C.

2.4 Characterization of the antibody

2.4.1 Western blot

In a western blot proteins are first transferred to a nitrocellulose membrane and can then be detected immunologically. First, proteins were separated by SDS-PAGE. For the following electrophoretic protein transfer a Semi-Dry-Blot was used. The nitrocellulose membrane was laid on a blot paper soaked with blotting buffer (48 mM Tris, 390 mM glycine, 0.04% SDS, 20% methanol). The gel was placed on the membrane and then covered with another soaked blot paper. The transfer was carried out at an amperage of 4 mA/cm^2 for 30 min. A pre-stained marker was used to control the transfer of the proteins. As an additional control membranes were stained with Ponceau red for 1 min after blotting to visualize bound proteins. Free binding sites of the membrane were blocked with 5% low-fat milk powder in Tris-buffered saline (TBS; 20 mM Tris-HCl, 150 mM NaCl, pH 7.4) for 30 min. Afterwards, membranes were incubated with the diluted antibody (in 5% milk powder in TBS) over night at 4 °C. The next day, membranes were washed in TBS (3x10 min), then placed in the alkaline phosphatase conjugated secondary antibody (aP-GaR, 1:10,000 in TBS) for 2 h. After washing in TBS and shortly in AP-buffer (100 mM NaCl, 5 mM $MgCl_2$ in 100 mM Tris-HCl, pH 9) the immunosignal was developed using *p*-nitro blue tetrazolium chloride (NBT; 75 mg/ml in 700 μl DMF + 300 μl H_2O; 50 μl/10 ml) and 5-bromo-4-chloro-3-indolyl-phosphate (BCIP; 50 mg/ml in 1 ml DMF; 37.5 μl/10ml). The reaction was stopped after 30 min, membranes were washed in A.dest and pictures were taken with a Leica camera.

Protein labeling with fluorescein The purity of the prepared recombinant proteins was controlled with a FLUOS (5(6)-carboxyfluorescein-N-hydroxysuccinimide ester)-labeling. Free amino groups of the proteins in the analyzed solution react with FLUOS by forming a stable amino bond. Therefore, following FLUOS labeling all proteins can be detected by using an anti-FLUOS antibody and an appropriate visualization system. Proteins were loaded on a gel, electrophoretically separated and

blotted to nitrocellulose membranes as described above. Membranes were washed in 50 mM PP (3x5 min) and treated with FLUOS (1:2000 in 50 mM PP pH 8, added with 0.001% Triton-X-100) for 1 h at RT. Following washing in TBS (3x5 min) free binding sites were blocked with 5% milk powder in TBS for 30 min, washed again in TBS (3x5 min) and incubated with the alkaline phosphatase conjugated anti-Fluos antibody (1:2000 in TBS) over night at 4 °C. Next day, membranes were washed and visualized with BCIP/ NBT as described before.

2.4.2 Preparation of membrane fractions

To analyze the TASK-3 expression in the brain by western blot, membrane fractions were prepared from rat brain. Animals were first anesthetized, then decapitated (see page 26). Brains were dissected out and crushed in liquid nitrogen. About 1 g whole rat or mouse brain samples were homogenized in homogenization buffer (10 mM TEA pH 7.5, 250 mM sucrose containing 1 tablet protease inhibitor) and sonicated for 1 min. After centrifugation for 10 min at 1000xg at 4 °C the supernatant was ultracentrifuged for 1 h at 200,000xg at 4 °C. Pellets were resuspended in homogenization buffer, sonicated, and stored in aliquots at -80 °C. The total protein concentration was determined by BCA (see page 21).

2.4.3 Detection of antibodies using the ELISA

The Enzyme Linked Immuno Sorbent Assay (ELISA) was used for detection of antibodies and determination of their binding specificity. Wells of the ELISA microtiter plates were coated over night each with 1 μg/ml of the antigen in coating buffer (50 mM Na_2CO_3 in H_2O pH 9.6, 100 μl/well). As control, IgGs from rabbit in different dilutions (0, 5, 25 and 199 μg/ml) were used. All incubations were carried out at RT. The next day, remaining binding sites were blocked with 150 μl/well of 1 mg/ml bovine hemoglobin (Hb) in ELISA wash buffer (EWB; 50 mM NaH_2PO_4, 150 mM NaCl, 0.5% Tween 200, 3 mM NaN_3 in H_2O, pH 7.2) for 1 h. After washing three times with EWB, wells were incubated with the antibody appropriately diluted in EWB-Hb (100 μl each, 2 h). Following washing with PBS, the antibody was labeled with an peroxidase-conjugated anti-rabbit antibody (P-GaR, 1:1000 in 1 mg/ml hemoglobin in PBS, 100 μl/well, 1 h). After washing with PBS, the enzymatic reaction leading to the visualization of the bound antibodies was started by pipetting 100 μl/well of 1 mg/ml ABTS (2,2‘-Azino-bis-[3-ethylbenzthiazolin-6-sulfonacid) in incubation buffer (50 mM NaH_2PO_4, 100 mM CH_3COONa in H_2O, pH 4.2) added with 0.03% H_2O_2. After 5 min the reaction was stopped by the addition of 100 μl sodium azide solution (0.1% in PBS). The extinction was photometrically measured with an ELISA reader (405 nm against 630 nm).

Competitive ELISA The competitive ELISA was used for the determination of the specificity of the antibody. Dilution series of different antigens were prepared and the appropriately diluted antibody was incubated with the antigen solutions. Incubation was carried out over night at 4 °C, after centrifugation the preincubated antibody was applied to the coated microtiter plate. Beside TASK-3-6HisTR, the paralogous TASK-1- and TASK-5-6HisTR fusion proteins and the carrier protein GST was used for the blockade.

2.5 Immunocytochemistry

2.5.1 Perfusion fixation of rat brains

Adult, male Wistar rats (250 to 320 g) obtained from an institutional breeder (FEM, Forschungseinrichtungen für Experimentelle Medizin) were handled in accordance with German animal protection laws and approved by the governmental authorities (Regional Berlin Animals Ethics Committee). Animals were maintained under controlled temperature (22 °C) and scheduled illumination (12 h light/dark cycle) conditions with water and food *ad libitum*. Rats were first anesthetized by placing them in an ether atmosphere. Following, a mixture of ketamine (0.1 mg/g body weight), 2% Rompun and heparin (2500 U) was injected intraperitoneally. The thorax was opened and the transcardial perfussion started with 10 sec of the prerinsing solution (12 g sodium 5,5-diethylbarbiturate, 8.2 g $Na(CH_3COO)$, 18 g NaCl, 0.4 g $CaCl_2$, 0.1 g Cl_2, 80 g dextran, ad 2000 ml, pH 7.6) followed by an immediate switch to the perfusion solution (4% paraformaldehyde, 0.05% glutaraldehyde, 0.2% pricric acidin 0.1 M, phosphate buffer, pH 7.4; 5 min at $1.998x10^4$ Pa and 20 min at $2.666x10^3$ Pa) and concluding 10 min with a postfixation solution (0.5% sucrose, 100 mM NaH_2PO_4, pH 7.4; $1.998x10^4$Pa). Brains were dissected out, embedded in 2% agarose and cut in coronal blocks of 2-3 mm. Brains were cryoprotected in 0.4 M sucrose (in 0.1 M PP pH 7.4) over night and 0.8 M sucrose (in 0.1 M PP pH 7.4) for at least 4 h, frozen in hexane at -60 °C and attached to a cork plate with tissue tec. The frozen blocks were stored at -80 °C until use.

2.5.2 Immunocytochemistry on brain sections

For the immunocytochemical examination 20-μm sections were cut on a microtome. Slices were transferred to 24-well tissue culture plates using a brush and washed for at least 20 min in PBS. Brain slices were incubated free floating in the culture plates. Incubation volume was 500 μl for all incubation steps and 1000 μl for washing. Incubation over night was carried out at 4 °C on a shaker. Slices were treated with 1% sodium borohydride (in PBS, 15 min) to reduce aldehyde groups, and following thorough washing (5 x PBS) preincubated for 30 min in 1% casein, 1% NHS, and 0.3% Triton-X-100 in 50 mM Tris-buffer pH 9.5, containing 0.05% phenylhydrazine to destroy endogenous peroxidases. Afterwards, slices were incubated with the primary antibody appropriately diluted in the incubation solution (1% casein, 1% NHS, 0.3% Triton-X-100, 0.01% thimerosal, 0.01% sodium azide in 50 mM Tris-buffer pH 9) for at least 48 h.

ABC-DAB/nickel-method Sections labeled with the primary antibody were washed in PBS (20 min and 40 min), followed by a 1-h treatment with PBS-A (2 mg BSA/ml PBS) and incubation for 24 h in the secondary antibody solution (biotinylated goat anti-rabbit IgG, 1:2000 in PBS-A containing 0.3% Triton-X-100 and 0.1 % sodium azide).

Next day, sections were washed twice in PBS and again preincubated in PBS-A for 1 h. Subsequently, signaling with the peroxidase-coupled avidin-biotin-complex (ABC; 1:200 in PBS-A) was carried out over night. Finally, tissue bound peroxidase was visualized with a DAB-solution (10 mM 3,3-diaminobenzidine tetrahydrochloride [DAB], 10 mM imidazole in 50 mM Tris-buffer pH 7.4). The visualization reaction was started by pipetting 25 μl 0.005 % H_2O_2 per well and 50 μl 3% ammonium

nickel sulfate (per 500 μl well). The solution was replaced by PBS after 15 min, sections were washed and mounted on coated slides. Following dehydration in a graded series of ethanol (70%, 90%, 96%, 100%, 100%, 3 min each) and treatment with xylole (2x5 min) sections were embedded in Entellan. Immunocytochemistry with mouse anti-TH (1:10,000), goat anti-vAChT (1:1000) and guinea pig-anti-HDC (1:1000) were performed as described before. The corresponding biotinylated secondary antibodies (horse anti-mouse, horse anti-goat and goat anti-guinea pig) were diluted 1:2000.

Pre-absorption with the specific antigen As a control for binding specificity the primary antibody was incubated with the specific antigen before incubation on brain sections. Varying amounts of TASK-3-GST were tested. Best blockades were obtained by using 5-10 μg antigen per ml antibody solution. Blockade was carried out over night and the antibody solution was centrifuged prior to use.

Fluorescence double-labeling For the fluorescence double-labeling the TASK-3 antibody and one of five other antibodies (mouse anti-TH, mouse anti-DBH, goat anti-vAChT, goat anti-5-HT, guinea pig anti-HDC) were co-applied and incubated for at least 36 h at 4 °C (treatment of brain sections and incubation solution as mentioned before, see page 26). Cy2- or AlexaFluor594 coupled anti-rabbit secondary antibody and Cy3-anti-mouse, Cy3-anti-goat or AlexaFluor488-anti-guinea pig antibodies were diluted 1:500 in PBS-A. Sections were incubated over night, washed and covered in a fluorescence mounting medium (14 g glycine, 17 g NaCl and 100 mg phenylenediamine in 1 l H_2O pH 8, diluted 1:2 in glycerine).

2.5.3 Staining with cresyl violet

To demonstrate the cytoarchitecture of the brain sections staining with cresyl violet was performed. This method, also referred to as nissl-staining, takes advantage of the alkaline properties of the aniline dye cresyl violet. Basophilic structures such as nuclei or RNA (Nissl-bodies) are stained violet. Slide-mounted sections were treated with 70% EtOH over night, rinsed in A.dest for 2 min and incubated in a solution of 0.2% cresyl violet acetate in 20 mM acetic acid, pH 4.5 for 30 min. Slides were again washed in A.dest (2 min), differentiated in 70% EtOH (max. 5 min) and dehydrated in a graded series of EtOH. Following the transfer to xylole, sections were embedded in Entellan.

2.5.4 Counterstaining with methyl green

Methyl green stains all nuclei. Immunocytochemically stained brain sections were mounted on coated slides and treated with 70% EtOH over night. Subsequently, slides were washed in A.dest (2 min) and stained with a methyl green solution (2% in 20 mM acetic buffer, pH 5) for 30 min. Following staining, slides were again washed in A.dest, dehydrated in 96% and 100% EtOH (30 sec, 5 min) and after replacing ethanol with xylole (2x5 min) embedded in Entellan.

2.5.5 Coating of slides

Glass slides were cleaned in a dishwasher and dried at 60 °C. For the preparation of the gelatine solution 15 g gelatine and 1.76 g potassium chromosulfate-12-hydrate were diluted in 630 ml H_2O at

70 °C. Subsequently, 300 ml of 100% ethanol and 70 ml acetic acid were added. The solution was filtered into a cuvette and the slides were transferred to the solution for 3 min each. Gelatine was used up to 5 times before replacing with fresh solution. Afterwards, slides were dried at room temperature in a dust-free environment.

2.6 Synthesis of rat TASK-3 specific riboprobes for *in situ* hybridization

2.6.1 Polymerase chain reaction (PCR)

For the amplification of TASK-3 fragments a cDNA gained from rat hippocampus was used. Two pairs of primers were chosen for the amplification of a C-terminal fragment of the TASK-3 sequence.

GenBank-Acc.No.	Primer	product size
NM_053405	5'agggagaagttgcgcagata 3'	
	5'ccggaagtaggtgttcctca 3'	341 bp
NM_053405	5'ctcctgttcctcctgctgtt 3'	
	5'atgtgcagcctgtggttttc 3'	204 bp

The PCR mixture for a 50 μl reaction was as follows:

5 μl	10 x buffer
10 μl	dNTP mix (25 mM each)
1 μl	forward primer (100 pmol/μl)
1 μl	reverse primer (100 pmol/μl)
5 μl	cDNA
27 μl	H_2O
1 μl	Advantage Taq Polymerase Mix 2

The PCR started with the denaturation of the DNA double-helix at 95 °C for 60 sec. Following, a cycle of denaturation (95 °C for 15 sec), primer annealing (58 °C for 15 sec) and elongation (72 °C for 60 sec) was repeated 35 times. Finally, heating to 72 °C for 180 sec served to terminate elongation of all PCR fragments.

2.6.2 Agarose gel electrophoresis and gelextraction

To isolate the amplified fragments, the PCR mixture was electrophoretically separated on a 1% agarose gel followed by the extraction of the DNA from the gel. 2 μl of loading buffer were added to 10 μl of the PCR reaction each and loaded on a 1% agarose gel in TAE (40 mM Tris-acetate, 1 mM Na_2EDTA in H_2O, pH 7.6) containing 1% ethidium bromide. The electrophoresis was run at 80 mV in a chamber with TAE for about 45 min. The DNA marker λ-Eco47I was co-applied to control the size of the bands. Visualization of the bands was carried out under UV-light using the fluorescence of ethidium

bromide, which intercalates into the DNA.
Bands corresponding to the estimated size of the PCR product were cut out under UV-light and DNA was isolated using a Gel extraction Kit. Instructions of the supplied protocol were followed, in a final step the DNA was eluted from the columns with 50 μl of H_2O. DNA probes were concentrated with a vacuum centrifuge for 20 min to about 20 μl.

2.6.3 Ligation, transformation and identification of positive clones

To transcribe the DNA fragment into RNA, it was cloned into the pGEM-T vector by TA cloning. This technique relies on the ability of adenine (A) to hybridize with thymidine (T). The DNA fragment carries 3‘ adenine overhangs added by the Taq polymerase. In the presence of a ligase the overhangs fuse with complementary 3‘ thymidine overhangs of the vector. The vector contains T7 and SP6 RNA polymerase promotors flanking the multiple cloning region. 3 μl DNA, 1 μl ligase and 1 μl pGEM-T vector were added to 5 μl of 2x Rapid Ligation Buffer. The ligation was carried out over night at RT. Afterwards, competent XL1 Blue *E.coli* cells were transformed with the vector and cells carrying the vector with the insert could be identified by blue-white screening. Therefore, 10 μl of the ligation mixture was added to 100 μl of cells each and incubated on ice for 45 min. Following, cells were crossed out on LB-A agar plates with 20 μl of 100 mM IPTG and 20 μl of 2% X-Gal (in DMF). Agar plates were incubated at 37 °C over night.

2.6.4 Preparation of plasmid-DNA

Positive clones were identified by their white color, picked with a sterile tooth pick and transferred to 1.5 ml of LB-A medium. Medium was incubated on a shaker at 37 °C over night. The culture was pelleted by centrifugation (5 min, 14,000xg), followed by the isolation of plasmid DNA using a miniprep kit. The miniprep was carried out following the instructions of the manufacturer (Qiagen). The DNA was eluted from the column with 70 μl of H_2O. To minimize the number of clones sent for sequencing a restriction analysis was carried out. Therefore, 1 μl of the enzyme *Pst*I, 1 μl of the enzyme *Cfr*42I and 1 μl of the corresponding buffer were added to 7 μl of DNA and incubated for 1 h at 37 °C. The vector contains one restriction site for *Cfr*42I and *Pst*I on the 5‘- and 3‘-sites of the multiple cloning side respectively. Hence, these enzymes cut the vector on either sides of the insert. An agarose gel electrophoresis shows if the size of the insert corresponds to the size determined for the cloned PCR product. Finally, two presumptive positive clones per primer were sent for sequencing (JenaGen, Jena). Sequencing verifies if the clone carries the right insert and shows in which orientation it is cloned.

2.6.5 Preparation of digoxigenine-labeled riboprobes

Non-radioactive riboprobes were prepared with the Dig RNA labeling kit from Roche. This kit uses SP6 and T7 RNA polymerases for the *in vitro* transcription of a template DNA. Furthermore, digoxigenine (Dig)-UTP is incorporated into the transcript. The Dig-labeled ribo probes can be detected with anti-digoxigenine antibodies and visualized using immunocytochemical methods.
A midiprep (Midiprep Kit, Qiagen) was performed to gain the plasmid DNA (TASK-3-pGEM-T).

Therefore, *E.coli* BL21DE3 cells were re-transformed with the positive clones. 2 μl plasmid DNA (from the miniprep, see page 29) were added to 100 μl of cells, incubated on ice for 45 min and plated on LB-A plates over night at 37 °C. Colonies were picked with a sterile tooth pick and transferred to 50 ml LB-A medium. The medium was incubated under shaking over night at 37 °C, then cultures were pelleted by centrifugation at 4500xg for 30 min. DNA was extracted by following the instructions of the manufacturer. Finally, DNA was precipitated by the addition of 0.8 Vol. isopropanol and immediate centrifugation at 15,000xg for 30 min at 4 °C. The pellet was washed with 2 ml of 80% ethanol and after centrifugation resuspended in 50 μl of RNase-free water. Subsequently, the DNA concentration was determined by measuring the extinction at 260 nm and calculating the value with a free program (http://www.pubquizhelp.com/other/dnacalculator.html). For linearization of the vector, two restriction reactions were performed each, one with an enzyme cutting on the 3‘-site of the insert and one cutting on the 5‘-site. It is important to choose enzymes that have no internal restriction sites in the insert. 3 μl of plasmid DNA and 5 μl of H_2O were mixed with 1 μl *Not*I or *Sph*I and 1 μl of the corresponding reaction buffer. Incubation was carried out at 37 °C for 3 h. Subsequently, the restriction mix was electrophoretically separated on an agarose gel, the bands corresponding to the linearized vector were cut out and the DNA was extracted from the gel using the Qiagen Gel extraction kit. The DNA was concentrated by centrifugation under vacuum. Following, each probe was transcribed with a SP6 and T7 polymerase; these RNA-polymerases read the insert from opposite directions. One transcript serves as the antisense probe that binds to the complementary mRNA. The other, called sense probe, does not hybridize to the mRNA and can be used as a negative control.
The following components were mixed as describe in the protocol:

13 μl	DNA
2 μl	10x NTP labeling mixture
2 μl	10x transcription buffer
1 μl	Protector RNase inhibitor
2 μl	RNA polymerase SP6 bzw. T7

Incubation was carried out at 37 °C for 2 h. In a final step, the template DNA was digested by adding 2 μl of DNase I and an additional incubation at 37 °C for 15 min. Riboprobes were stored frozen at -80 °C.

2.7 *In situ* hybridization on brain sections

20-μm sections were taken on a microtome, washed in PBS for 20 min and treated with 1% sodium borohydrid in PBS for 15 min. Following thorough washing in PBS, sections were preincubated in hybridization buffer (50 % formamide, 10 mM Tris, 50 mM $NaHPO_4$, 60 mM sodium citrate, 5 mM EDTA, 100 μg/ml tRNA, 5% dextran sulphate, 1% ficoll, 1% polyvinyl-pyrrolidone) for 30 min and then incubated with the digoxygenine-labeled TASK-3 specific riboprobes appropriately diluted in hybridization buffer (0.1-0.3 μg/ml). Incubation was carried out free floating for 16 h at 56 °C. A 30 min stringency wash at 56 °C in citrate buffer (15 mM NaCl, 2 mM sodium citrate, pH 7.5) was followed by RNase A digestion (10 μg/ml, 0.2% BSA in PBS, pH 7.4) for 30 min. Subsequently,

slices were washed in PBS, preincubated in maleat buffered saline (MBS; 100 mM maleic acid, 100 mM NaCl in H_2O, pH 7.5) containing 2% casein and 1% NHS and then incubated with the mouse anti-digoxigenine antibody (diluted 1:10,000 in MBS containing 1% NHS, 1% casein and 0.1% sodium azide) for 24 h at 4 °C. The next day, sections were washed in PBS (20 and 40 min), preincubated in PBS-A (2 mg BSA/ml PBS) for 60 min and then treated with the biotinylated horse anti-mouse IgG secondary antibody (1:2000 in 0.2% BSA in PBS, 0.1% sodium azide). 24 h later, sections were washed in PBS (20 and 40 min) and preincubated again in PBS-A for 60 min. Bound antibodies were labeled with avidin-biotin-complexes from the Vectastain Elite ABC kit (1:200 in PBS-A, over night at 4 °C). Following washing (10, 20 and 30 min in PBS), further signal amplification was provided by treatment with biotinyl-thyramide (5 μM in 50 mM Tris/HCl pH 7.6, added with 10 mM imidazole) which was supplemented with 0.0015% H_2O_2 (final concentration) after 15 min to start the reaction. 15 min later the reaction was stopped by replacing the incubation mixture with PBS, sections were washed in PBS (10, 20, 30 min) and again incubated in the ABC solution (over night, 4 °C). Finally, slices were developed with DAB and mounted in Entellan as described above (see 26).

3 Results

3.1 Preparation and purification of recombinant TASK proteins

The TASK-3 channel of the K_{2P} family has been subject to many studies about its function in different cellular processes, contribution to native leak currents or its occurrence and distribution in peripheral or central nervous tissue. At least two reports described the localization of TASK-3 channels in the CNS by *in situ* hybridization experiments [Karschin et al., 2001, Talley et al., 2001], showing a widespread distribution of TASK-3 mRNA. Less comprehensive data are available on the immuno localization, hence the expression pattern of the TASK-3 channel protein. This is largely due to the lack of a specific, commercially available antibody. Therefore, in the present work a TASK-3 antibody was raised in rabbit, freed from cross reactivities to other K_{2P} proteins and affinity purified to obtain a polyclonal, monospecific antibody. This antibody was used to study the distribution of TASK-3 in the rat brain, with a special focus on neurons associated with monoaminergic and cholinergic systems.

3.1.1 The TASK-3 region used for immunization

To ensure the specificity of the antibody it is crucial to chose an appropriate sequence for the TASK-3 fusion protein used for the immunization of the rabbits. Therefore, a region of the TASK-3 protein was used that shares only little homology with other proteins. Figure 3.1 illustrates an alignment of the amino acid sequence of three rat TASK channels. The amino acid sequence of TASK-3 shares 54% and 51% over all identity with that of TASK-1 and TASK-5 respectively. Within M1 and M4 the sequence of TASK-1, TASK-3 and TASK-5 share about 80% identity. Besides the high conservation, the regions of the transmembrane segments should not be used for immunization because of their hydrophilic properties. A comparison of the three proteins reveals only little similarity at the carboxy-terminal ends, as can be seen by the gaps in the alignment (amino acid identitiy about 17%). In contrast to the low homology to paralogous proteins, this region shows the highest homology to orthologous proteins. This is important for the preparation of antibodies that can be used in several species, e.g not only for immunocytochemistry on rat tissues, but also on mouse and human tissues. In addition, the C-terminal end is located extracellularly and therefore provides good access for the antibody. Concluding, this region is ideally suited for use as an antigen in the antibody production. The sequence chosen for preparing the TASK-3-GST fusion protein is assigned in yellow and comprises amino acids 323 to 396.

3.1.2 The recombinant fusion proteins

Anti-TASK-3 antibodies were gained by immunization of two rabbits with the bona fide fragment of the protein. For the immunization the protein fragment was linked to a carrier protein. This is important

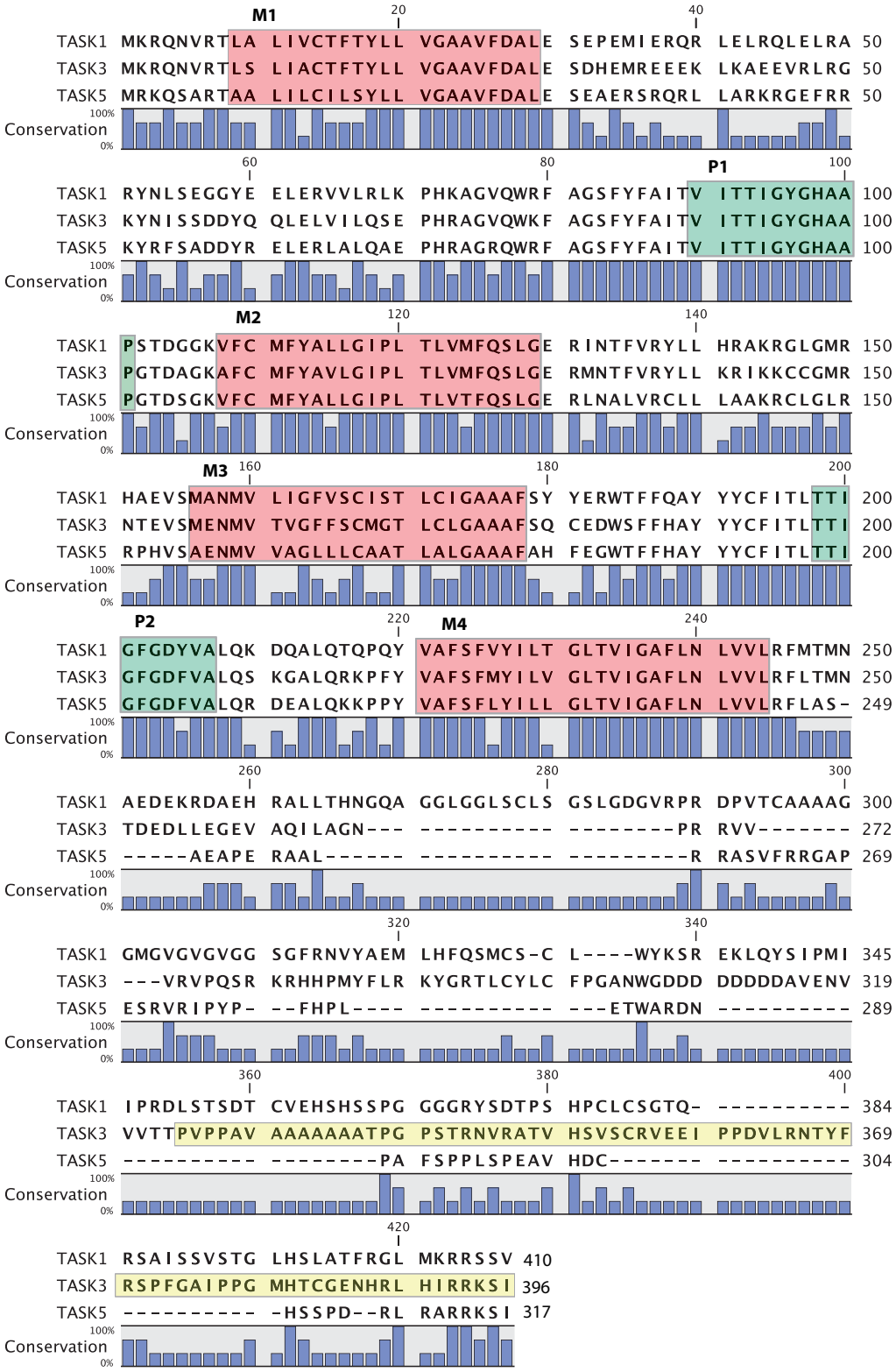

Figure 3.1 – Alignment of the amino acid sequence of members of the TASK family. Sequence comparison of TASK channels from *Rattus norvegicus* reveals only little conservation at the carboxy-terminal ends of the proteins. A sequence of 73 amino acids in this area was chosen for antibody production (marked in yellow). Regions of high conservation are the transmembrane domains (M1-M4, red) and the pore-forming regions (P1 and P2, green). Bars indicate the degree of conservation between the three channel proteins (with 100%= all three share the same amino acid).

for the stability of the protein and the following purification. The chosen fragment of 73 amino acids from TASK-3 was cloned into the expression vector pGEX-4T-1. Transformation and subsequent preparative expression in *E.coli* bacteria led to a fusion protein of gluthation-S-tranferase with the TASK-3 fragment bound to its C-terminal end (TASK-3-GST). GST was used for the purification of the fusion protein by performing an affinity chromatography with GST-sepharose. In addition, fusion proteins with GST and C-terminal fragments of TASK-1 or TASK-5 were expressed and purified.
The purified paralogous proteins were used for the removal of cross reactivities and for tests of the antibody specificity. The purity of the fusion proteins was checked in SDS-PAGE (Fig. 3.2A) and by western blot analyses. When applied to the gel and visualized directly with blue stain reagent all three proteins showed a single band with the expected molecular weight (TASK-1-GST, 44.3 kDa; TASK-3-GST, 42 kDa; TASK-5-GST, 34.8 kDa). Furthermore, a western blot analysis of the fusion proteins with an anti-GST antibody detected a band with the correct size each for TASK-1-GST, TASK-3-GST, and TASK-5-GST (not shown).
In addition, fusion proteins of the corresponding TASK fragments and thioredoxin with a six-histidine N-terminal extension (6HisTR) were expressed. The six-histidine tail was used for the purification by ion-exchange-chromatography with Ni^{2+}-NTA agarose. TASK-1-6HisTR and TASK-5-6HisTR were required for removal of cross reactivities and tests of the monospecific antibody. An SDS-PAGE of the purified proteins revealed a single band with the expected molecular weight for the TASK-1 and TASK-5 fusion proteins (TASK-1-6HisTR, 37.2 kDa; TASK-5-6HisTR, 27.7 kDa; Fig. 3.2B).

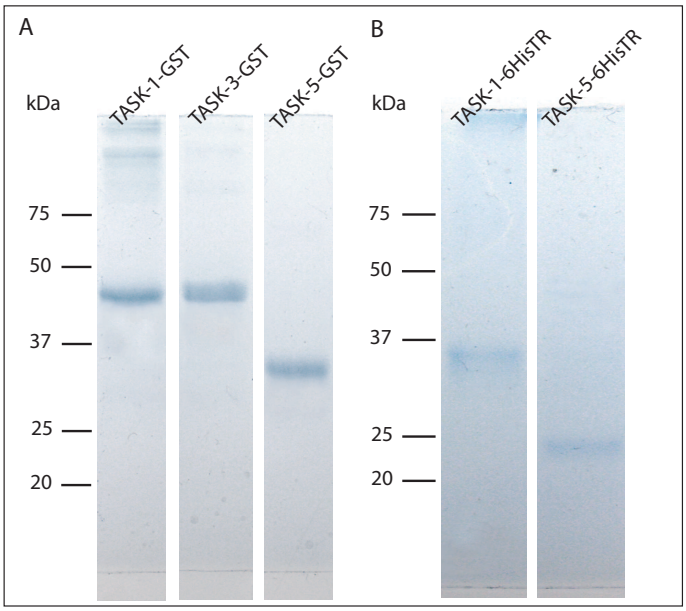

Figure 3.2 – SDS-PAGE of recombinant TASK fusion proteins. The recombinant proteins were applied to a 12% polyacrylamide gel and electrophoretically separated. (A) SDS-PAGE of the purified TASK-1-, TASK-3- and TASK-5-gluthation-S-transferase (GST) fusion proteins. Visualization with blue stain reagent revealed single bands with about the expected molecular weight for each protein (TASK-1-GST, 44.3 kDA; TASK-3-GST, 42 kDa; TASK-5-GST, 34.8 kDa). (B) SDS-PAGE of the purified TASK-1- and TASK-5-6HisTR (TASK fragment fused to thioredoxin with a 6-histidine N-terminal extension) fusion proteins. Visualization of the proteins revealed a single band with about the expected molecular weight for both proteins (TASK-1-6HisTR, 37.2 kDA; TASK-5-6HisTR, 27.7 kDa). Marker precision plus protein standard (Bio-Rad) is indicated.

TASK-3-6HisTR was required for the affinity purification, therefore particular accuracy was set on the purification of this protein. Western blot analyses of the purified TASK-3-6HisTR protein showed several bands besides the expected band of the recombinant protein at 27 kDa. The crude serum of the TASK-3 antibody and an anti-HisTag antibody detected at least 5 bands with molecular weights between 20 to 30 kDa (Fig. 3.3, 1 and 2). The crude serum detected an additional protein with a molecular weight of about 45 kDa (Fig. 3.3A, 2). It was assumed that the 45-kDa band corresponds to a dimer of the TASK-3-6HisTR protein.

To test this assumption, the previously purified TASK-3-6HisTR protein was applied to a superdex 75 column, to separate individual proteins by their molecular weight. The outflow was collected in fractions, Figure 3.3B shows a western blot with a commercial anti-TASK-3 antibody of selected fractions. No bands are visible in the early fraction 23 and the late fraction 53. Fractions 28 and 31 display the same composition of bands as the load, with several bands in the 27-kDa range and a band at around 45 kDa. These data are in line with the idea that the recombinant protein forms larger complexes, which elute together in the higher molecular weight range. In a next step, the pre-purified

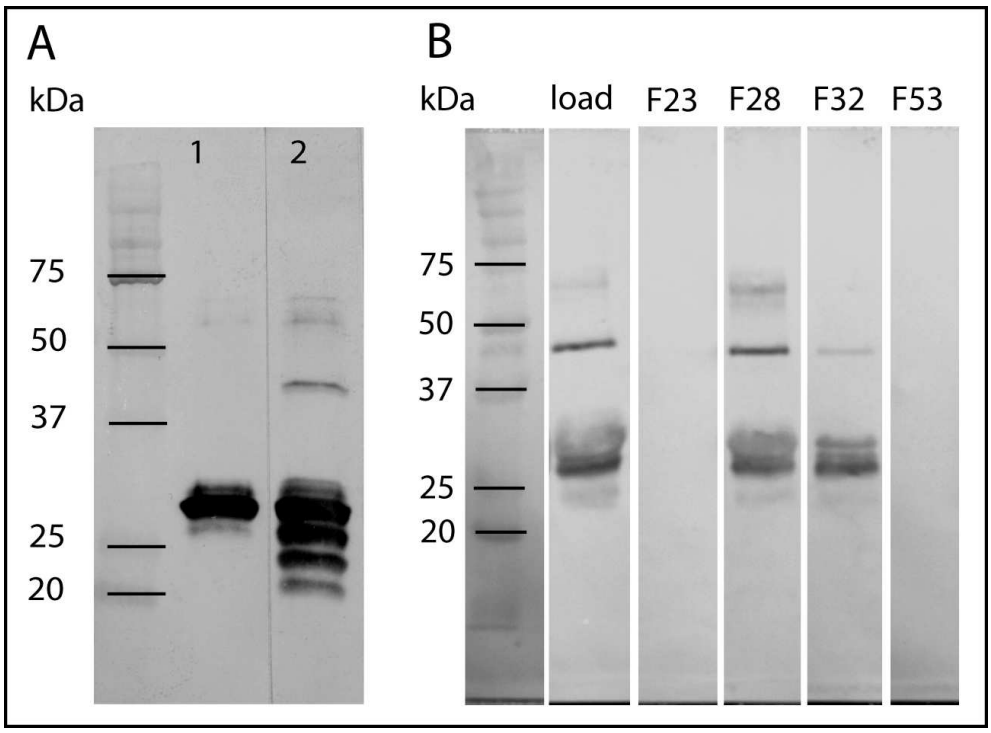

Figure 3.3 – Western blot analysis of the purified TASK-3-6HisTR (A) A western blot analysis of the pre-purified TASK-3-6HisTR fusion protein with an anti-HisTag antibody (1) and the crude serum of TASK-3 (2) revealed several bands beside the expected band of the recombinant protein at 27 kDa. The crude serum detected an additional band with about twice the molecular weight (about 45 kDa, in 2). (B) The pre-purified TASK-3-6HisTR protein was applied to a superdex 75 column and selected fractions were tested in an ELISA with a commercial anti-TASK-3 antibody. Load and fractions 28 and 32 show the same composition of bands, with several band in the 27-kDa-range an a band with about 45 kDa. No bands are visible for the early fraction 23 and the late fraction 53. Marker dual color (Bio-Rad) is indicated.

protein was electrophoretically separated on a maxi-gel. A band at around 27 kDa, corresponding to the TASK-3-6HisTR protein, was cut of the gel and the protein was extracted from the gel by electroelution. A western blot analysis with an anti-TASK-3 antibody again revealed several bands around 27 kDa. When higher amounts of the extracted protein are loaded on the gel the additional

band at about 45 kDa appears. It can be concluded that the 45-kDa band corresponds to a dimer of the TASK-3-6HisTR protein. Smaller bands around 27 kDa presumably correspond to proteolytic fragments of the protein.

3.2 Purification and characterization of the TASK-3 antibody

Two New Zealand rabbits were immunized with a C-terminal fragment (amino acids 323-396) of rat TASK-3 fused to GST. Beginning with the third week, blood samples were taken weekly for the next 12 weeks and finally rabbits were killed and exsanguinated. The blood samples were tested in an ELISA to follow the process of immunization. The immunoreactivity of the early samples was low against TASK-3-6HisTR and the carrier protein GST, but increased beginning with week 7, indicating the success of the immunization (see Fig. 3.4). The pooled sera were freed from unspecific antibodies by absorption with liver extract. Subsequently, IgMs were removed by gel filtration on a superdex 200 column. In a next step cross reactivities against the carrier protein (GST) were removed by absorption to autoclaved and fixed bacterial pellets from *E.coli* over-expressing the GST protein. Cross reactivities against TASK-1 as well as TASK-5 were removed by adsorption to nitrocellulose membranes loaded before with the corresponding recombinant proteins (TASK-1-GST and TASK-5-6HisTR). Finally, the antibody was affinity-purified using the purified TASK-3-6HisTR fusion protein and concentrated.

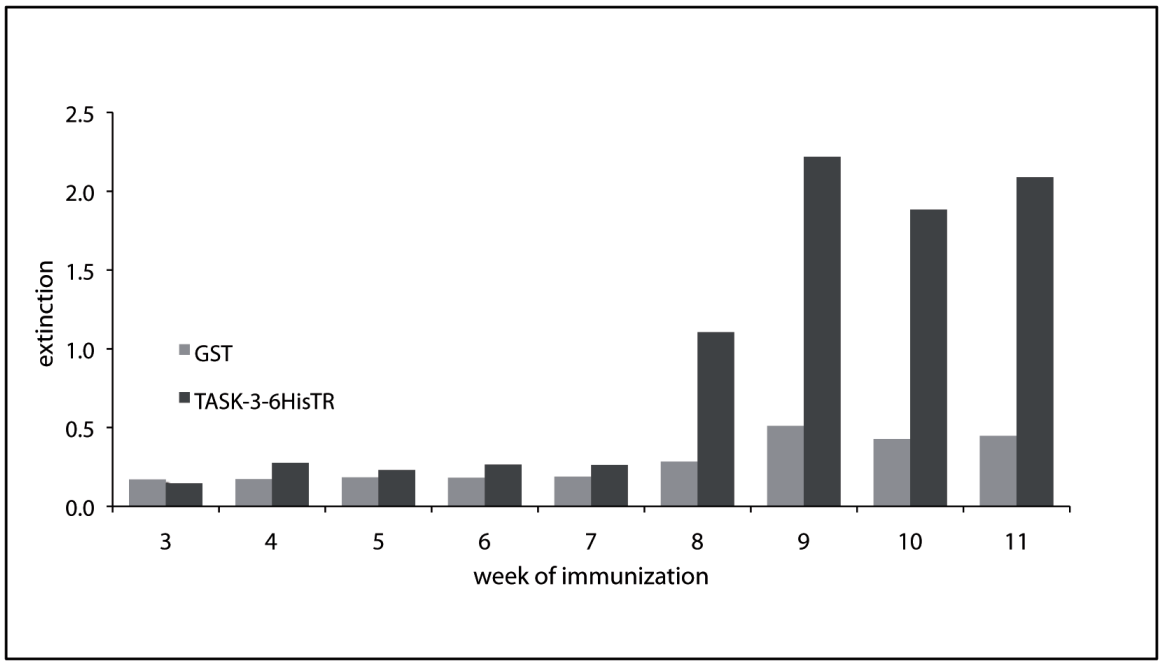

Figure 3.4 – Progress of immunization. Following immunization of the rabbits, blood samples were taken weekly (starting with week 3) and checked in an ELISA for reactivity against GST and TASK-3-6HisTR. Microtiter plates were coated with the respective proteins and incubated with the serum samples. Immunoreactivity of the early samples was low for both proteins. An increased signal beginning in week 8 indicates the presence of antibodies, hence the progress of the immunization.

3.2.1 Removal of unspecific serum proteins and IgMs from the serum

In a first step the serum was freed from antibodies against extracellular matrix and house-keeping proteins by absorption to rat liver acetone powder. These antibodies bind to the respective proteins in the extract, thus can be removed from the crude serum by centrifugation. Subsequently, the serum was loaded to a superdex 200 column to separate the serum proteins by their molecular weight. This step is essential not for the specificity but for the reactivity of the gained antibody. IgMs can bind fast to the antigen and compete with the IgGs for binding sides. However, due to their low affinity, IgMs dissociate fast in the following washing steps. Therefore, they cannot be visualized, leading to a loss of the specific signal. The pentameric IgMs are much larger than the IgGs, thus can be excluded from the serum by pooling the appropriate later fractions. Figure 3.5 illustrates the total protein amount of each fraction (blue line) and the specific anti-TASK-3 activity of chosen fractions as determined in an ELISA (red line). Based on the two curves, fractions 31 to 40 were pooled for further purification.

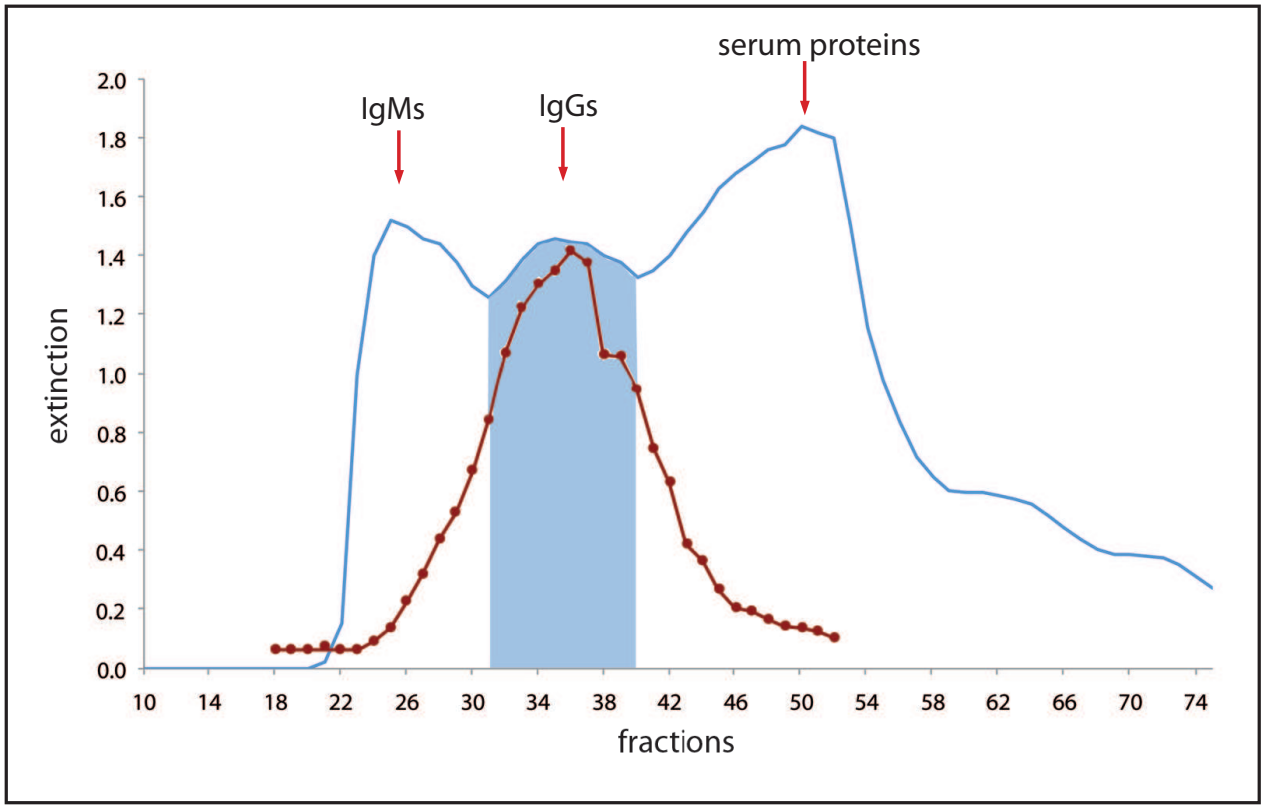

Figure 3.5 – Removal of IgM antibodies by serum separation on a superdex 200 column. 2 ml of the serum were separated on a superdex 200 column. The blue line delineates the protein concentration of the fractions (E_{280}). IgMs are contained in the early fractions corresponding to the first peak. The red line represents the specific immunoreactivity of chosen fractions against the recombinant protein TASK3-6HisTR (checked in an ELISA). The colored area under the curve indicates the fractions pooled for further purification, corresponding to the second peak of the blue curve (F31-F40).

3.2.2 Removal of anti-GST-activity

The rabbits were immunized with a recombinant protein consisting of a TASK-3 fragment and the carrier protein gluthation-S-tranferase (GST). Consequently, besides antibodies against TASK-3 the

serum pool contains antibodies against GST. These antibodies were removed from the serum by absorption to autoclaved and fixed bacterial pellets from *E. coli* BL21DE3 cells over-expressing the GST protein. In a pilot experiment the amounts of pellet per serum sufficient for removal of the anti-GST-activity were determined (see Fig. 3.6). Absorption to the bacterial pellets caused a decrease of the anti-GST-activity in a concentration dependent manner with only minor changes when more than 4 mg bacterial pellet per 100 μl serum were used. The specific activity against TASK-3 was not affected. Finally, 4 mg bacterial pellet per 100 μl serum were used for bulk absorption.

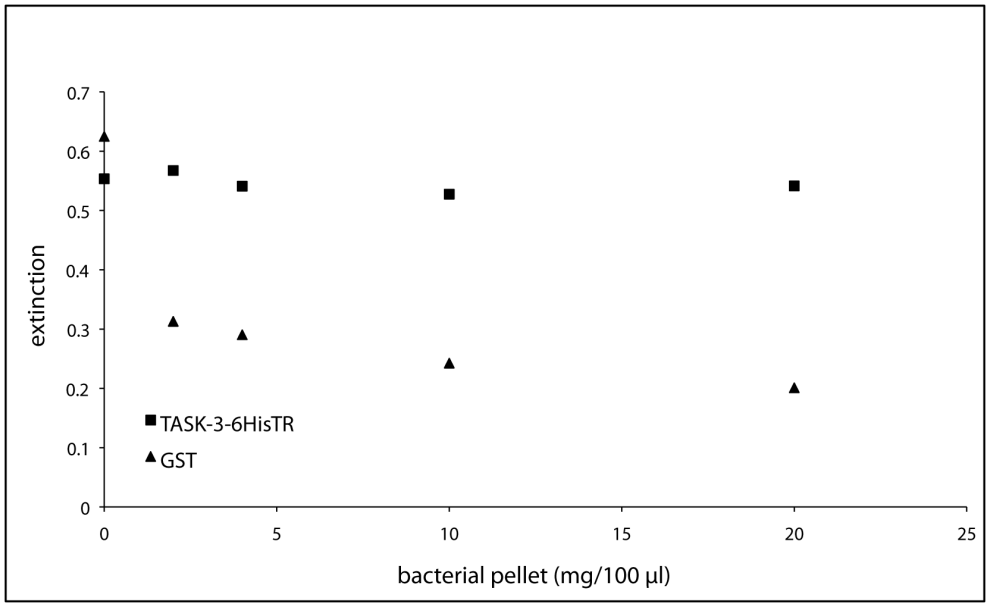

Figure 3.6 – Removal of anti-GST activity. The superdex pool was absorbed to varying amounts of autoclaved and fixated bacterial pellets from *E.coli* BL21DE3 over-expressing the GST protein. Following centrifugation, the anti-GST- and anti-TASK-3-6HisTR-reactivity were determined in an ELISA. Absorption to the bacterial pellet caused a considerable decrease of the immunoreactivity against GST with only minor changes when higher pellet amounts ($\geq$ 4 mg/100 μl) were used. The specific anti-TASK-3 activity was not affected by this procedure. Note that different serum dilutions were chosen for TASK-3-6HisTR (1:10,000) and GST (1:2000).

3.2.3 Preparation of monospecific antibodies

The aim of the next purification step was to remove cross reactivities against paralogous proteins. First, the activity of the serum pool against various K_{2P} proteins was determined in an ELISA (Fig. 3.7). Beside the closely related TASK-1 and TASK-5, sharing strong homology with TASK-3, C-terminal fragments of two other members of the K_{2P} family, THIK-1 and THIK-2, were tested. Additionally, the reactivity against the carrier protein GST was determined. The serum exhibited a remaining reactivity against GST and a considerable reactivity against TASK-1-GST. There was only marginal reactivity against the other 6HisTR fusion proteins; highest reactivities were observed against TASK-1- and TASK-5-6HisTR. The removal of cross reactivities was performed in two steps with two different proteins: in a first step with TASK-1-GST and in a second step with TASK-5-6HisTR. This enabled us not only to remove antibodies against the paralogous TASK-1 and TASK-5 proteins, but also remaining activity against the carrier protein GST. Thereafter, pure monospecific antibodies were obtained by affinity purification.

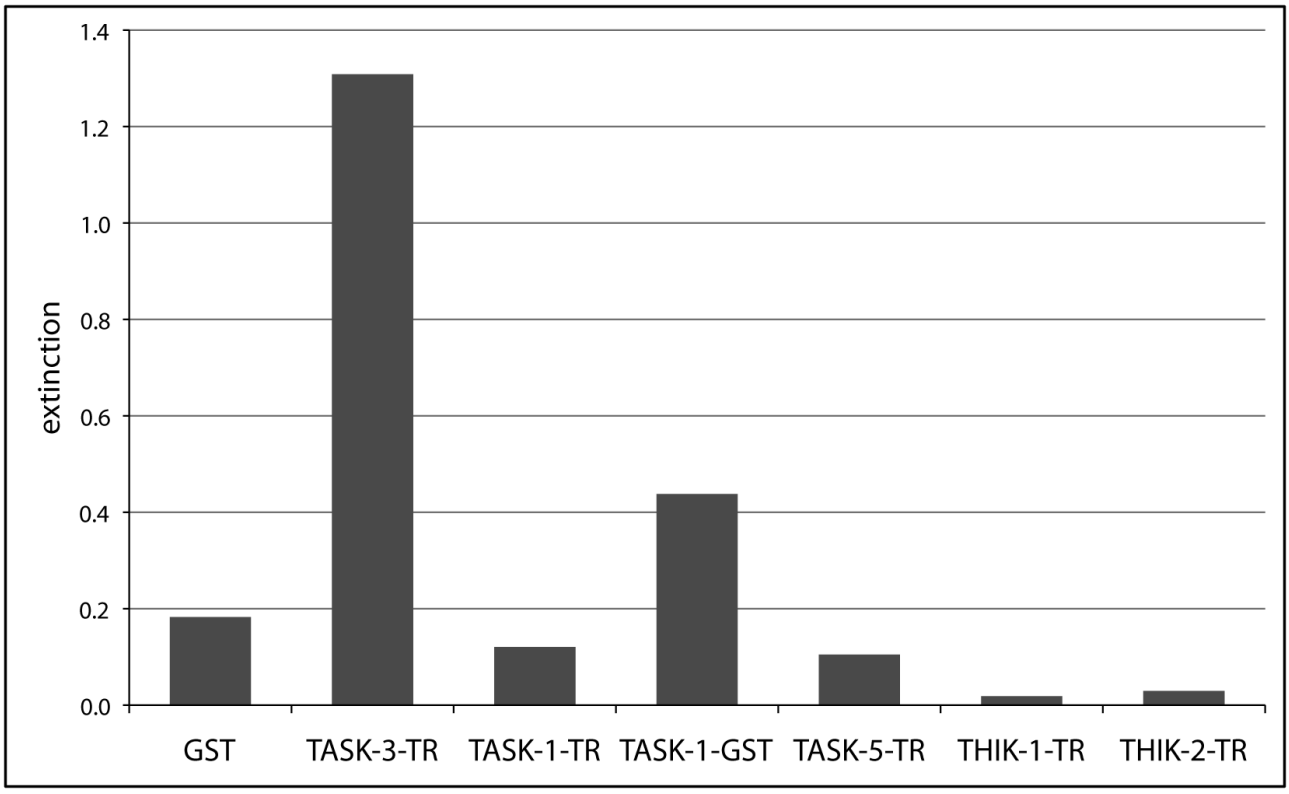

Figure 3.7 – Cross reactivity of the serum pool after absorption to bacterial pellets. An ELISA plate was coated with GST, TASK-3-6HisTR, TASK-1-6HisTR, TASK-1-GST and TASK-5-, THIK-1-, and THIK-2-6HisTR and then incubated with the serum to determine the corresponding immunoreactivities. Beside the specific reactivity against TASK-3-6HisTR highest cross reactivity was observed against GST and TASK-1-GST. Minor reactivities were detected against TASK-1- and TASK-5-6HisTR. Immunoreactivity against proteins of the THIK family was only marginal.

3.2.4 Comparison of the two antibodies gained from immunization of the two rabbits

Purified antibodies were obtained from two animals (serum1, s1 antibody; serum 2, s2 antibody). Subsequently, the antibodies were characterized to compare them with regard to sensitivity and specificity.

A western blot with the recombinant TASK-6HisTR fusion proteins and the carrier proteins 6HisTR and GST confirmed that both antibodies recognize the recombinant TASK-3-6HisTR protein. Though, when membranes were loaded with high amounts of protein the s1 serum exhibited cross reactivity against TASK-1-6HisTR, GST and particularly TR (Fig. 3.8, serum 1). The s2 antibody specifically recognized the TASK-3-6HisTR protein, showing no cross reactivities (Fig. 3.8, serum 2). Furthermore, in an immunocytochemical analysis of rat brain sections preincubation with the specific antigen (TASK-3-GST) blocked the immunosignal of the s2 antibody, but not the signal of the s1 antibody (not shown). Consequently, the s2 antibody was selected for all further experiments.

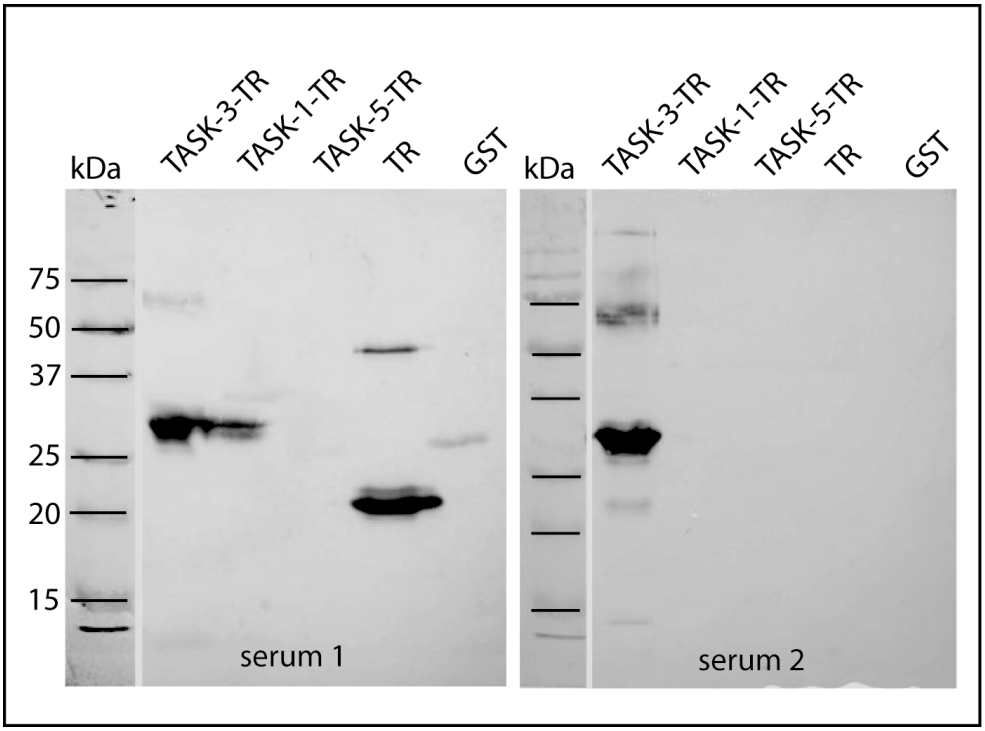

Figure 3.8 – Comparison of TASK-3 antibodies purified from the sera (s1 and s2) of two animals. In a western blot with recombinant proteins (5 μg/ml each) both antibodies recognized a band around 28 kDa, close to the predicted molecular weight of TASK-3-6HisTR (26.7 kDa). A second band is visible at around 60 kDa, presumably corresponding to a dimer. While the s2 antibody exposed no cross reactivities, the s1 antibody revealed additional immunoreactive bands for TASK-1-6HisTR, TR and GST. Marker dual color (Bio-Rad) is indicated.

3.3 Characterization of the TASK-3 antibody

After the removal of cross reactivity and affinity purification, a set of experiments was performed to characterize the respective polyclonal TASK-3 antibody as monospecific. These experiments comprised ELISA and western blot analyses and immunocytochemical experiments on rat brain sections.

3.3.1 Competitive ELISA

First, a competitive ELISA was performed. The purified monospecific antibody was preincubated with varying concentrations (from 1 ng/ml to 10 μg/ml) of the competitive TASK-6HisTR proteins or the GST protein before testing it in an ELISA against TASK-3-6HisTR. Only incubation with the cognate TASK-3-6HisTR decreased the immunosignal in a concentration-dependent manner (Fig. 3.9). Preincubation with GST, TASK-1- or TASK-5-6HisTR had no effect, indicating that the antibody does not recognize and bind to these proteins.

3.3.2 Western blot analyses

In a next step two different western blots demonstrated that the anti-TASK-3 antibody specifically recognizes the TASK-3 fusion proteins and the native TASK-3 protein and no other proteins.

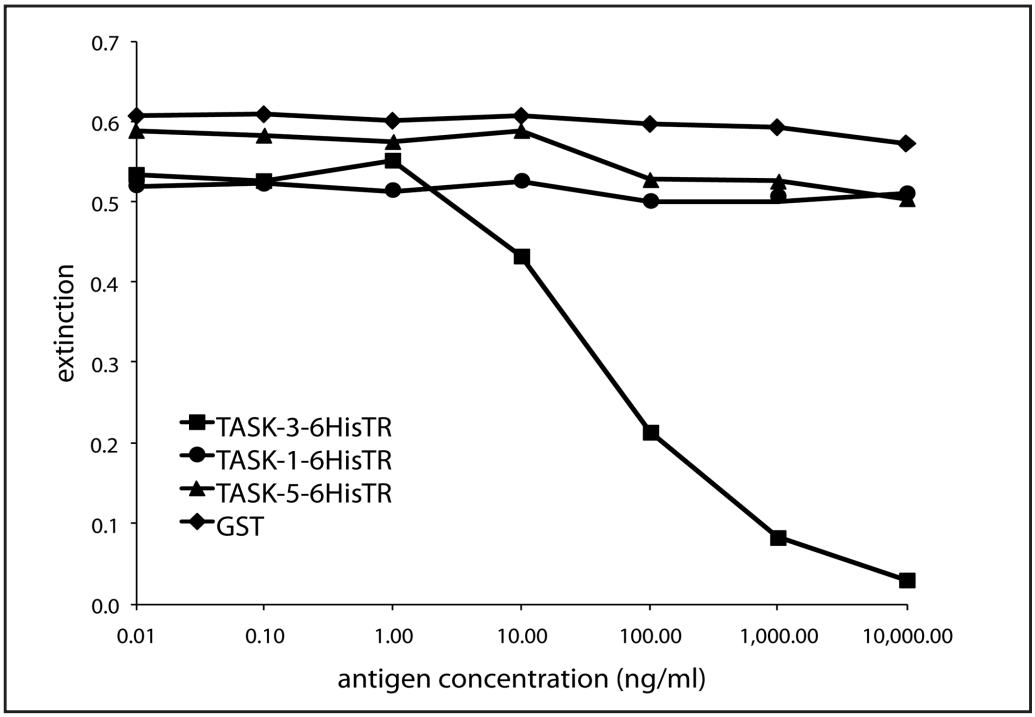

Figure 3.9 – Competitive ELISA. Microtiter plates were coated with TASK-3-6HisTR and the anti-TASK-3 antibody was preincubated with varying amounts of the specific antigen and the recombinant TASK-1-6HisTR, TASK-5-6HisTR and GST proteins. Only incubation with the cognate antigen (TASK-3-6HisTR) decreased the immunoreactivity in a concentration-dependent manner. Incubation with the other proteins had no effect.

Western blot analysis of recombinant proteins A western blot analysis with recombinant 6HisTR fusion proteins confirmed that the antibody only detects the cognate TASK-3-6HisTR fusion protein (Fig. 3.10). The respective 6HisTR fusion proteins were loaded on a gel. Following electrophoresis and blotting the antibody revealed a strong band around 28 kDa, close to the predicted molecular weight of TASK-3-6HisTR (26.7 kDa). A second faint band is visible around 60 kDa, presumably corresponding to a dimer. The paralogous TASK-1- and TASK-5-6HisTR proteins displayed no immunosignal, indicating that the antibody did not recognize them. Furthermore, incubation with 50 μg/ml of the recombinant TASK-3-6HisTR protein completely blocked the TASK-3 specific immunoreactivity.

Western blot analysis of rat brain membrane fractions Western blot analyses of rat brain membrane fractions illustrated that the anti-TASK-3 antibody specifically recognizes the actual TASK-3 protein. Isolated rat cerebellum and forebrain membrane fractions were loaded on a gel, electrophoretically separated and blotted. The antibody only detected a single band at about 45 kDa (Fig. 3.11A) in accordance with the predicted molecular weight of the native TASK-3 channel protein of 44.4 kDa. This experiment supports the specificity of the antibody, as well as the expression of TASK-3 in the rat brain. Once again incubation with the recombinant TASK-3-6HisTR protein completely blocked the specific immunoreaction of both membrane fractions (Fig. 3.11B). Furthermore, anti-TASK-3 recognized a single band with the expected molecular weight (45 kDa) in a western blot of mouse brain membrane fractions (Fig. 3.11C). This is not surprising, as the orthologous rat and mouse TASK-3 proteins share about 90% amino acid identity.

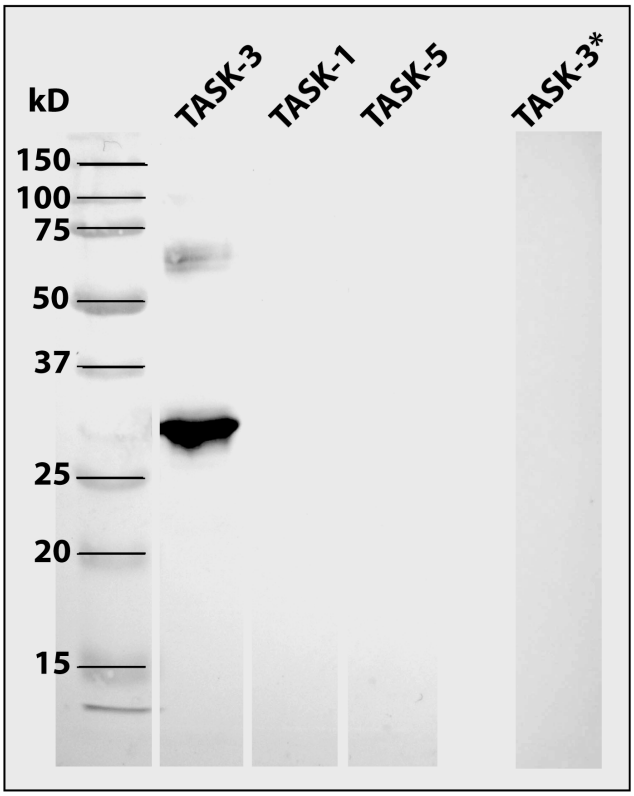

Figure 3.10 – Western blot analysis of the anti-TASK-3 antibody using recombinant TASK-1-, TASK - 3-, and TASK-5-6HisTR fusion proteins. The gel was loaded with the respective recombinant proteins (5 μg/lane). After electrophoresis and blotting the anti-TASK-3 antibody detected a strong band about 28 kDa, close to the predicted molecular weight of the TASK-3-6HisTR protein (26.7 kDa). A second faint band is visible at around 60 kDa, presumably corresponding to a dimer. The antibody did not recognize the paralogous TASK-1- and TASK-5-6HisTR proteins. The TASK-3-specific immunoreactivity was completely blocked by preincubation with 50 μg/ml of the TASK-3-6HisTR protein (outer right lane). Marker dual color (Bio-Rad) is indicated (outer left lane).

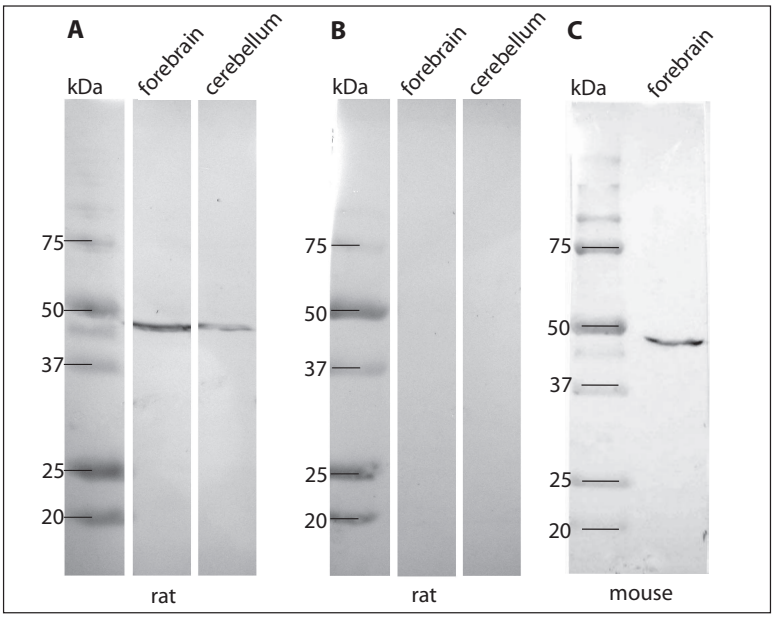

Figure 3.11 – Western blot analysis of brain membrane fractions with the anti-TASK-3 antibody. The gel was loaded with rat cerebellum and forebrain membrane fractions or mouse whole brain membrane fractions (150 μg). Following electrophoresis and blotting, the anti-TASK-3 antibody revealed a single band around 45 kDa, corresponding to the calculated molecular weight of the rat TASK-3 channel protein (A, 44.4 kDa). Preincubation with TASK-3-6HisTR completely blocked the specific immunoreaction in both membrane fractions (B). In a western blot of mouse membrane fractions the anti-TASK-3 antibody also detected a single band of the correct size (C, about 45 kDa).

3.3.3 Blockade of immunostaining of rat brain sections

Together with the competitive ELISA, the staining of single bands of the correct size in western blots indicates that the purified TASK-3 antibody is monospecific. To verify this assumption, the antibody was tested on rat brain sections and the specific signal was blocked by incubation with TASK-3-GST. Immunocytochemistry on rat brain sections revealed a widespread distribution of TASK-3. Among other neurons, staining was especially strong in neurons of the dorsal raphe. Incubation with varying amounts of TASK-3-GST blocked the immunostaining in a concentration dependent manner (Fig. 3.12). A complete block of the immunosignal was achieved by incubation with 10 μg/ml TASK-3-GST, incubation with lower protein concentrations led to a marked decrease, but failed to completely block the immunosignal. Incubation with higher protein amounts (20 μg/ml) led to anew increase of the immunosignal, presumably caused by the formation of soluble antibody-antigen-complexes.

3.4 Distribution of TASK-3 in the rat brain

Previously, *in situ* hybridization analyses of two different groups revealed a widespread distribution of TASK-3 mRNA throughout the rat brain [Karschin et al., 2001, Talley et al., 2001]. The western blot analysis of rat brain membrane fractions confirmed the expression of the TASK-3 protein in the rat brain. Accordingly, immunocytochemistry on rat brain sections with the anti-TASK-3 antibody demonstrated a widespread distribution of the TASK-3 channel protein. Immunocytochemical staining with anti-TASK-3 of different brain sections revealed positive neurons in all areas examined, including neurons in the forebrain, midbrain, hindbrain, brainstem, cerebellum and medulla oblongata. In table 1 all examined nuclei are listed and the corresponding expression strength of TASK-3 is indicated. Some areas displayed considerable staining of the neuropil (indicated in tabel 1), this was most obvious for the central grey, the dentate gyrus, the superficial grey layer of the superior colliculi and the substantia nigra pars reticulata. Results are compared with the data of Karschin et al. [2001] and Talley et al. [2001] that were gained by *in situ* hybridization experiments.The comparison shows no apparent differences in the expression of the TASK-3 protein and TASK-3 mRNA.
At a first glance, all neurons appear to be positive for TASK-3. However, intensity of the immunosignal greatly varied between different neurons, with some neurons showing strong immunoreactivity and others displaying intermediate or only weak TASK-3 expression. Furthermore, detailed analyses using a counter-staining with methyl green revealed neurons without TASK-3 immunoreactivity, as shown here for sections of the basal forebrain (Fig. 3.13). Methyl green labels all nuclei, therefore also revealing the cells without immunoreactivity against anti-TASK-3.

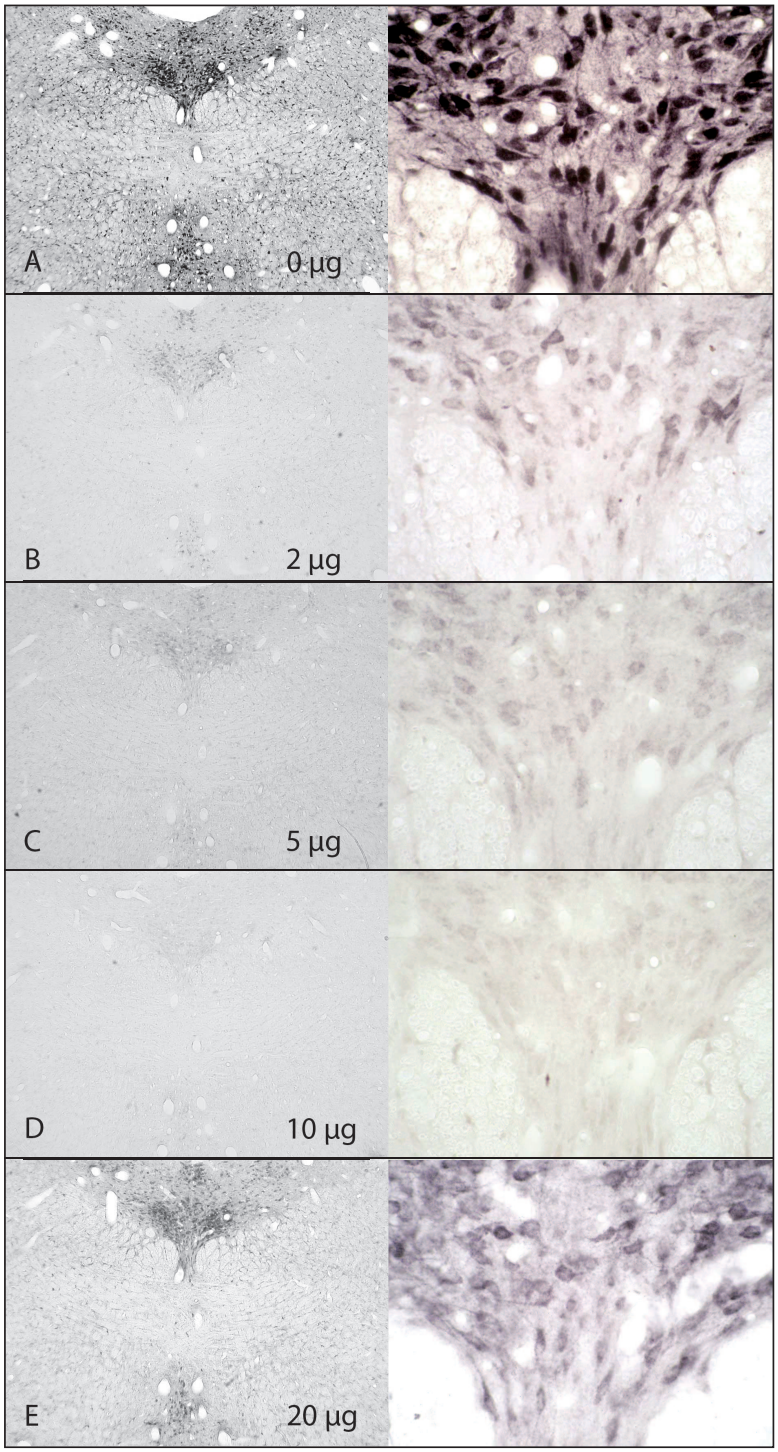

Figure 3.12 – Block of anti-TASK-3 immunoreactivity by incubation with varying amounts of TASK-3-GST. (A) Immunocytochemistry on rat midbrain sections with the anti-TASK-3 antibody reveals strong immunoreactivity of dorsal raphe neurons. (B)-(E) Incubation of the antibody with varying amounts of TASK-3-GST decreased the immunostaining in a concentration dependent manner. Incubation with 10 μg/ml caused a complete loss of the specific signal (D), while incubation with higher or minor TASK-3-GST amounts failed to completely block the signal ((B),(C), and (E))

Table 3.1 – Distribution of TASK-3 in the rat brain. Expression of TASK-3 in the rat brain as obtained by immunocytochemistry with the TASK-3 antibody on rat brain sections. Areas showing strong staining of the neuropil are indicated. Results are compared with the data of Karschin et al, 2001 and Talley, et al. 2001 gained by *in situ* hybridization experiments. Expression strength is indicated by the number of +; -, no expression; n.e., not examined; Ch, only cholinergic neurons labeled

	cell bodies	neuropil	Talley	Karschin
Bulbus olfactorius	+++		++	+++
Neocortex	+/++/+++		++	++
Hippocampus				
CA1	++		++	+
CA2	++		+	n.e.
CA3	++		-/++	+/-
Dentate gyrus	+++	+	+	+/++++
Basal forebrain				
Caudate putamen	+, few +++	+	-/++++	Ch
Accumbens nucleus	++		n.e.	n.e.
Globus pallidus	+		+/++	Ch
Basal nucleus of Meynert	+++		n.e.	Ch
Ventral pallidum	+, few+++		n.e.	n.e.
Island of Calleja	-/+		n.e.	n.e.
Septohippocampal nucleus	++		n.e.	n.e.
Tenia tecta	+++		n.e.	n.e.
Indusium griseum	++		n.e.	n.e.
Lateral septal nucleus	++		n.e.	+++
Medial septal nucleus	+++		n.e.	Few +++
Diagonal band	+, few+++		+/++	Few +++
Bed nucleus stria terminalis	++		++++	+++
Central amygdaloid ncl.	++	+	+	+/-
Basolateral amygdaloid ncl.	++		+	+++
Hypothalamus				
Preoptic nucleus	+++		+++	+++
Supraoptic nucleus	+++		n.e.	n.e.
Anterior hypoth. area	+		n.e.	n.e.
Lateral hypoth. area	++		n.e.	n.e.
Ventromedial hypoth. ncl.	++		+++++	++
Arcuate hypoth. nucleus	+, few+++		++++	+++
Periventricular hypoth. ncl.	++/+++		++	+++
Dorsomedial hypoth. ncl.	++		++	+++
Ventral tuberomammillary ncl.	++/+++		n.e.	n.e.
Dorsal tuberomammillary ncl.	++		n.e.	n.e.
Lateral mammillary ncl.	++/+++		+++/++++	+++

	cell bodies	neuropil	Talley	Karschin
Medial mammillary ncl.	++		+++/++++	+++
Medial habenula	+/++		+/++	n.e.
Lateral habenula	+/++		+/++	n.e.
Thalamus				
Central thalamic ncl.	++		n.e.	n.e
Intermedial thalamic ncl.	++/+++		n.e.	n.e.
Anteroventral thalamic ncl.	++/+++	+	n.e.	+++
Anterodorsal thalamic ncl.	+++	+	n.e.	++++
Reticular thalamic ncl.	++/+++		n.e.	n.e.
Anteromedial thalamic ncl.	++		n.e.	n.e.
Paraventricular thalamic ncl.	++		n.e.	+/-
Entopeduncular ncl.	++		n.e.	n.e.
Lateral geniculate ncl.	++	+	n.e.	+++
Medial geniculate ncl.	++		n.e.	+
Laterodorsal thalamic ncl.	+/++		n.e.	+++
Midbrain, brainstem				
Superior colliculus	++	+	+	+
Substantia nigra, reticulata	+	+	-	-
Substantia nigra, compacta	-/+		-	Few '++
VTA	+, few +++		n.e.	Few +++
Edinger-Westphal nucleus	+++		n.e.	n.e.
Caudal linear raphe	++		n.e.	n.e.
Red nucleus	++		+++	++
Interpeduncular nucleus	+++		+++	+++
Interstitial nucleus	++		n.e.	n.e.
Oculomotor nucleus	++++		+++++	++++
Central gray, dorsal	++/+++	+	n.e.	n.e.
Trochlear nucleus	+++		+++++	++++
Dorsal raphe	++++		+++	++++
Median raphe	+++		n.e.	n.e.
Pontine nuclei	++		+++	++
Pedunculopontine tegment. ncl.	++		n.e.	+++
Ventral tegmental nucleus	++		n.e.	n.e.
Dorsal tegemental nucleus	+		n.e.	n.e.
Motor trigeminal nucleus	++++		n.e.	n.e.
Locus coeruleus	++++		+++++	++
Central grey, pons	++	+	n.e.	n.e.
Raphe pontis	+++		n.e.	n.e.
Raphe magnus	++/+++		n.e.	n.e.
Trapezoid body	++/+++		n.e.	n.e.

	cell bodies	neuropil	Talley	Karschin
Mesencephalic trigeminal ncl.	-/+		n.e.	-
Superior olivary nuclei	++/+++		n.e.	n.e.
Abducens nucleus	+++		+++++	++++
Accessory facial nucleus	++++		n.e.	n.e.
Facial nucleus	++++		+++++	++++
Vestibular nucleus	++	+	+	+/few++
Cerebellum				
Molecular layer	++	+	n.e.	-
Purkinje cells	-/+		n.e.	-
Granule cell layer	++		+++++	++
Medulla/ and spinal cord				
Raphe pallidus	++		n.e.	n.e.
Spinal trigeminal nucleus	++	+	++	++
Nucleus solitary tract	++	+	++++	n.e.
Ventral cochlear nucleus	++	+	++	+/++
Ambiguus nucleus	++++		+++++	++++
Inferior olivary nuclei	++/+++	+	n.e.	n.e.
Hypoglossal nucleus	++++		+++++	++++
Dorsal vagal motoneurons	+++		n.e.	n.e.
Cuneate nucleus	++	+	n.e.	n.e.
Gracile nucleus	++	+	n.e.	n.e.
Raphe obscurus	++		n.e.	n.e.
Nucleus solitary tract	++		n.e.	n.e.
Spinal motoneurons	++++		+++++	++++

Immunocytochemistry with the anti-TASK-3 antibody detected immunoreactive neurons in all forebrain areas (Fig. 3.13B). However, a closer look demonstrated marked differences in the intensity of the immunosignal between the neurons, as apparent from staining of the ventral pallidum and the cortex (see Fig. 3.13CE). Analysis at higher magnification following counter-staining with methyl green shows that most neurons from the Island of Calleja are free from staining or display staining intensity near to background (indicated by dashed lines in Fig. 3.13D). Other adjacent neurons in the ventral striatum also display no TASK-3 immunoreactivity (indicated by red arrows in Fig. 3.13D). Detection of TASK-3 in the forelimb area of the cortex reveals differences in the staining intensity of neurons; some neurons strongly express TASK-3, while others demonstrate intermediate, weak or no TASK-3 immunosignal (see Fig. 3.13E, red arrows mark negative cells). In addition, endothelial and glial cells were devoid of staining. It can be concluded that TASK-3 is widely distributed, but displays a diverse and not ubiquitous expression in the brain.

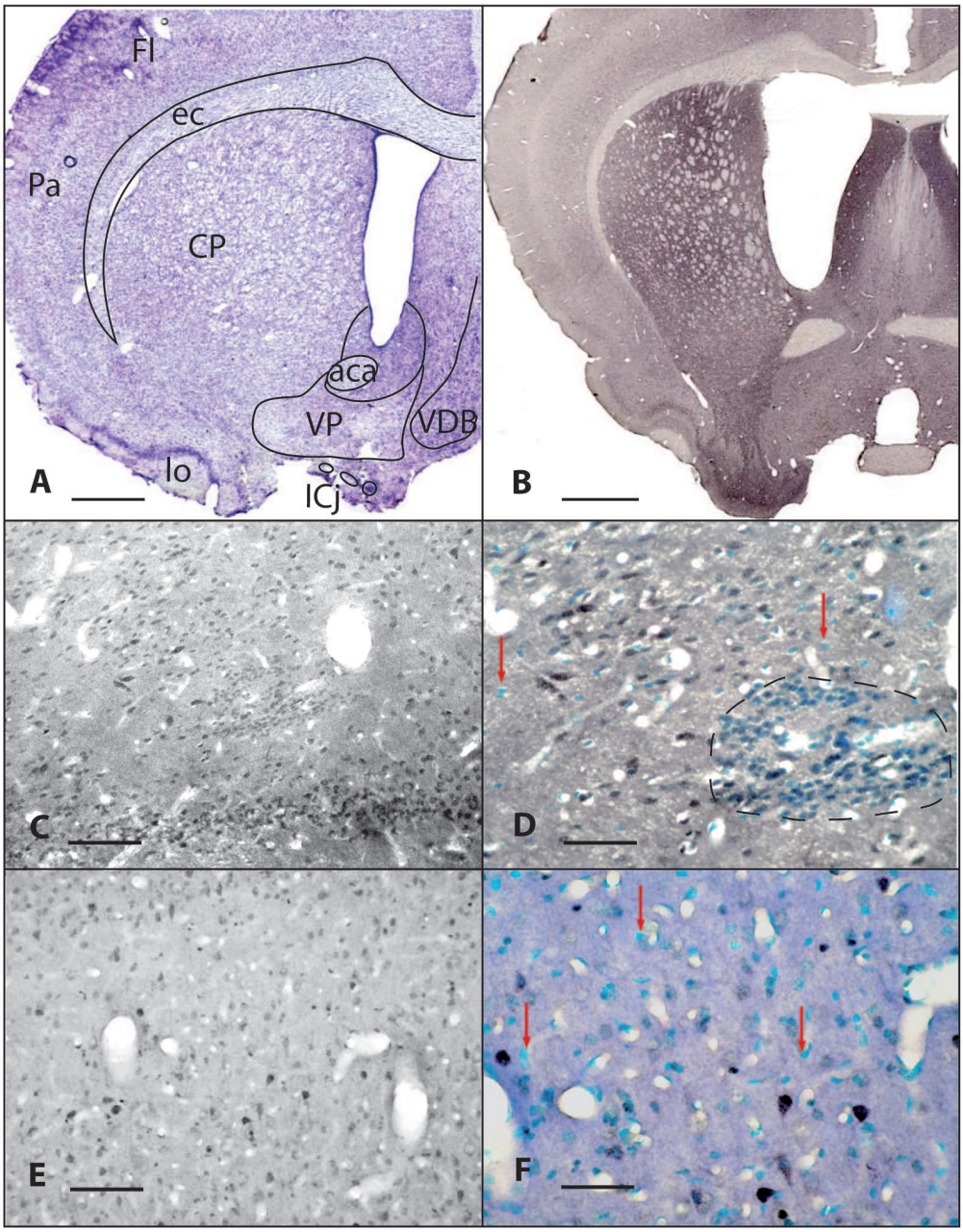

Figure 3.13 – Immunocytochemistry of rat forebrain sections reveals a widespread but not ubiquitous distribution of TASK-3 immunoreactivity. A cresyl violet staining illsutrates the region of the basal forebrain (A). Immunocytochemistry of forebrain sections demonstrates a widespread expression of TASK-3 (B). A closer look reveals clear differences in the staining intensity between different neurons in the ventral pallidum (C). Counter-staining with methyl green detected neurons absent of TASK3 immunoreactivity (red arrows in (D)). Especially, most neurons of the Island of Calleja are not labeled (dashed line). The forelimb area of the cortex also displays strong and weak TASK-3 immunoreactive neurons (E). Methyl green also staining reveals TASK-3-negative cells (red arrows in (F)). Abbreviations: aca, anterior commissure, anterior; CP, caudate putamen; ec, external capsule; Fb, forelimb area of the cortex; ICj, island of Calleja; lo, lateral olfactory tract; Par, parietal cortex; VDB, nucleus vertical limb diagonal band. Bar represent 1 mm in (A), and (B), 50 μm in (E), and 20 μm in (C), (D), and (F).

3.5 TASK-3 expression in neurons of the monoaminergic and cholinergic system

Several reports described that TASK-3, or at least TASK-3 mRNA, is widely distributed throughout the brain. This was also confirmed by immunocytochemistry with our TASK-3 antibody on rat brain sections. However, staining intensity varied between different brain regions, and some nuclei or neurons showed conspicuous strong TASK-3 expression. Karschin et al. [2001] found high levels of TASK-3 mRNA in cholinergic motoneurons and several other cholinergic neurons. *In situ* hybridization experiments also revealed high levels of TASK-3 mRNA in neurons of the raphe and the locus coeruleus [Karschin et al., 2001, Talley et al., 2001, Washburn et al., 2002]. First immunocytochemical experiments with the anti-TASK-3 antibody confirmed these results. Therefore, in this work the focus was set on the expression of TASK-3 in cholinergic and monoaminergic neurons. In addition to serotoninergic raphe neurons and noradrenergic locus coeruleus neurons I focused on histaminergic neurons of the tuberomammillary nucleus and dopaminergic neurons of the ventral tegmental area and the substantia nigra pars compacta. Analysis of the cholinergic system comprised motoneurons of cranial nerve nuclei and spinal cord and neurons of the basal nucleus of Meynert as well as striatal interneurons.

3.5.1 TASK-3 is strongly expressed in cholinergic motoneurons

The output of the central nervous system (CNS) is manifested by a motor behavior, which implies the contraction of muscles. Motoneurons in the CNS sending their axons to muscles or glandular tissues in the periphery provide a link between these two systems. Cranial and spinal α-motoneurons directly innervating muscles and therefore initiating their contraction, are among the largest neurons in the CNS with diameters up to 50 μm. All vertebrate motoneurons release the neurotransmitter acetylcholine (cholinergic neurons) and can be identified using antibodies against the vesicular acetylcholine transporter (anti-vAChT) or choline acetyl transferase (anti-ChAT), the enzyme catalyzing the transfer of the acetyl group of acetyl CoA to choline. All analyzed motoneurons showed strong to very strong TASK-3 expression.

The four nuclei of the oculomotor complex are located in the midline of the midbrain and pons [Büttner-Ennever and Büttner, 1992]. The oculomotor nucleus is located in the midbrain in the ventral part of the aqueductal grey. Its neurons innervate the external eye muscles except the superior oblique and lateral rectus muscle. The somatic motoneurons exhibit strong TASK-3 expression, with a clear somatodendritic distribution of the channel (Fig. 3.14BC). Neurons of the accessory oculomotor nucleus (Edinger-Westphal nucleus) lay just rostral to the oculomotor nucleus at the level of the superior colliculi. They send parasymphatetic fibers to the eyes that mediate the pupil reflex and lens accommodation. These neurons display a considerable strong TASK-3 immunoreactivity, but weaker as compared to somatic motoneurons (Fig. 3.14DE). In addition, *in situ* hybridization experiments with TASK-3 specific riboprobes detected TASK-3 mRNA in oculomotor neurons (shown for Edinger-Westphal nucleus, Fig. 3.14F). The superior oblique muscles are innervated by somatic motoneurons of the trochlear nucleus. This nucleus lays ventral to the aqueduct in the caudal midbrain at the level of the inferior colliculi. Trochlear neurons are strongly positive for TASK-3, the immunosignal

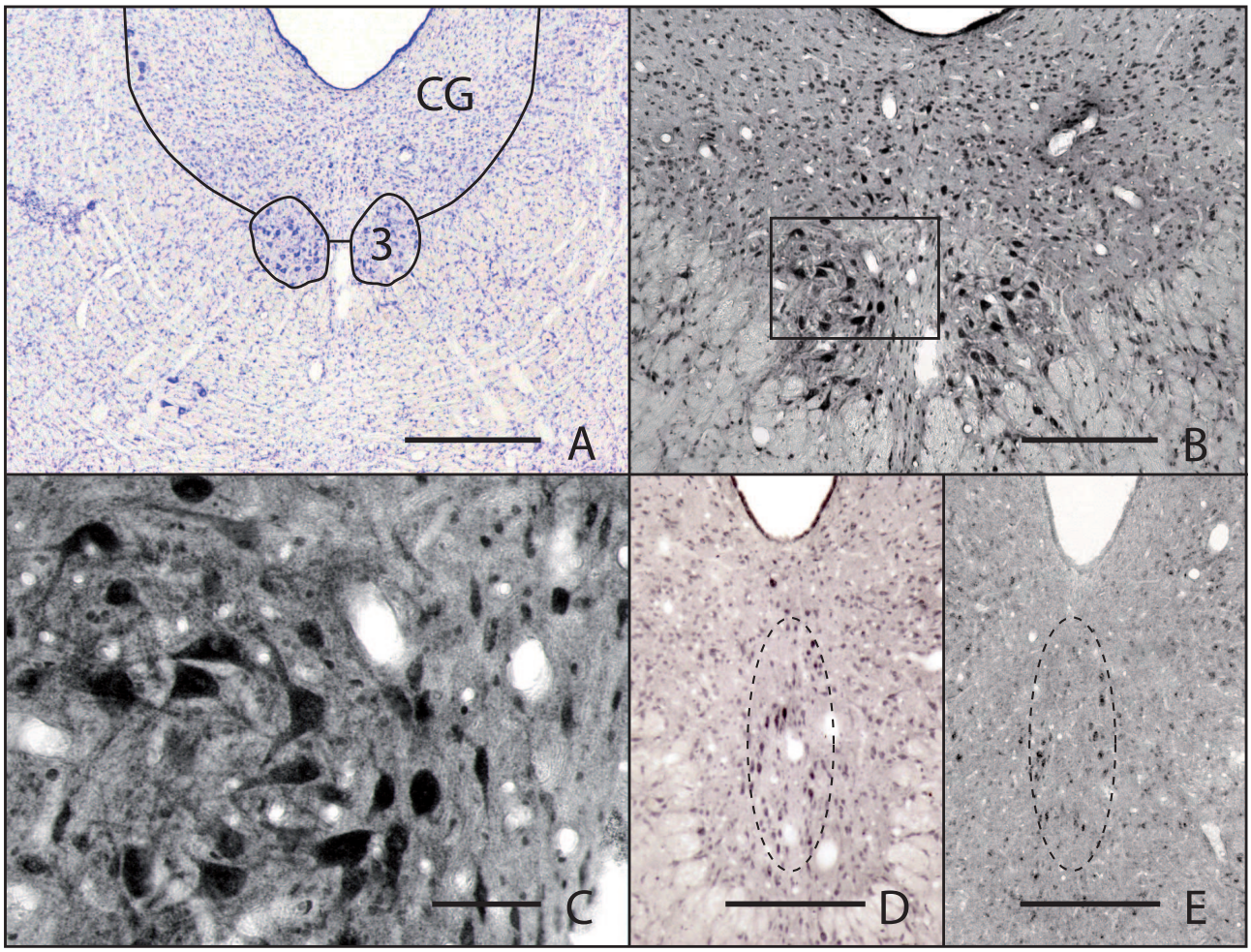

Figure 3.14 – TASK-3 expression in neurons of the oculomotor nucleus. Cresyl violet staining of a midbrain sections at the level of the superior colliculi reveals the somatic motoneurons of the oculomotor nucleus, located in the ventral part of the central grey (A). Immunolabeling with the anti-TASK-3 antibody demonstrates strong TASK-3 expression in these neurons (B). The immunosignal can be found in the somata and several dendrites (C). Neurons of the accessory oculomotor nucleus (Edinger-Westphal nucleus, indicated by the dashed line in D) that lay just rostral to the oculomotor nucleus display strong but comparably weaker TASK-3 immunoreactivity. TASK-3 presence in these neurons was supported by the detection of TASK-3 mRNA using TASK-3 specific riboprobes. Abbreviations: 3, oculomotor nucleus; CG, central grey; EW, Edinger-Westphal nucleus. Bar represent 1 mm in (A), 500 μm in (B), (D), (E), and 100 μm in (C).

is visible in somata and dendrites (Fig. 3.15BC). The fourth nucleus controlling eye movements is the abducens nucleus located in the caudal pons beneath the fourth ventricle. Its motoneurons innervate the lateral rectus muscle. Immunocytochemistry with the anti-TASK-3 antibody displays strong TASK-3 expression in abducens motoneurons (Fig. 3.15EF).

The motor nucleus of the trigeminal nerve (Mo5) is located in the lateral part of the pons, within the lateral portion of the pontine reticular nucleus (PRN). Beside the RPN it is flanked by the supratrigeminal nucleus and the motor root of the trigeminal nerve (see Fig. 3.24 for an cresyl violet stained overview of this region). Mo5 comprises branchial motoneurons that innervate the muscles of mastication. Immunocytochemical staining with anti-TASK-3 of the lateral pons shows that TASK-3 is very strongly expressed in these neurons (Fig. 3.16A) with a clearly somatodendritic distribution of the channel protein, as seen in a higher magnification (Fig. 3.16B). These findings were confirmed by the detection of TASK-3 mRNA using TASK-3 specific riboprobes (Fig. 3.16C). Immunofluorescence double-labeling with anti-TASK-3 and anti-vAChT antibodies supported the localization of TASK-3 in cholinergic neurons (Fig. 3.16D-E).

The nucleus of the facial nerve is located in the caudal part of the ventrolateral pontine tegmentum. The somatic motoneurons of the facial nucleus innervate the muscles of the facial expression and the stapedius muscle [Hinrichsen and Watson, 1984]. These neurons display very strong TASK-3 expression (Fig. 3.17B) with a somatodendritic distribution of the immunosignal (Fig. 3.17C). In addition, neurons of the accessory facial nucleus show strong TASK-3 immunoreactivity comparable to facial neurons. These neurons can be seen just dorsal to the main nucleus (Fig. 3.17B); they innervate the posterior belly of the digastric muscle [Hinrichsen and Watson, 1984].

The branchial motoneurons of the nucleus ambiguus lay in the rostral medulla oblongata dorsal to the inferior olivary nucleus. They innervate laryngeal and pharyngeal muscles through the vagus nerve and the glossopharyngeal nerve. Ambiguus neurons display strong TASK-3 immunoreactivity. A likewise strong TASK-3 expression and a clearly somatodendritic channel distribution can be seen in premotoneurons of the retroambiguus nucleus (Fig. 3.18CD). This nucleus is located in the caudal medulla and is important for the control of respiration and respiration related activities such as vocalization and vomiting [Subramanian and Holstege, 2009].

Furthermore, somatic motoneurons of the hypoglossal nucleus exhibit very strong TASK-3 expression (Fig. 3.19B). These neurons can be found in the medulla oblongata at the bottom of the fossa rhomboidea and innervate muscles of the tongue [Sawczuk and Mosier, 2001]. Immunocytochemistry with the anti-TASK-3 antibody revealed a localization of the channel to somata and dendrites (Fig. 3.19C). The dorsal vagal nucleus is located just ventral to the Nucleus nervi hypoglossi and contains visceral motoneurons that supply the internal organs [Jänig, 1996]. These neurons also present strong TASK-3 immunoreactivity (Fig. 3.19B). However, staining intensity is slightly weaker as compared to the hypoglossal motoneurons.

Finally, the motoneurons of the spinal cord display strong TASK-3 expression (shown for cervical spinal cord, Fig. 3.20B). Staining intensity is comparable to that of other somatic motoneurons with a clear labeling of somata and dendrites (Fig. 3.20C).

In summary, all examined motoneurons demonstrated strong TASK-3 expression. Highest TASK-3 levels can be found in trigeminal, hypoglossal, facial and ambiguus neurons. Ocuolomotor, trochlear,

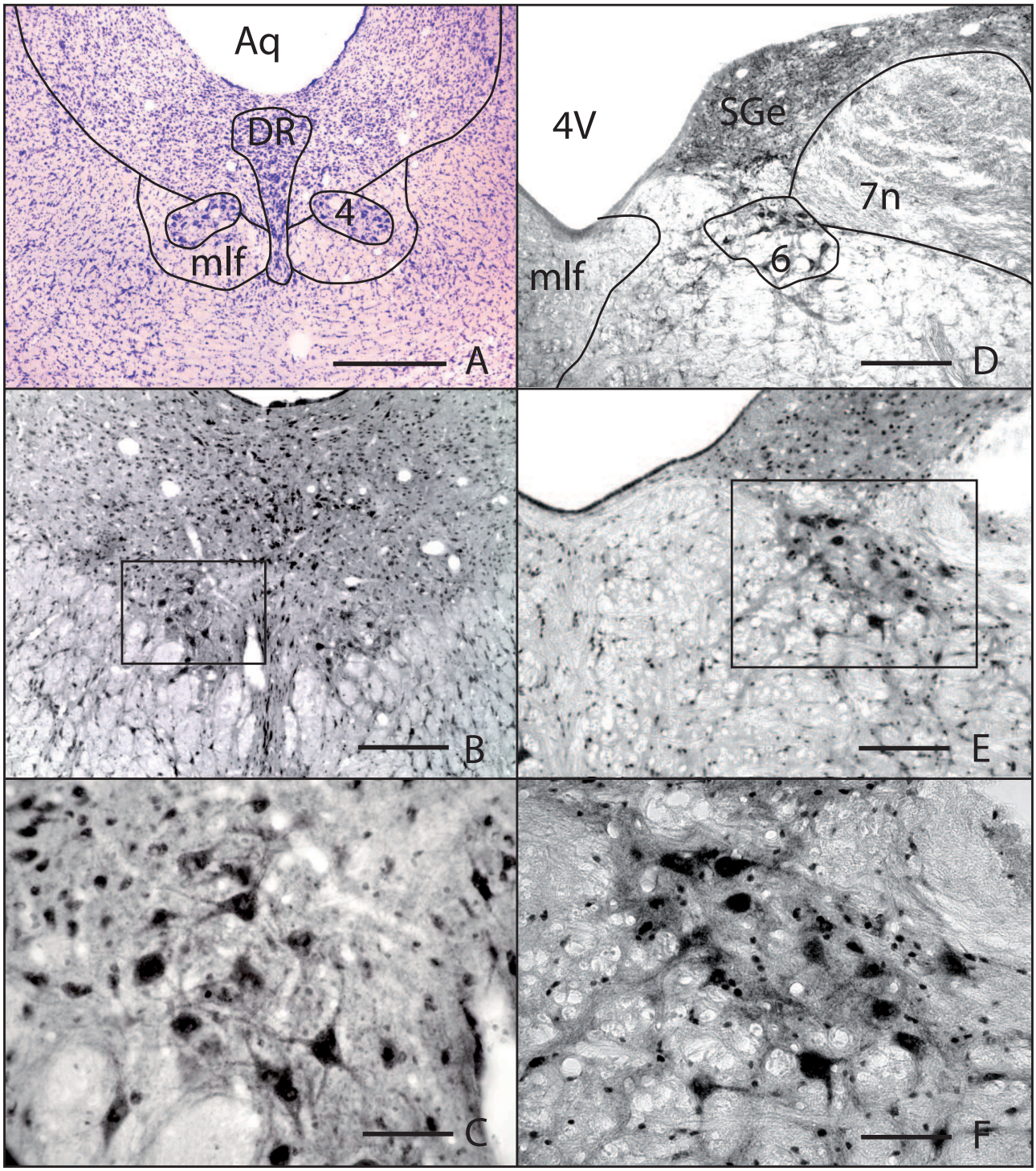

Figure 3.15 – Immunocytochemical detection of TASK-3 channels in trochlear and abducens nuclei. The trochlear nucleus is located in the caudal midbrain at the level of the inferior colliculi ventral to the aqueduct (see cresyl violet staining (A)). The anti-TASK-3 antibody detects high levels of the channel protein in trochlear motoneurons (B). Somata as well as dendrites demonstrate strong immunoreactivity (C). Motoneurons of the abducens nucleus lay in the caudal pons beneath the fourth ventricle and can be visualized with an anti-vAChT antibody (D). Using the anti-TASK-3 antibody, TASK-3 channels can be detected in these neurons (E). At higher magnification labeling of somata and dendrites is obvious (F). Abbreviations: 4, trochlear nucleus; 4V, 4th ventricle; 6, abducens nucleus; 7n, facial nerve; Aq, aqueduct; DR, dorsal raphe; mlf, medial longitudinal fasciculus. Bar represent 1 mm in (A), 400 μm in (D), and (B), 200 μm in (E), and 100 μm in (C), and (F).

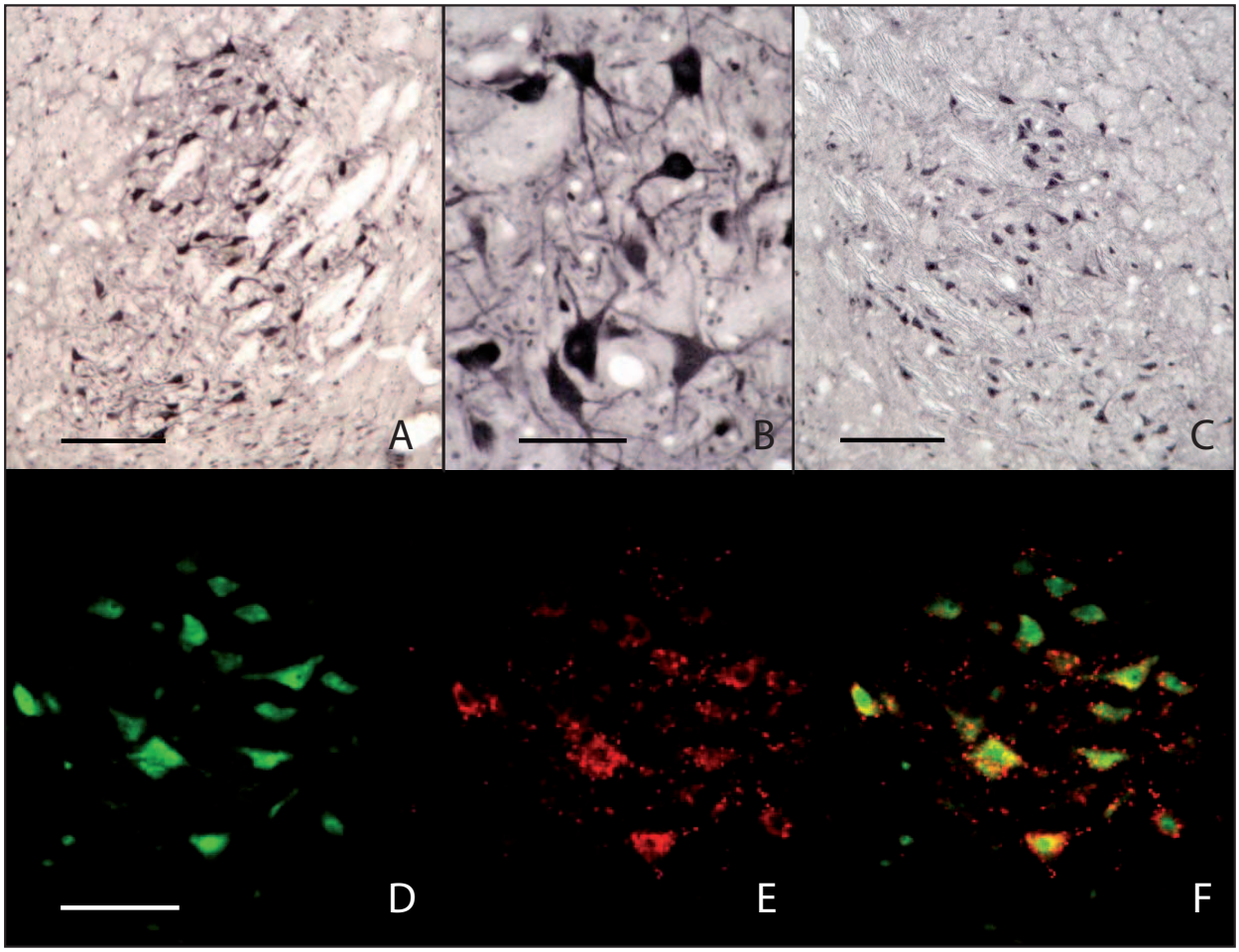

Figure 3.16 – TASK-3 is expressed in neurons of the trigeminal motor nucleus. The trigeminal motor nucleus can be found in the lateral part of the pons, ventrolateral to the locus coeruleus. Immunocytochemistry with the anti-TASK-3 antibody displays very strong TASK-3 expression in these large motoneurons (A). The immunosignal can be observed in the somata and several dendrites (B). Furthermore, the detection of TASK-3 mRNA supports the expression of the channels in Mo5 neurons (C). Immunofluorescence co-labeling with anti-TASK-3 (D, Cy2, green) and anti-vAChT (E, Cy3, red) antibodies confirmed the expression of TASK-3 in cholinergic neurons (overlay E, yellow). Bar represent 200 μm in (A), and (C), and 50 μm in (B), and (D)-(F).

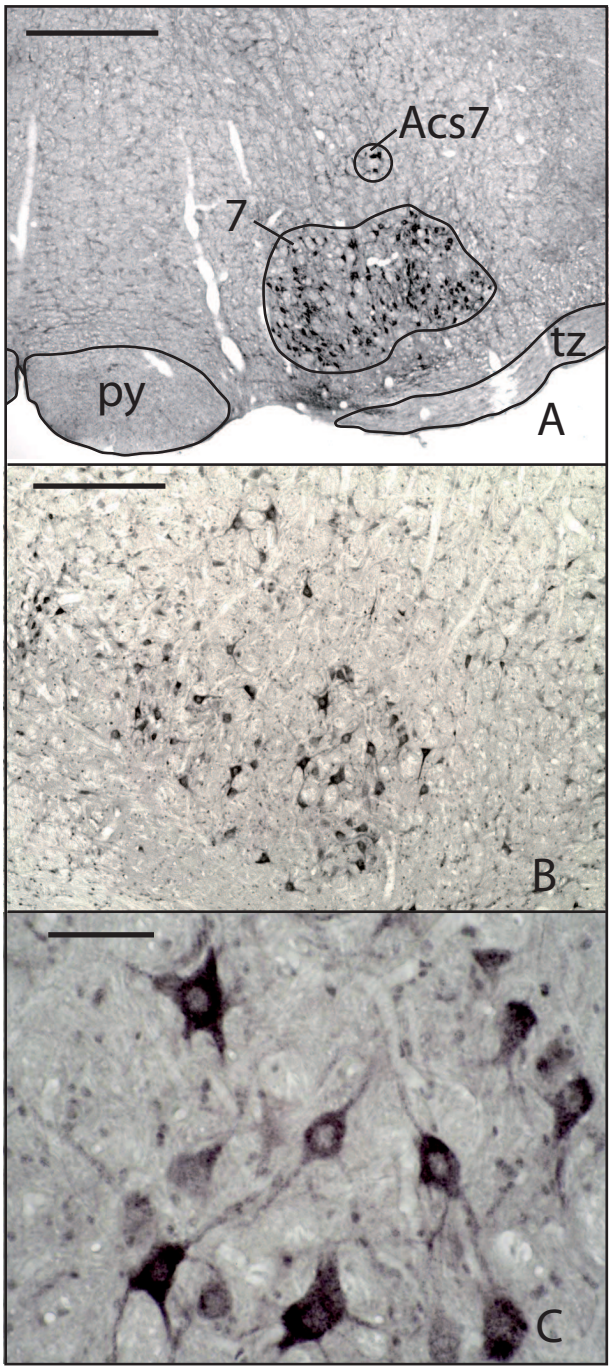

Figure 3.17 – Immunocytochemical staining of TASK-3 channels in motoneurons of the facial nucleus. The facial nucleus is located in the caudal part of the ventrolateral pontine tegmentum. The cholinergic motoneurons can be visualized with an anti-vAChT antibody (A). Immunocytochemistry with the anti-TASK-3 antibody demonstrates strong TASK-3 expression in neurons of the facial nucleus and adjacent neurons of the accessory facial nucleus (B). At higher magnification the localization of the TASK-3 protein in somata and dendrites can be recognized (C). Abbreviations: 7, facial nucleus; Acs7, accessory facial nucleus; py, pyramidal tract; tz, trapezoid body. Bar represent 1 mm in (A), 500 μm in (B), and 100 μm in (C)

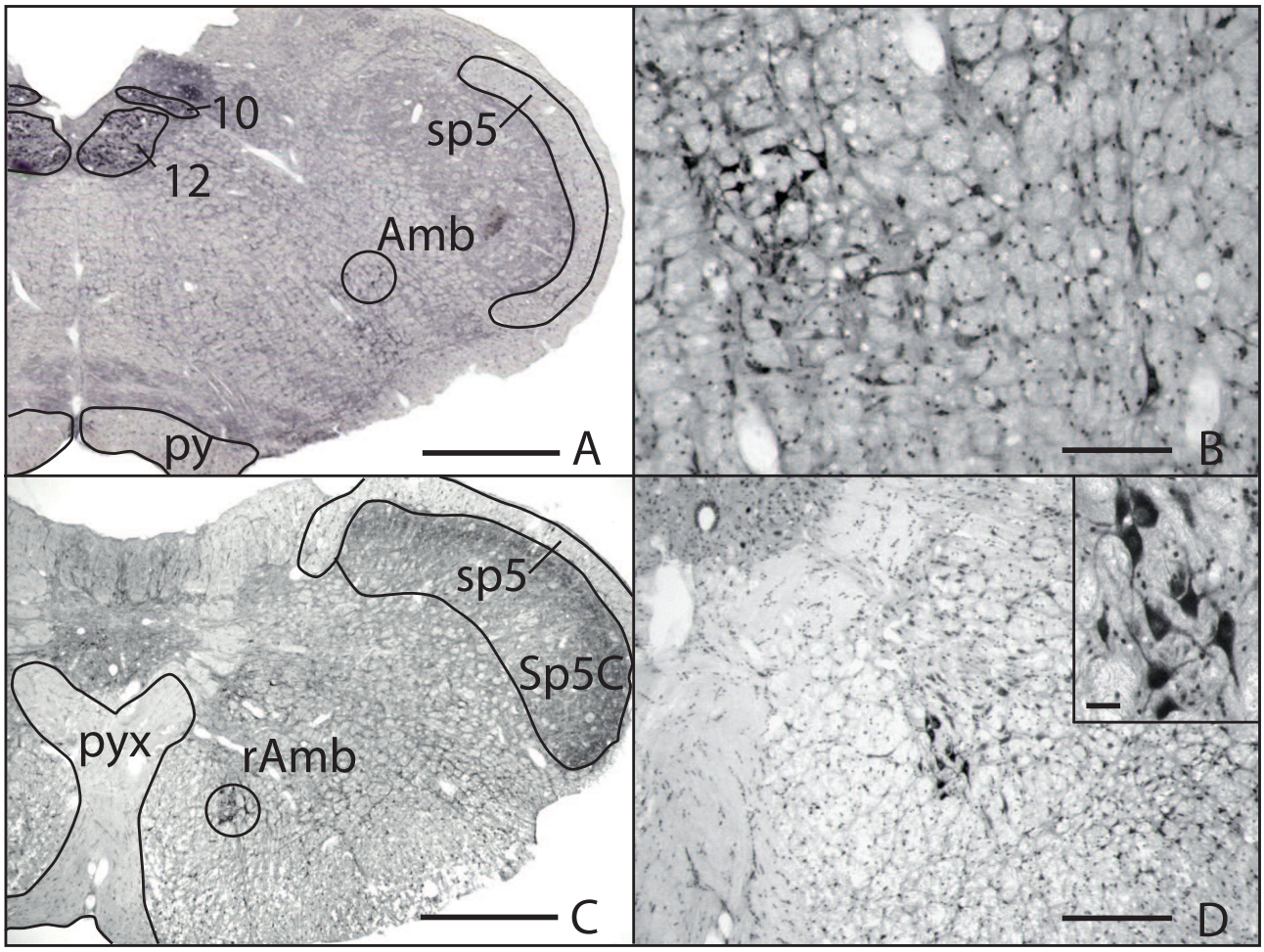

Figure 3.18 – Immunocytochemical staining of TASK-3 channels in neurons of the ambiguus nucleus. Staining with an anti-vAChT antibody on sections of the rostral medulla oblongata reveals the motoneurons of the ambiguus nucleus dorsal to the inferior olivary nucleus (A). TASK-3 channels are strongly expressed in neurons of the ambiguus nucleus (B) Motoneurons of the retroambiguus nucleus can be found on more caudal sections stained with an anti-vAChT antibody (C). Immunocytochemistry with anti-TASK-3 demonstrates high TASK-3 levels in these neurons (D) and a localization of the channel protein to somata and dendrites (see inlay). Abbreviations: 10, dorsal n.vagus nucleus; 12, hypoglossal nucleus; Amb, ambiguus nucleus; py, pyramidal tract; pyx, pyramidal decussation; rAmb, retroambiguus nucleus; sp5, spinal trigeminal tract; Sp5C, spinal trigeminal nucleus. Bar represent 1 mm in (A), and (C), 400 μm in (D), 200 μm in (B), and 50 μm in the inlay.

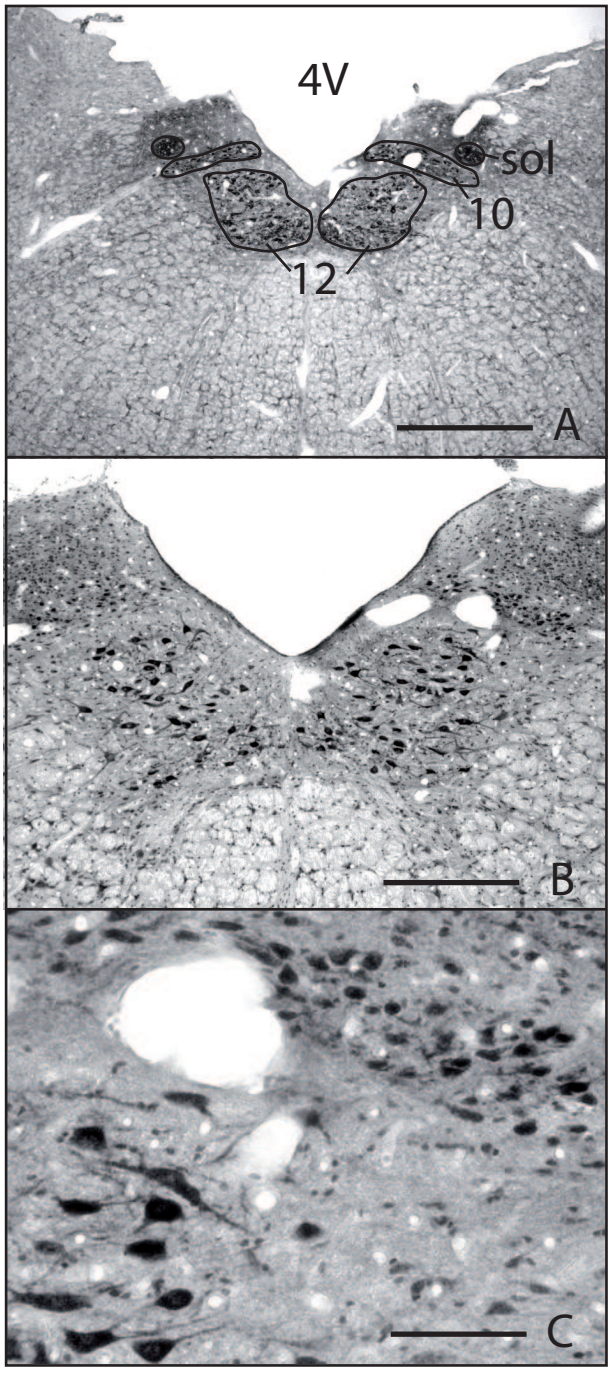

Figure 3.19 – TASK-3 expression in hypoglossal and dorsal vagal motoneurons. Motoneurons of the hypoglossal nucleus and the dorsal vagal nucleus are located in the medulla oblongata at the bottom of the fossa rhomboidea, as can be seen following immunocytochemistry with an anti-vAChT antibody (A). Both motonuclei display strong TASK-3 immunoreactivity (B). A closer look reveals that TASK-3 expression in parasympathetic dorsal vagal neurons is slightly weaker as compared to somatomotoric hypoglossal neurons. Abbreviations: 4V, 4th ventricle; 10, dorsal vagal nucleus; 12, hypoglossal nucleus; sol, solitary nucleus. Bar represent 800 μm in (A), 400 μm in (B), and 100 μm in (C).

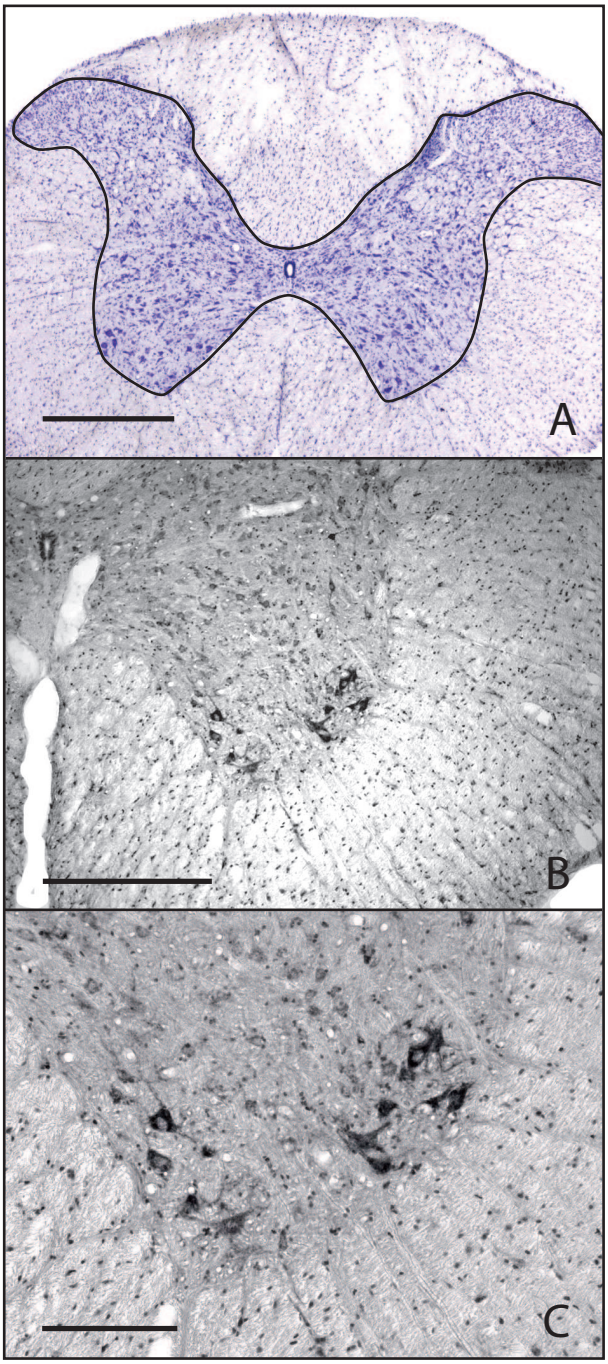

Figure 3.20 – Localization of TASK-3 channels in spinal cord motoneurons. Cresyl violet staining of a spinal cord section from the cervical region shows the α-motoneurons in the anterior horn (A). Immunocytochemical staining with the anti-TASK-3 antibody displays strong TASK-3 expression in these motoneurons (B). The channel protein can be found in somata and dendrites (C). Bar represent 1 mm in (A), 500 μm in (B), and 200 μm in (C)

abducens and spinal motoneurons expose a comparable strong TASK-3 immunoreactivity. TASK-3 expression in the parasympathetic Edinger-Westphal nucleus and the dorsal vagal nucleus is slightly weaker as compared to somatic and branchial motoneurons.

3.5.2 TASK-3 is strongly expressed in neurons of the basal nucleus of Meynert

Besides in motor systems, acetylcholine is the main neurotransmitter in the basal nucleus of Meynert (NBM). This nucleus comprises a group of neurons in the substantia innominata, localized at the ventromedial border of the pallidum. It exerts an important control over cognitive and limbic cortical areas in the forebrain and represents the major source of ascending cholinergic inputs [Ezrin-Waters and Resch, 1986]. Cholinergic neurons of the NBM were identified by immunocytochemistry with an anti-VAChT antibody (Fig. 3.21A). Immunocytochemical analysis of TASK-3 expression of adjacent sections revealed neuronal subsets with strong staining in the area of the globus pallidus and internal capsule (Fig. 3.21C), a region corresponding to the NBM. Analyses at higher magnification demonstrate a somatodendritic distribution of the channel protein (Fig. 3.21D). Immunofluorescence double-labeling with anti-TASK-3 and anti-vAChT confirmed the expression of TASK-3 in cholinergic neurons of the NBM (Fig. 3.21E-G). *In situ* hybridization experiments with TASK-3 specific riboprobes supported the presence of TASK-3 in these cells (Fig. 3.21B).

3.5.3 Striatal cholinergic interneurons demonstrate strong TASK-3 expression

Immunocytochemical staining for acetylcholine reveals a sparse group of large, aspiny interneurons in the striatum. These neurons provide the sole source of striatal acetylcholine. They receive prominent inputs from the thalamus, substantia nigra and the cortex, while exhibiting modulatory influences over striatal projection neurons and GABAergic interneurons. Therefore, they play a role in motivationally relevant events, learning and synaptic plasticity [Calabresi et al., 2000]. These cholinergic neurons display very strong TASK-3 immunoreactivity (Fig. 3.22B). Higher magnification indicate the somatodendritic localization of the channel protein (Fig. 3.22CD). Staining intensity is even stronger than that of cholinergic neurons in the basal nucleus of Meynert.

3.5.4 TASK-3 is strongly expressed in serotoninergic raphe neurons

The raphe nuclei are a group of mostly serotoninergic medium-sized neurons located in the midline of the brainstem along its entire rostral to caudal extension; it is considered to be the medial portion of the reticular formation. Serotonin (5-HT) plays an important role in the modulation of sleep, appetite, metabolism, body temperature, aggression and anxiety, implicating a role of raphe neurons in the regulation of these functions. The rostral raphe complex, which comprises the caudal linear, dorsal and median raphe nuclei, projects mainly to the forebrain and provides the major serotoninergic input to the forebrain [Hornung, 2003].

Dorsal raphe neurons display strong TASK-3 immunoreactivity (Fig. 3.23 C). Higher magnification indicates a somatodendritic localization of the TASK-3 protein (Fig. 3.23 E). *In situ* hybridization analyses of adjacent brain sections also detected TASK-3 mRNA in dorsal raphe neurons (see Fig. 3.23D). Beside the dorsal raphe, the median (Fig. 3.23B) and caudal linear raphe (not shown) show a noticeable

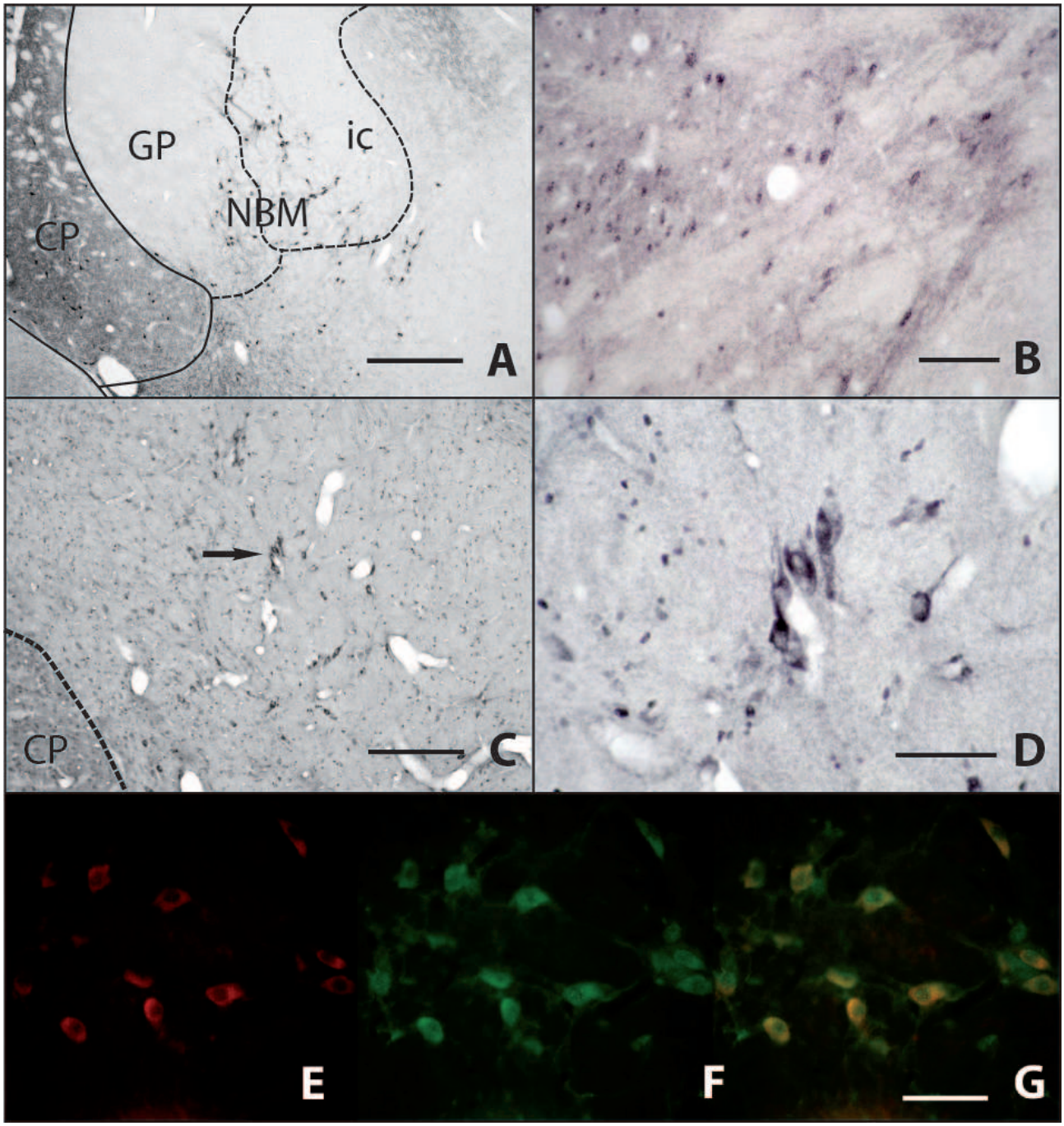

Figure 3.21 – TASK-3 expression in cholinergic neurons of the basal nucleus of Meynert. Immunocytochemical staining of the basal forebrain with an anti-vAChT antibody identified cholinergic neurons of the basal nucleus of Meynert at the ventromedial border of the pallidum (A). Immunocytochemical staining with the anti-TASK-3 antibody of adjacent sections displays strongly TASK-3 immunoreactive neurons in this area (C). At higher magnification of C (see arrow) the localization of TASK-3 protein in somata and dendrites is visible (D). Immunofluorescence double-labeling with anti-TASK-3 (E, Cy2, green) and anti-vAChT (F, Cy3, red) supported the expression of TASK-3 in cholinergic neurons of the basal nucleus of Meynert (G, merge, yellow). TASK-3 mRNA was also detected in such neurons using TASK-3 specific riboprobes (B). Abbreviations: NBM, basal nucleus of Meynert; CP, caudate putamen; GP, globus pallidus; ic, internal capsule. Bar represent 400 μm in (A), 100 μm in (B), (C), and (D), and 50 μm in (E), (G), and (F).

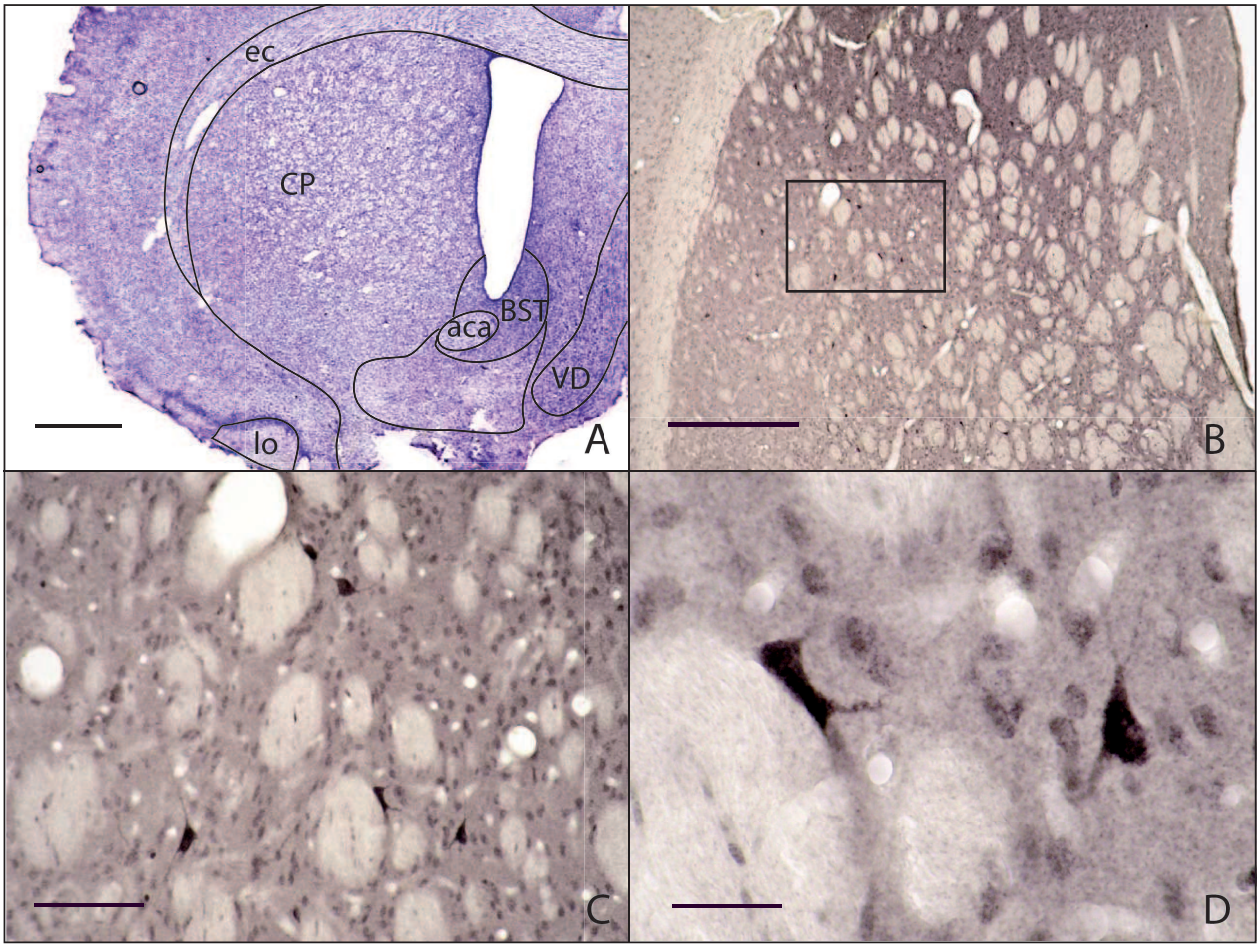

Figure 3.22 – TASK-3 channels are expressed in striatal cholinergic interneurons. Cresyl violet staining of forebrain sections shows the area of the caudate putamen (A). Within this area a group of large, cholinergic neurons can be found. These striatal interneurons display strong TASK-3 immunoreactivity (C and D). At higher magnification the somatodendritic distribution of the TASK-3 protein is more obvious (D). Abbreviations: aca, anterior commissure anterior; BST, bed nucleus of the stria terminalis; CP, caudate putamen; ec, external capsule; lo, lateral olfactory tract; VP, ventral pallidum. Bar represents 1 mm in (A), 500 μm in (B), 100 μm in (C), and 25 μm in (D).

antibody staining, however weaker as compared to dorsal raphe neurons. This was also affirmed by ISH. The expression of TASK-3 in serotoninergic neurons was demonstrated by fluorescence double-labeling (Fig. 3.23 F), revealing extensive co-expression of TASK-3 and 5-HT in these neurons (as indicated by the yellow signal).

3.5.5 Locus coeruleus neurons display very strong TASK-3 expression

The locus coeruleus (LC) is the major noradrenaline-containing nucleus in the brain and provides the main source of noradrenaline to the forebrain. Together with other brain stem nuclei the LC is a part of the ascending reticular activating system, therefore plays an important role in processes related with arousal and wakefulness [Sara, 2009]. The LC is located in the rostral tegmentum of the pons. Nissl-stained sections show a cluster of darkly stained mostly medium-sized neurons ventrolateral to the 4th ventricle and adjacent to the very large neurons of the mesencephalic trigeminal nucleus (see Fig. 3.24A for an cresyl violet overview). Neurons of the LC deisply very strong TASK-3 expression, as shown by immunocytochemistry with the anti-TASK-3 antibody (Fig. 3.24C, arrowheads). Examination at higher magnification identifies labeling of perikarya and dendrites, indicating a somatodendritic distribution of the channel (see inlay in Fig. 3.24C). The expression of TASK-3 in LC neurons was supported by the detection of mRNA by ISH experiments (Fig. 3.24D, arrowheads). However, ICC and ISH analyses revealed differences in the expression of mRNA and the channel protein. While TASK-3 riboprobes apparently detected some mRNA in the somata of the giant pseudounipolar neurons of the trigeminal mesencephalic nucleus (Fig. 3.24D, asterisks), the TASK-3 protein was only weakly detected in these cell bodies (see Fig. 3.24C, asterisks). This may indicate that in sensory systems TASK-3 proteins may have a different subcellular localization as compared to noradrenergic LC neurons or neurons of other monoaminergic systems. Co-localization of the channel with noradrenaline in LC neurons was confirmed by fluorescence double-labeling of brain stem sections with anti-TASK-3 and an anti dopamine-β-hydroxylase antibody (anti-DBH), the enzyme that converts dopamine to noradrenaline. Merging of the images showing labeling of anti-TASK-3 with Cy3 (green) and anti-DBH with Cy2 (red) indicates expression of TASK-3 in noradrenaline containing LC neurons (identified by the yellow labeling, Fig. 3.24B).

3.5.6 TASK-3 is expressed in histaminergic neurons of the tuberomammillary nucleus

The tuberomammillary nucleus is a part of the posterior hypothalamus and the main histaminergic cell group in the brain, providing histaminergic input to many regions including the brain stem, hypothalamus and cerebral cortex[Panula et al., 1984]. It activates the cerebral cortex through a direct projection. In addition, tuberomammillary neurons activate cholinergic neurons in the basal forebrain, therefore increasing the release of acetylcholine in the cerebral cortex. The tuberomammillary nucleus plays a role in the regulation of arousal and the sleep-wake-cycle [Haas and Panula, 2003]. The complex includes the dorsomedial TM (TMD, see Fig. 3.25E), located dorsal to the rostral part of the posterior periventricular nucleus, and a ventral nucleus (TMV, see Fig. 3.25B), which lays on the base of the hypothalamus (Fig. 3.25A). The location of histaminergic neurons can be demonstrated by immunolabeling with an antibody against histidine decarboxylase (anti-HDC, Fig. 3.25BE). HDC is the enzyme that catalyzes the production of histamine from histidine and consequently, can only

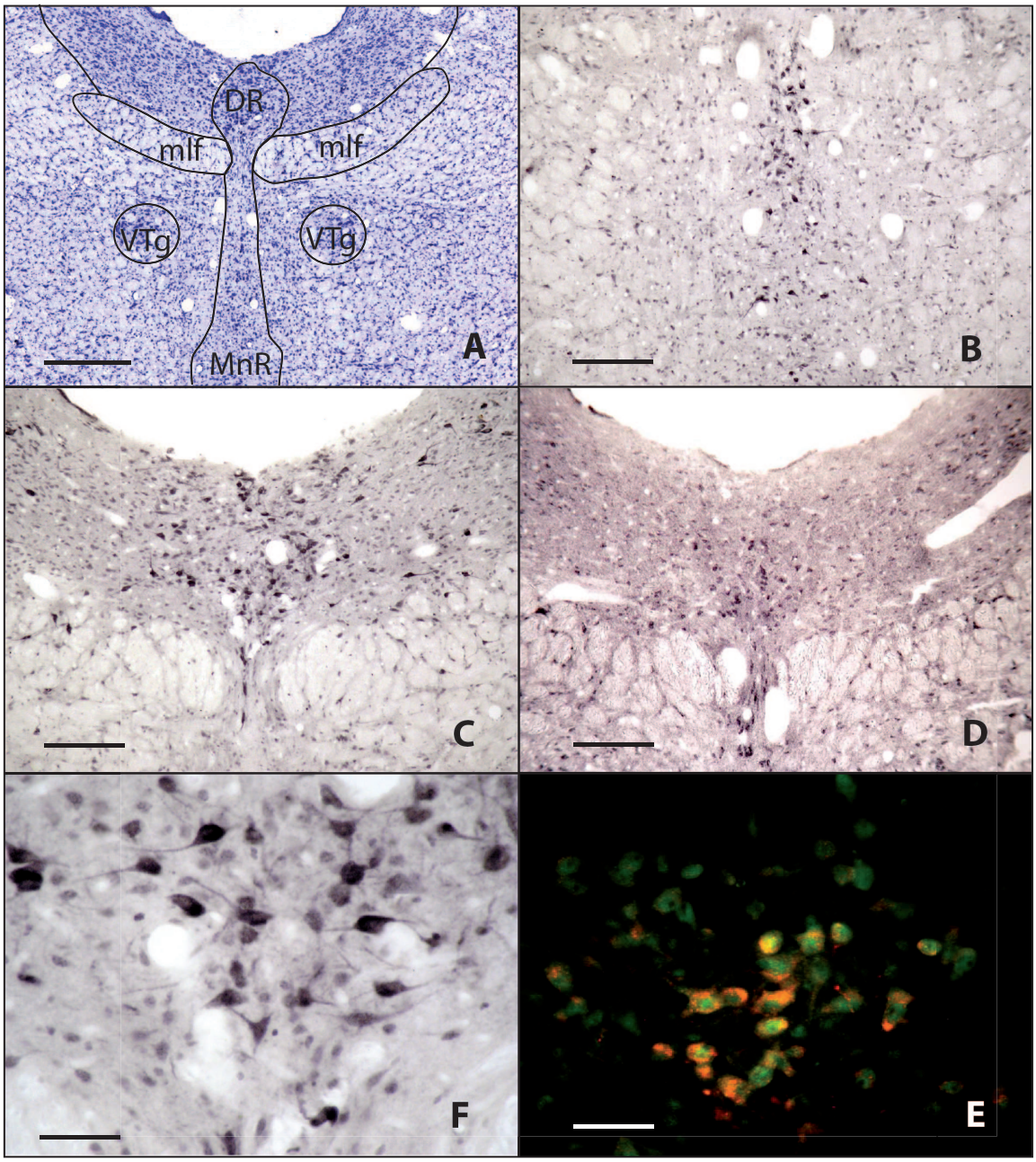

Figure 3.23 – TASK-3 expression in serotoninergic neurons of the raphe nuclei. The raphe nuclei are located in the midline of the brainstem. Cresyl violet staining of caudal midbrain sections show dorsal and median raphe neurons ventral to the aqueduct (A). Immunocytochemistry using the anti-TASK-3 antibody demonstrates considerable TASK-3 expression in median raphe neurons (B). However, TASK-3 immunoreactivity of dorsal raphe neurons is much stronger (C). The localization of the channel protein to somata and dendrites can be recognized at higher magnification (E). ISH with TASK-3 specific riboprobes of adjacent sections confirmed the presence of TASK-3 mRNA in these neurons (D). Immunofluorescence double-labeling of dorsal raphe neurons (F) with anti-TASK-3 (Cy2, green) and anti-5-HT (Cy3, red) antibodies revealed extensive co-expression in these neurons (yellow). Abbreviations: DR, dorsal raphe; MnR, median raphe, VTg, ventral tegmental nucleus; mlf, medial longitudinal fasciculus. Bar represent 1 mm in (A), 200 μm in (B), (C), (D), and 40 μm in (E), and (F).

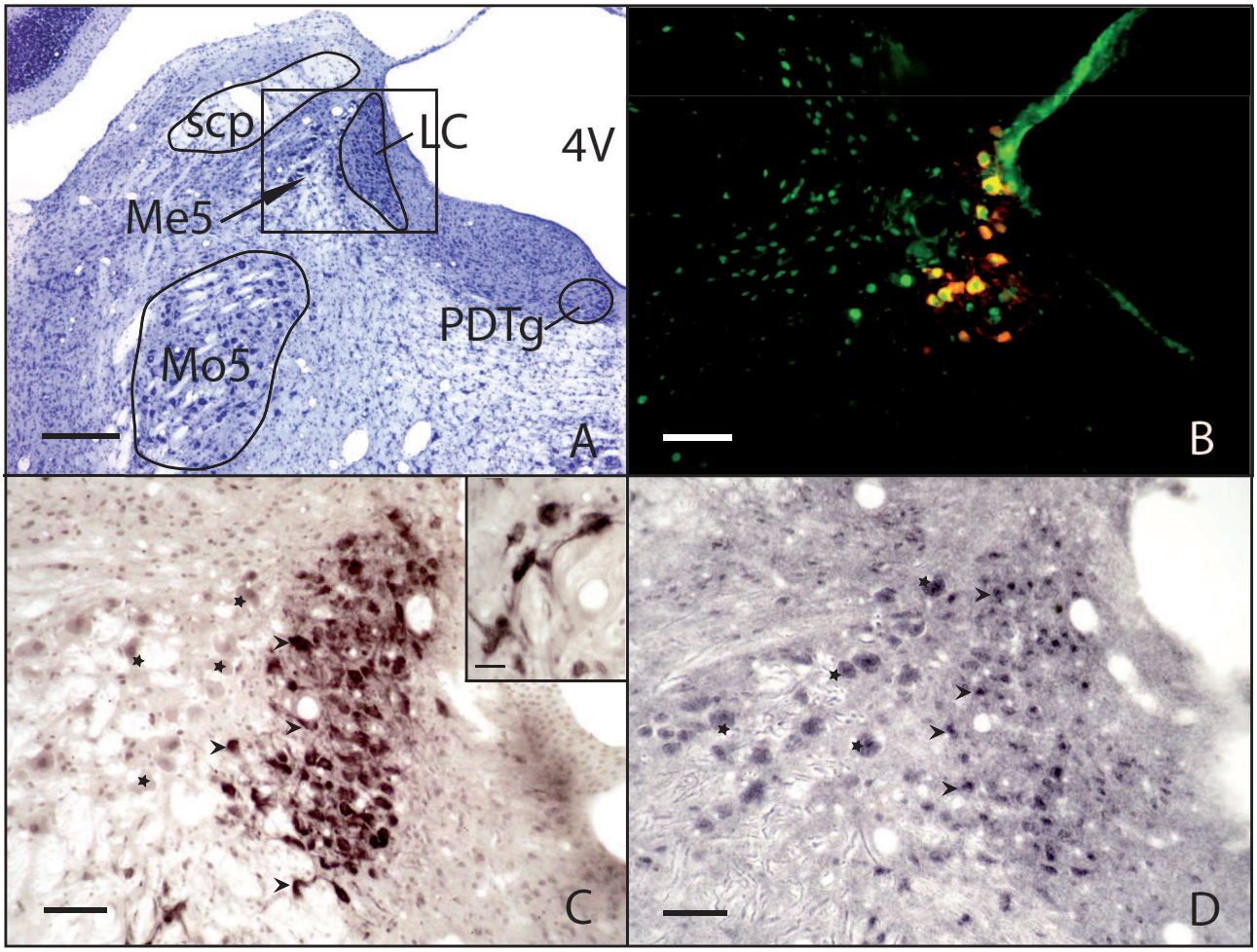

Figure 3.24 – Immunocytochemical detection of TASK-3 in noradrenergic neurons of the locus coeruleus. The locus coeruleus can be clearly identified on cresyl violet stained sections of the hindbrain region, ventrolateral to the fourth ventricle (A). LC neurons display very strong TASK-3 immunoreactivity (asterisks in C). At higher magnification the localization of TASK-3 in the somatodendritic compartment is visible (inset in C). In addition, ISH experiments detected TASK-3 mRNA in LC neurons (asterisks in D). The adjacent pseudo unipolar neurons of the mesencephalic trigeminal nucleus (arrowhead) were also positive for TASK-3 mRNA, but exhibited only weak expression of TASK-3 protein in their somata (arrowhead in C). Immunofluorescence double-labeling (B) using anti-TASK-3 (Cy2, green) and anti-dopamine-β-hydroxylase (Cy3, red) antibodies affirmed the expression of TASK-3 in noradrenergic LC neurons (yellow). Abbreviations: LC, locus coeruleus; mlf, medial longitudinal fasciculus; Me5, mesencephalic trigeminal nucleus; Mo5, motor trigeminal nucleus; PDTg, posterodorsal tegmental nucleus; scp, superior cerebellar peduncle. Bar represent 500 μm in (A), 100 μm in (B), (C), and (D), inlay 25 μm.

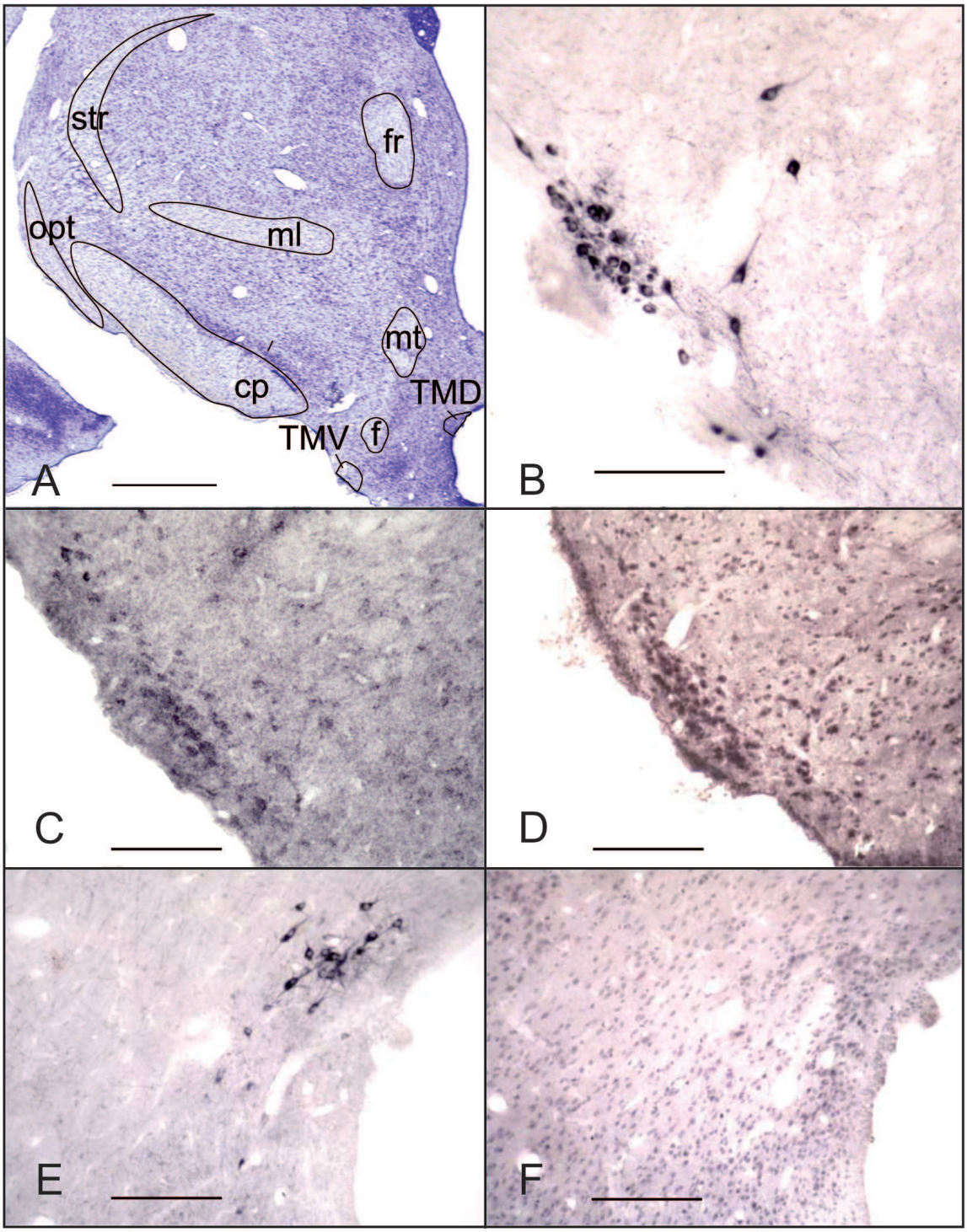

Figure 3.25 – TASK-3 expression in histaminergic neurons of the tuberomammillary nucleus. The tuberomammillary nuclei are located in the dorsal hypothalamic region lateral to the mammillary recessus of the third ventricle (seen in cresyl violet stained sections in A). Immunocytochemistry with an anti-histidine decarboxylase antibody identified the histaminergic neurons in the ventral tuberomammillary nucleus (TMV in B) and the dorsal tuberomammillary nucleus (TMD, in E). Neurons of the TMV display considerable TASK-3 immunoreactivity (C), whereas immunoreactivity of TMD neurons is comparably weaker (F). The expression of TASK-3 in the TMV was supported by the detection of TASK-3 mRNA in these neurons (D). Abbreviations: f, fornix; fr, fasciculus retroflexus; ml, medial lemniscus; mt, mammillothalamic tract; opt, optic tract; str, superior thalamic radiation. Bar represent 1 mm in (A), and 100 μm in (B)-(F).

be found in histaminergic neurons. Immunocytochemistry with the anti-TASK-3 antibody of adjacent brain sections shows that TASK-3 is expressed in neurons of the tuberomammillary nucleus (dorsal and ventral part). Immunoreactivity of neurons of the ventral nucleus (Fig. 3.25D) is weaker than compared to other monoaminergic neurons (e.g. dorsal raphe or locus coeruleus). However, the signal intensity is clearly distinguishable from the surrounding weakly labeled neurons. Immunoreactivity of the dorsal tuberomammillary neurons is somewhat weaker as compared to the ventral nucleus (see Fig. 3.25F). Moreover, ISH experiments detected TASK-3 mRNA in neurons of the tuberomammillary complex (shown only for TMV, Fig. 3.25C). Fluorescence double-labeling with anti-TASK-3 and anti-HDC supported the co-localization of TASK-3 and histamine in tuberomammillary neurons (data not shown).

3.5.7 TASK-3 is differentially expressed in dopaminergic midbrain neurons

The substantia nigra is a part of the basal ganglia located just dorsal to the cerebral peduncles. It consists of two parts. The substantia nigra pars compacta (SNc) is situated dorsal to the pars reticulata and is one of the major sources of striatal dopamine. Situated between the left and right SNc lays the ventral tegmental area (VTA) also harboring dopaminergic neurons. The VTA can be divided into several sub-nuclei. Both, VTA and SNc, play an important role in the reward system and addiction [Chinta and Andersen, 2005]. In the dopaminergic neurons of the midbrain (for cresyl violet overview see Fig. 3.27A) the TASK-3 channel protein is differently expressed. Immunocytochemistry of midbrain sections with an anti-tyrosine hydroxylase antibody demonstrates the localization of dopaminergic neurons of the SNc and VTA (see Fig. 3.26A). Labeling of adjacent sections with the anti-TASK-3 antibody reveals differences in the intensity of the immunosignal. While neurons of the SNc are only weakly labeled, neurons of the VTA demonstrate a moderate TASK-3 expression with some strongly immunoreactive neurons (Fig. 3.26B). This becomes more evident at higher magnifications. Some neurons of the VTA demonstrate strong TASK-3 expression with a clearly somatodendritic labeling (Fig. 3.26C). In contrast, neurons of the SNc display a labeling of the nuclei (Fig. 3.26D, asterisk), while the surrounding somata are only very weakly labeled and hard to distinguish from background staining (Fig. 3.26D, arrows). TASK-3 is expressed in several sub-nuclei of the VTA (Fig. 3.27). Dopaminergic neurons of the anterior VTA (for anti-TH labeling see Fig. 3.27B) are clearly TASK-3 positive (see Fig. 3.27C). Indeed, at higher magnification the somatodendritic compartment of neurons in the VTA displays prominent TASK-3 immunoreactivity (see Fig. 3.27D). The expression of TASK-3 mRNA was confirmed by ISH (Fig. 3.27E). Additionally, TASK-3 expression was also demonstrated in neurons of the interfascicular VTA (Fig. 3.27G) and the paranigral VTA (Fig. 3.27H). However, TASK-3 expression in these VTA sub-nuclei is comparably weaker.

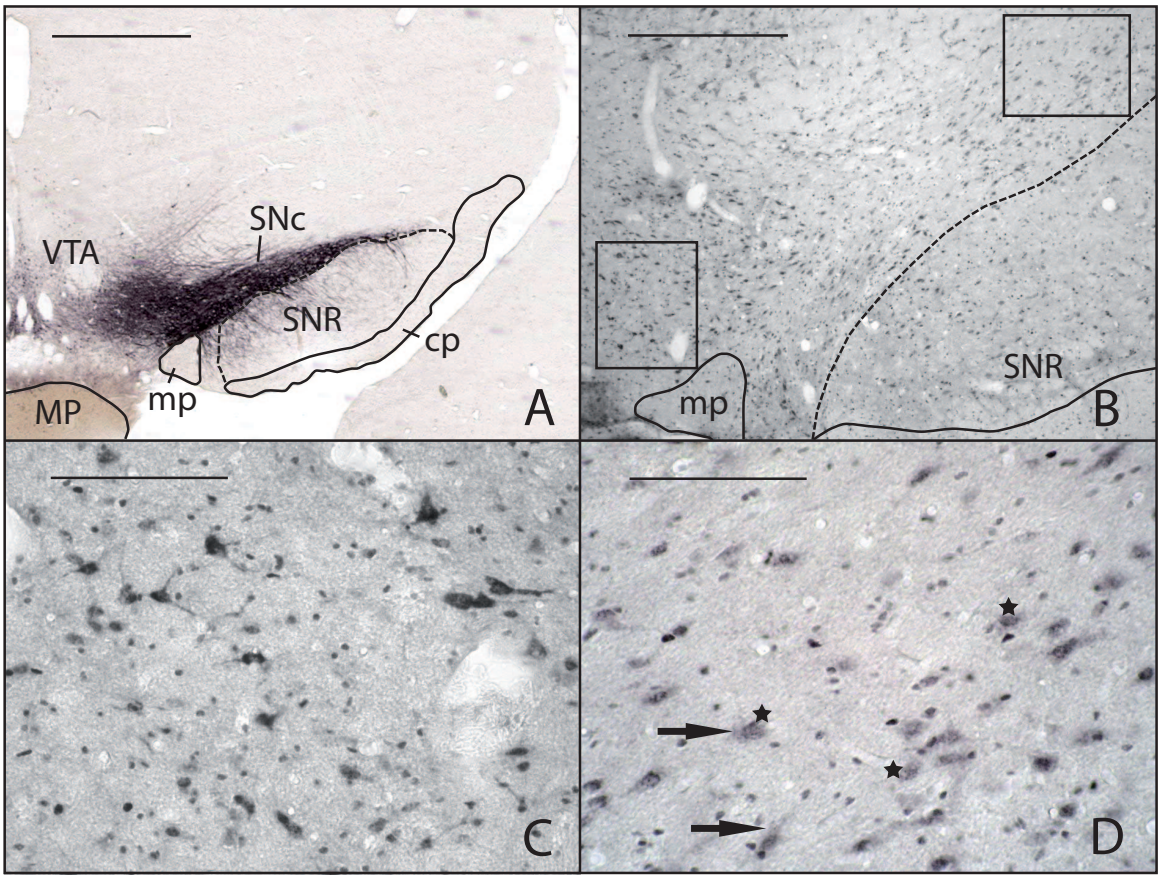

Figure 3.26 – Differential expression of TASK-3 in VTA and SNc neurons. Immunocytochemistry of rostral midbrain sections with an anti-tyrosine hydroxylase antibody reveals dopaminergic neurons of the ventral tegmental area and substantia nigra pars compacta (A). Immunocytochemistry of adjacent sections with the anti-TASK-3 antibody demonstrates TASK-3 expression in VTA and SNc neurons (B). At higher magnification a difference in staining intensity becomes obvious. VTA neurons expose a moderate to strong TASK-3 expression with a somatodendritic localization of the channel (C). In contrast, SNc neurons demonstrate only weak TASK-3 immunoreactivity (D) with a clear labeling of the nuclei (asterisks) but only marginal labeling of somata (arrows). Abbreviations: cp, cerebral peduncle; MP, nucleus of the mammillary peduncle; SNc, substantia nigra pars compacta; SNR, substantia nigra pars reticulata; VTA, ventral tegmental area. Bar represents 1 mm in (A), 500 μm in (B), and 50 μm in (C), and (D).

Figure 3.27 – TASK-3 channels are detected in dopaminergic neurons of the VTA. The VTA comprises dopaminergic neurons close to the midline at the bottom of the midbrain (see cresyl violet staining in A). Dopaminergic neurons of the anterior VTA can be visualized with an anti-tyrosine hydroxylase antibody (B). Immunocytochemistry with the anti-TASK-3 antibody also reveals TASK-3 positive neurons in this region (C). At higher magnification the expression of the channel protein in somata and dendrites can be recognized (D). Furthermore, the detection of TASK-3 mRNA supported the expression of TASK-3 channels in VTA neurons (E). Other VTA sub-nuclei (F) including the interfascicular VTA (G) and paranigral VTA (H) display a somewhat weaker TASK-3 immunoreactivity. Abbreviations: CG, central gray; cp, cerebral peduncle; medial lemniscus; iVTA, interfascicular VTA; MG, medial geniculate nucleus; pVTA, paranigral VTA; SNc, substantia nigra pars compacta; SNR substantia nigra pars reticularis, VTA, ventral tegmental area. Bar represent 1 mm in (A), (B), (F), 100 μm in (C), (E), 50 μm in (H), and 25 μm in (D), and (G).

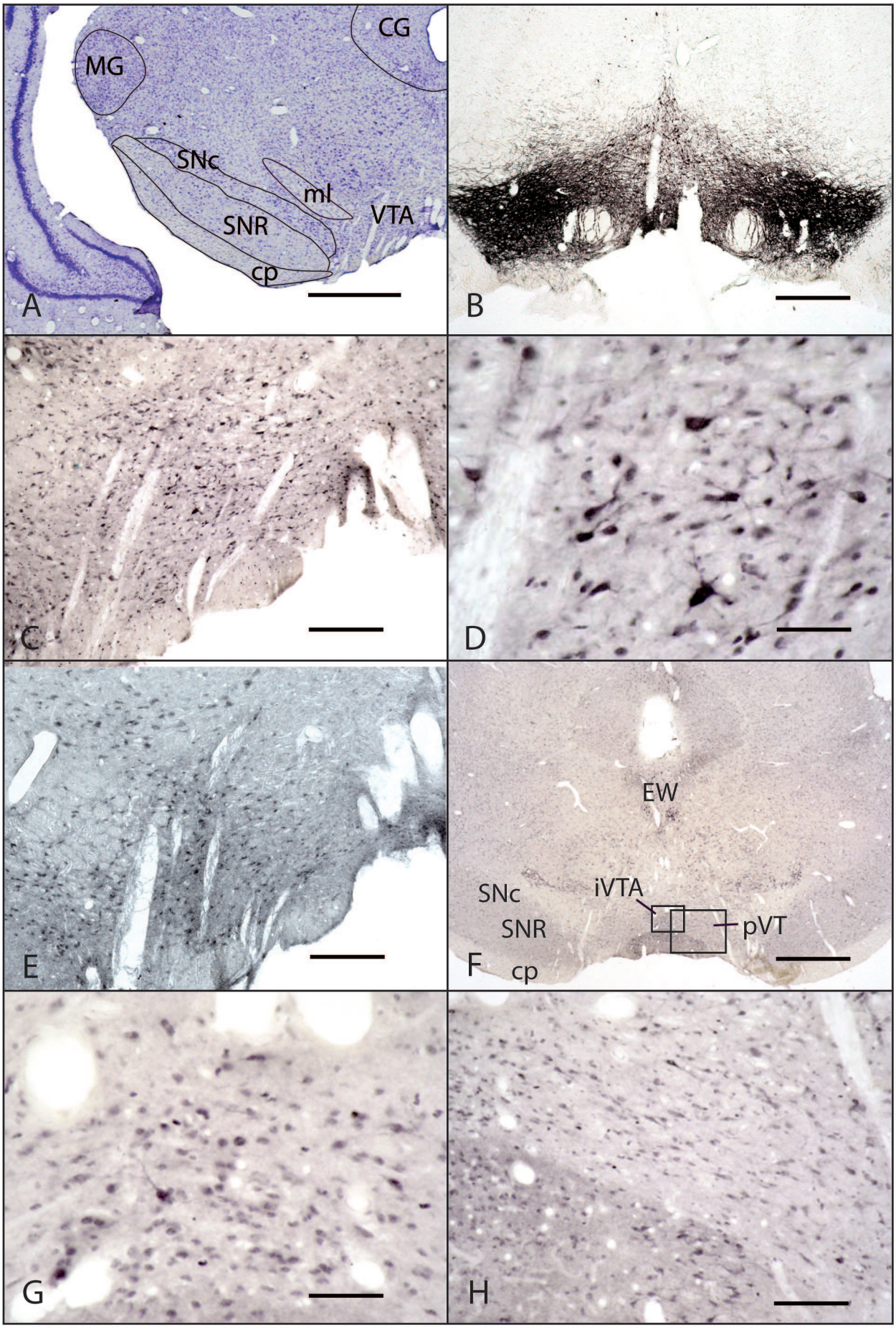
CG
MG
SNc
ml
VTA
SNR
cp
A
B
C
D
E
EW
SNc
iVTA
SNR
pVT
cp
F
G
H

3.6 TASK-3 expression in the adrenal glands

The adrenal glands are a pair of endocrine glands located on the upper poles of the kidneys. The adrenal glands comprise the outer cortex and the inner part which is called medulla. Cells of the medulla originate from the neural crest, therefore can be regarded as modified neurons. Medullary cells can produce adrenaline and noradrenaline that on demand are released into the blood stream. The adrenal cortex consists of the most superficial zona glomerulosa, the zona fasciculata and the zona reticularis that borders on the medulla. An increased potassium level or a decreased sodium level in the blood mediate the production of aldosterone in glomerulosa cells. Cells of the zona fasciculata predominantly produce glucocorticoids like cortisol in humans or corticosterone in rats. In the zona reticularis glucocorticoids and androgens like androsterone are produced. Cross sections of the adrenal gland display a very strong TASK-3 immunoreactivity in cells of the zona glomerulosa (Fig. 3.28D) and the medullary cells (Fig. 3.28C). Cells of the zona fasciculata and reticularis expose no specific signal.

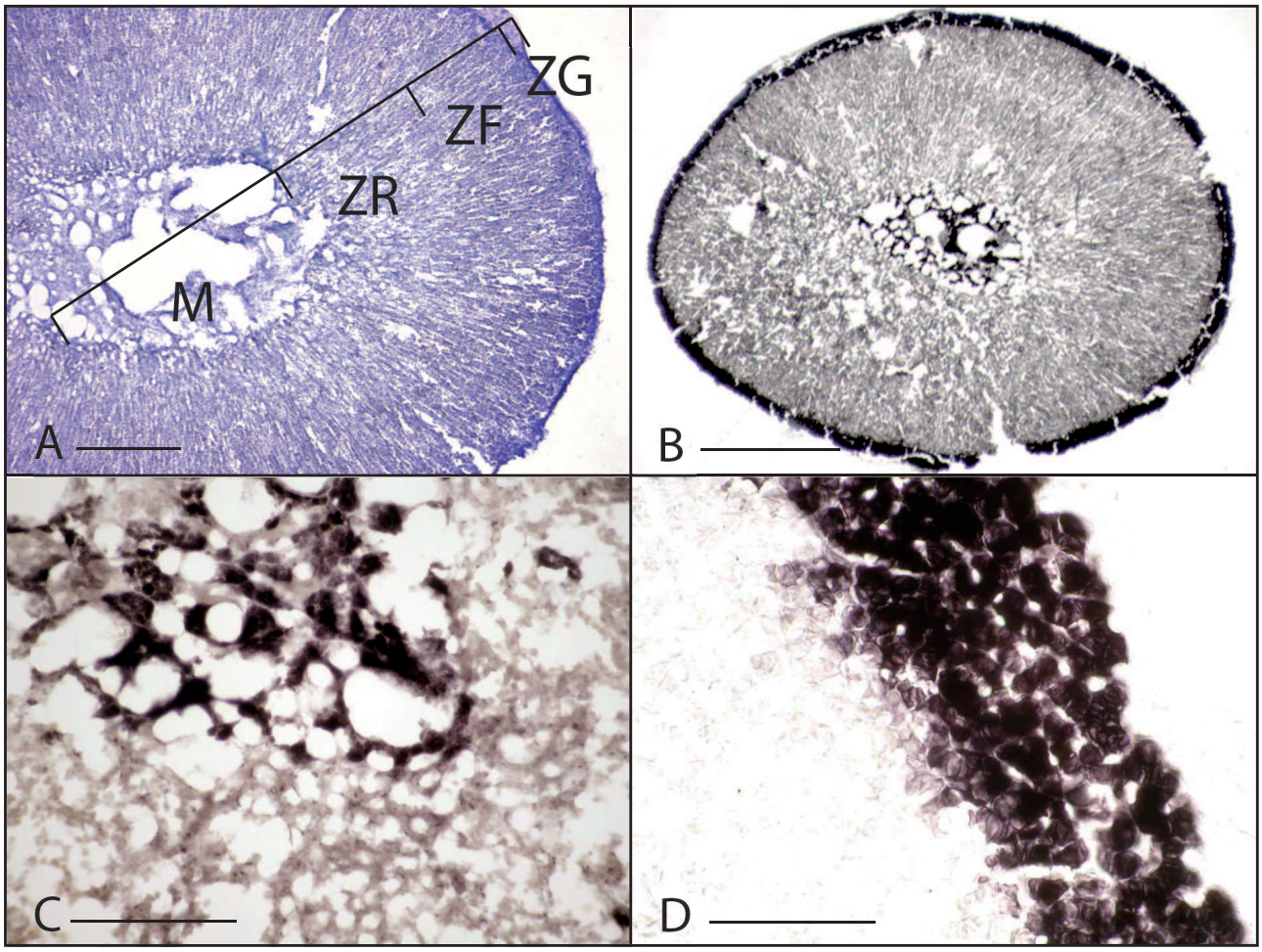

Figure 3.28 – Immuncytochemistry with anti-TASK-3 of the adrenal glands. The adrenal glands can be divided into cortex, comprising zona glomerulosa, zona fasciculata and zona reticularis and the inner medulla (A). Immunocytochemistry with anti-TASK-3 of adrenal gland sections display strong TASK-3 immunoreactivity of zona glomerulosa cells and cells of the medulla (B). At higher magnification it is obvious that only medullary cells (C) and zona glomerulosa cells (D) express TASK-3, other cells only display background staining. Abbreviations: M, medulla; ZF, zona fasciculata; ZG, zona glomerulosa, ZR, zona reticularis. Bar represents 1 mm in (B), 500 μm in (A), and 50 μm in (C), and (D).

4 Discussion

4.1 Are there protein interaction domains within the C-terminal TASK-3 fragment?

For the affinity purification of the anti-TASK-3 antibody a fusion protein of a C-terminal fragment of TASK-3 and thioredoxin with a tail of six histidine molecules (TASK-3-6HisTR, 27 kDa) was used. Western blot analyses of the purified fusion protein revealed an additional large band at around 45 kDa besides the expected 27 kDa band. Further analyses suggested that this band corresponds to a dimer of the recombinant TASK-3 protein. It can be guessed that disulfide bonds form these dimers, as the TASK-3 fragment comprises two cysteine residues. However, the sample buffer (Laemmli buffer) contains the agents mercaptoethanol and DTT that should reduce and split up sulfide bonds. Furthermore, in an additional analysis the protein was treated with iodacetamide that prevents reoxidation of thiol groups by alkylating them. In an subsequent western blot analysis the 45 kDa band was still visible (see Fig. 3.3). Therefore, a dimer formation by disulfid bonds is unlikely.
Another possible explanation for the formation of stable dimers is an interaction of specialized domains within the C-terminal TASK-3 fragment. A well-known functional domain within the C-terminal end of TASK-3 is the 14-3-3-binding motif. This is a conserved sequence of TASK-3 as well as TASK-1, comprising a pentapeptide (RRx(S/T)x) at the extreme C-terminus. This motif is necessary for the interaction with isoforms of the adapter protein 14-3-3. Binding of the adapter protein promotes channel trafficking to the surface membrane [Rajan et al., 2002]. Possibly, such a conserved binding motif could also enable the direct interaction of TASK-3 fragments with each other.
Some potassium channels require a C-terminal coiled-coil domain for correct subunit assembly (tetramerization). This is a protein-protein interaction domain with a helical secondary structure because of a special amino acid sequence. The amino acids are arranged in such a way that every first and fourth position is preferably occupied by a hydrophobic amino acid [Lupas, 1996]. In an aqueous environment this amphipathic sequence causes the formation of multimers. A contribution of such domains to potassium channel subunit assembly has been described for voltage-gated channels of the ether-a-go-go superfamily [Jenke et al., 2003] and for M-type KCNQ (K_v7) channels [Schwake et al., 2006]. A section of the C-terminal sequence of TASK-3 resembles a coiled-coil domain. Beginning at position 342 there is an amino acid arrangement with predominantly hydrophobic amino acids (valine, isoleucine, phenylalanine, methionine) or at least non-hydrophilic (cysteine) or less hydrophilic (proline, threonine, histidine) amino acids on every first and fourth position. However, the proline residues in the C-terminal sequence may avoid the formation of a helical structure. Actually, the program Marcoil version 1.0 (http://www.ch.embnet.org) predicted that there would not be a formation of a coiled-coil structure within the C-terminal fragment of TASK-3. Though, the hydrophobic amino

acids could promote the formation of other secondary structures and there may be other structural features within the C-terminal sequence that enable subunit assembly. Interaction of TASK-3-6HisTR proteins that are based on motifs for channel dimerization could explain the stable aggregates and therefore the 45 kDa band. This is not exactly twice the molecular weight of the 27-kDa fusion protein. Thought, the formation of secondary structures and protein interactions influences the migration of the protein in the acrylamide gel, explaining aberrations from the expected values.

4.2 Antibody-specificity

In 1942, Coons et al. introduced the method of immunocytochemical staining using antibodies labeled with fluorescent dyes [Coons et al., 1942]. In the last 70 years this technique has evolved greatly and been applied to various fields of biology and medicine. Due to its apparent simplicity, the immunocytochemical localization of antigens such as proteins or other macromolecules has become a standard method. Nowadays, a multiplicity of antibodies against a variety of antigens is commercially available. Commercially acquired antibodies, however, are often assumed to be specific and are used without further testing. In recent years, several reports raised serious concerns on the use of largely uncharacterized commercial antibodies [Saper, 2009, Pradidarcheep et al., 2008]. These antibodies often show a lack of specificity and sensitivity as well as cross reactivies.

The anti-HDC antibody is a good example for the importance to choose the appropriate antibodies and to control their specificity before use. At least two antibodies against HDC are commercially available. The anti-HDC antibody from DPC Biermann cross reacts with DOPA-decarboxylase. Consequently, this antibody not only visualizes histaminergic neurons, but also dopaminergic and adrenergic neurons. Therefore, in my thesis I used an antibody from Acris that specifically detects histidine decarboxylase and unambiguously identifies histaminergic neurons.

The unavailability of a reliable commercial anti-TASK-3 antibody may be the main reason for the rare reports about the localization of TASK-3 on the protein level. Brickley et al. [2007] claimed that the anti-TASK-3 antibody from Alomone gave equally high signals in WT and TASK-3 knockout mice, even though absence of TASK-mRNA in knockout mice was demonstrated by ISH and quantitative PCR. Another group reported that the anti-TASK-3 antibody from Santa Cruz not detected the protein in homogenates of the adrenal gland [Inoue et al., 2008]. Strong expression of TASK-3 in adrenal zona glomerulosa cells has been demonstrated by several reports (see page 68). Furthermore, Rusznak et al. [2004] used the Santa Cruz antibody to study TASK channel distribution in the rat and human cerebellum and detected TASK-3 in astrocytes. A quantitative PCR (Data provided by Dr. Christian Derst) detected no TASK-3-DNA in astrocytes nor are there any other hints in literature for a TASK-3 expression in astrocytes.

In the present investigation, a polyclonal, monospecific anti-TASK-3 antibody was prepared, to have a reliable tool to study the distribution of TASK-3 in the rat brain. I used an extensive protocol that was established in our laboratory for the generation, purification and characterization of antibodies directed against defined soluble domains of 50-100 amino acids [Veh et al., 1995, Prüss et al., 2005, Eulitz et al., 2007].

To avoid cross reactivity of the antibody a 73 amino acid long fragment from the C-terminal end of

the TASK-3 protein was chosen for the preparation of the GST fusion protein that was used for the subsequent immunization of the rabbits. The C-terminal region shows only low homology to other paralogous channel proteins (e.g. TASK-1 and TASK-5). To rule out any homologies between the chosen 73 amino acids and other proteins, the sequence was compared with database entrees using NCBI-BLAST (www.ncbi.nlm.nih.gov/BLAST). All blast hits were entrees of TASK-3 from different species.

The purified anti-TASK-3 antibody was carefully tested in several experiments to confirm its sensitivity and specificity. ELISA and western blot analyses of recombinant proteins showed that the antibody specifically recognizes the TASK-3 sequence in recombinant fusion proteins with GST and 6HisTR.

However, these tests with selected recombinant proteins do not tell anything about other proteins the antibody could bind in tissue, nor if it also binds the native TASK-3 channel protein. These questions were answered by western blot analyses of rat brain membrane fractions. Anti-TASK-3 staining revealed a single band with the expected molecular weight (44.4 kDa) in fractions of rat forebrain and cerebellum, demonstrating that the antibody recognizes the native channel protein and no other proteins expressed in the brain. In addition, immunocytochemistry of transfected HT22 cells confirmed the specificity of the antibody (data friendly provided by Dr. Harald Prüss). HT22 cells transfected with the TASK-3/pcDNA3.1 vector (full length clone) exposed a specific TASK-3 immunoreactivity, whereas signal was absent from cells transfected with TASK-1 or TASK-5. This experiment shows that the antibody detects the full-length protein in a cellular environment, arguing for its suitability in immunocytochemistry on brain sections.

RT-PCR experiments not only detected TASK-3 in the brain, but also in kidney, liver, lung, colon, stomach, spleen, testis, and skeletal muscle, and at very low levels in the heart and small intestine [Kim et al., 2000]. In a western blot with membrane fractions of other rat tissues I found minor TASK-3 expression only in heart, kidney and liver. It could be assumed that TASK-3 expression in tissues other than the brain is very low. This is also supported by the fact that Kim et al. [2000] could not detect TASK-3 mRNA in other tissues than brain by northern blot experiments. Likewise, Talley et al. [2000] only detected TASK-3 at very low levels in the kidney and other tissues, when running up to 80 RT-PCR-cycles. The aberrations in tissue distribution could be due to a divergence in expression of TASK-3 mRNA and the channel protein. Thought, it is most likely that the immunocytochemical detection by western blot analysis is not sensitive enough to detect low levels of protein. Interestingly, the anti-TASK-3 antibody detected two bands in a western blot of liver tissue; one with the molecular weight expected for the native TASK-3 channel and a bigger one. The same result was observed in a reverse-transcriptase PCR analysis of rat liver tissue [Kim et al., 2000]. No other tested tissue showed a double-band. This might indicate the existence of a TASK-3 splice variant in liver cells of the rat.

Further evidence for the specificity of TASK-3 was provided by preincubation experiments. In western blot analyses with the recombinant TASK-3 protein and membrane fractions as well as in immunocytochemical experiments on brain sections the specific immunosignal could completely be blocked by preincubation of the antibody with TASK-3-GST. Interestingly, the immunosignal of brain sections was completely blocked by preincubation with 10 μg/ml of TASK-3-GST, while higher protein

amounts lead to a decline, but failed to completely block the immunosignal. It can be guessed that at an optimal ratio of antibody and antigen complexes are formed in that all binding sites on both reagents, antibody and antigene, are occupied. These complexes are insoluble and can be removed from the solution by centrifugation. With an excess of either antigen or antibody, complexes are formed with free combining sites on one of the reagents. These complexes are soluble and might interact with the native occurring protein in the tissue.
Another useful tool in the characterization of antibody specificity is the immunocytochemical staining of tissues from knockout animals. Immunocytochemistry on brain sections revealed an equally strong and widely distributed immunosignal for wild type and TASK-3 knockout mice. However, this can be explained by the possible fact that these animals were functional knockouts [Brickley et al., 2007]. Supposedly , these mice do not express a functional channel, but a residual that is recognized by the antibody. However, further experiments are needed to confirm this assumption.
In conclusion, the new anti-TASK-3 antibody recognizes the native as well as the recombinant TASK-3 protein and no other proteins. Thus, it provides a useful tool to study the distribution of the channel in the rat brain.

4.3 TASK-3 channels are widely distributed throughout the rat brain.

Immunocytochemical staining of rat brain sections with the anti-TASK-3 antibody demonstrated a widespread signal. Detailed immunocytochemical analysis with the anti-TASK-3 antibody revealed TASK-3 positive neurons in all areas examined including forebrain regions, hippocampus, hypothalamus, thalamus, midbrain, cerebellum, pons, medulla oblongata, and the spinal cord. Comparison with the *in situ* hybridization data of Karschin et al. [2001] and Talley et al. [2001] revealed that the expression of the TASK-3 protein matches the mRNA expression, no obvious aberrations were observed (see table 3.1). ISH experiments detected no TASK-3 mRNA in the substantia nigra [Karschin et al., 2001, Talley et al., 2001], whereas the anti-TASK-3 antibody indicated a weak expression of the protein. Thought, these and other minor discrepancies could be caused by differences in the detection systems or intensity of the detection systems.
The TASK-3 protein is widely distributed but not ubiquitously expressed in the brain. Counterstaining with methyl green illustrated the mainly neuronal expression of the channel; endothelial and ependymal cells were clearly devoid of labeling. In contrast to the commercial antibody from Santa Cruz, our new anti-TASK-3 antibody did not label astrocytes. This result is consistent with the aforementioned (see 70) quantitative PCR data, confirming specificity of the antibody and also the doubts about the specificity of the commercial antibody.
Most obvious was the strong expression in monoaminergic and cholinergic neurons. This is in accordance with the reports of Karschin et al. [2001] and Talley et al. [2001], describing an especially strong expression of TASK-3 mRNA in most cholinergic neurons, including motoneurons, serotoninergic neurons of the raphe nuclei and noradrenergic neurons of the locus coeruleus. It is of interest to see if other monoaminergic neurons demonstrate a likewise strong TASK-3 expression. Therefore, besides serotoninergic, noradrenergic and cholinergic neurons, TASK-3 immunoreactivity of dopaminergic and histaminergic neurons was examined.

4.3.1 TASK-3 expression in serotoninergic raphe neurons

The raphe nuclei are a complex group of neurons located along the midline of the brainstem, most of them using the neurotransmitter serotonin. Arising in the raphe nuclei, serotoninergic fibers extend through virtually all brain areas, regulating many types of behavior and making the serotoninergic system the most expansive neurochemical system in the brain [Hornung, 2003]. Dorsal raphe neurons strongly express TASK-3 channels as can be seen by immunocytochemistry with the anti-TASK-3 antibody (see Fig. 3.23). Accordingly, TASK-3 mRNA was detected in raphe neurons by *in situ* hybridization experiments. Immunofluorescence double-labeling with anti-TASK-3 and anti-5-HT supported the expression of TASK-3 in serotoninergic dorsal raphe neurons.
Expression of TASK-3 mRNA in raphe nuclei has been demonstrated before by ISH studies on the distribution of TASK-3 in the rat brain [Karschin et al., 2001, Talley et al., 2001]. Washburn et al. [2002] confirmed these findings by combining ISH with the immunocytochemical localization of tryptophan hydroxylase. This enzyme catalyzes the hydroxylation of L-tryptophan to 5-HT and can be used to identify serotoninergic neurons. TASK-1 and TASK-3 mRNA were detected in most serotoninergic dorsal and caudal raphe neurons and by applying voltage clamp recordings a K^+ conductance with corresponding properties was identified [Washburn et al., 2003].
Several studies suggested that raphe neurons contribute to the control of breathing. Inadequate ventilation causes an accumulation of carbon dioxide in the blood, leading to a fall in arterial blood pH (acidosis). To maintain pH-homeostasis there are pH- and pCO_2-sensing neurons in the brainstem that control and adjust the rate and depth of breathing. This mechanism is called central respiratory chemoreception [Nattie, 1999, Feldman and Del Negro, 2006]. Serotoninergic raphe neurons can act as sensors for carbon dioxide- and pH-changes [Richerson, 1995] and serotoninergic medullary raphe neurons are activated by acidosis [Wang et al., 2001]. As TASK-3 is strongly expressed in raphe neurons and inhibited by acidification, a role for TASK-3 channels in arousal and ventilatory reflexes associated with extracellular acidosis appears likely [Washburn et al., 2002].
However, a potential role of TASK-1 and TASK-3 in central respiratory chemoreception is still under discussion. Studies on TASK-knockout mice indicated that TASK channels determine the pH-sensitivity of many brainstem respiratory neurons, but do not contribute to central respiratory chemoreception [Mulkey et al., 2007]. In these knockout mice pH-sensitivity of raphe neurons was abolished, while the ventilatory response to CO_2 was not impaired. Further investigations are needed to determine the exact role of TASK-3 in raphe neurons in respiratory control.

4.3.2 Expression of TASK-3 in noradrenergic locus coeruleus neurons

The locus coeruleus (LC) is a small nucleus of noradrenergic neurons located in the rostral tegmentum of the pons. Through a widespread efferent projection system the LC provides the major source of noradrenaline to the forebrain. The LC is involved in the regulation of attention, arousal and the sleep-wake-cycle and also in mechanisms as learning, memory, anxiety and pain. All these mechanisms serve two general functions, the adjustment of the activity state to incoming important or interesting events and the collection and processing of salient information [Sara, 2009]. Accordingly, the LC is involved in a range of psychiatric disorders associated with a dysfunction of cognition and arousal,

including attention-deficit hyperactivity, sleep and arousal disorders or post-traumatic stress disorders [Berridge and Waterhouse, 2003].
Immunocytochemistry of pontine sections revealed very strong TASK-3 immunoreactivity of locus coeruleus neurons (see Fig. 3.24). Beside several motoneurons, TASK-3 expression in LC neurons is strongest compared to all other nuclei. Immunofluorescence double-labeling with anti-TASK-3 and an anti-DBH antibodies showed that all noradrenergic neurons also express the TASK-3 channel. These findings were supported by the detection of TASK-3 mRNA.
Strong expression of TASK-3 mRNA in LC neurons has been reported by the groups of Karschin et al. [2001] and Talley et al. [2001]. These neurons also express TASK-1 mRNA [Talley et al., 2001, Sirois et al., 2000, Karschin et al., 2001, Talley and Bayliss, 2002]. Halothane depresses the neuronal activity of these neurons [Camproux et al., 1996] and TASK-1 channels contribute to the halothane and pH-sensitive current in LC neurons [Sirois et al., 2000, Bayliss et al., 2001]. Accordingly, a role for TASK-1 channels in mediating the hypnotic effects of anesthetics and also the chemosensitivity associated with respiratory control was suggested [Sirois et al., 2000, Bayliss et al., 2001]. Given that TASK-3 is also activated by halothane and inhibited by acidification a role for TASK-3 channels in controlling excitability of LC neurons can be expected as well as a potential contribution of TASK1/TASK-3 heterodimeric channels.
The presence of TASK channels on LC neurons provides a target for modulatory influences, because these channels are regulated by the action of many neurotransmitters [Bayliss et al., 2003]. In electrophysiological experiments LC neurons respond to the application of various neurotransmitters and several afferent pathways using these transmitters have been revealed. The LC receives for example serotoninergic input from dorsal raphe neurons [Pickel et al., 1977] and glutamatergic input from the nucleus gigantocellularis [Ennis and Aston-Jones, 1988]. Serotoninergic and glutamatergic mediated inhibition of TASK-3 channels could, at least partly, contribute to the activating effects of these transmitters upon LC neurons.

4.3.3 TASK-3 expression in histaminergic tuberomammillary neurons

The tuberomammillary nucleus (TM) is a group of neurons located in the posterior hypothalamus that provide the sole source of histamine in the brain [Panula et al., 1984]. Ascending and descending fibers from these neurons innervate most parts of the CNS. The TM is involved in the regulation of arousal and the sleep-wake-cycle. Activity of TM neurons strongly depends on the behavioral state, with no activity during REM sleep, low activity during slow-wave-sleep and tonical firing during waking [Vanni-Mercier et al., 1984]. Furthermore, the TM is involved in the control of other vital functions such as appetite.
Immunocytochemical staining with the anti-TASK-3 antibody revealed TASK-3 immunoreactive neurons in the tuberomammillary nucleus (see Fig. 3.25). In addition, TASK-3 mRNA was detetcted in TM neurons by ISH experiments. Immunofluorescence double-labeling with anti-TASK-3 and anti-histamine decarboxylase supported the expression of TASK-3 channels in histaminergic neurons.
So far, an expression of TASK channels in tuberomammillary neurons was not known. Karschin et al. [2001] reported about the expression in several hypothalamic nuclei, including a strong expression in the premammillary nucleus and a somewhat weaker, but nevertheless strong expression in neurons

of the mammillary nuclei (dorsal and ventral). Higher levels of TASK-3 mRNA in the mammillary nuclei were also detected by Talley and Bayliss [2002]. However, they did not recognize the relevance of TASK-3 expression in tuberomammillary neurons.
Among others, orexin excites the histaminergic neurons of the TM [Eriksson et al., 2001]. In paraventricular hypothalamic neurons (PVT) orexinergic activation is mediated by the suppression of TASK-like channels. Pharmacological investigations argued for a stronger contribution of TASK-3 than of TASK-1 channels [Doroshenko and Renaud, 2009]. It is likely that orexin can also act on TM neurons by mediating the inhibition of TASK-3 channels. However, orexin-induced depolarization of TM neurons was largely unaffected by manipulation of the external K^+ concentration and Eriksson et al. [2001] found strong evidence for an implication of Na^+/Ca^{2+} exchanger and Ca^{2+} channels rather than a K^+ conductance. Therefore, a role of TASK-3 in orexin-mediated depolarization seems to be questionable.
A role of histaminergic neurons in central respiratory control is also discussed. Neurons of the nucleus of the solitary tract (NTS) are heavily innervated by histaminergic fibers [Panula et al., 1984]. A direct activation of NTS neurons by histaminergic efferents following an increase in CO_2 or H^+ may affect central respiratory drive [Panula et al., 1984]. Studies of c-FOS expression following hypercapnic stress identified a subset of tuberomammillary neurons that were activated by an increase in CO_2 [Haxhiu et al., 2001]. Thus, TASK-3 expressed in the TM could contribute to central chemoreception by conferring chemosensitivity to these neurons. Meaning, an increase in pH following hypercapnation may inhibit TASK-3 channels, causing enhanced activity or even depolarization of the TM neurons. Furthermore, tuberomammillary neurons receive monoaminergic innervations, including a serotoninergic input from several raphe nuclei (cell groups B5-B9) and noradrenergic input from C1-C3 and A1-A2 cell groups [Ericson et al., 1989]. TASK-3 channels are inhibited by noradrenalin and 5-HT. Therefore, noradrenergic and serotoninergic innervations of tuberomammillary neurons could influence cell excitability by the modulation of TASK-3 channel activity.

4.3.4 TASK-3 expression in dopaminergic neurons

Dopaminergic neurons are distributed throughout the brain, but two closely related cell groups are most important. The ventral tegmental area (VTA) is a heterogeneous region located in the midline on the bottom of the mesencephalon. Dopaminergic neurons of the VTA innervate a region of the telencephalon, including the prefrontal cortex and parts of the limbic system (accumbens nucleus, amygdala, hippocampus). Accordingly, the VTA has been ascribed a role in the reward system, motivation, cognition and the pathology of several psychiatric disorders and drug addiction [Koob and Nestler, 1997]. The other important dopaminergic cell group lays lateral to the VTA and just dorsal to the cerebral peduncles, the substantia nigra pars compacta (SNc). The SNc is a part of the basal ganglia, provides an input to the basal ganglia circuit and supplies the striatum with dopamine. The SNc plays an important role in motor control [Hodge and Butcher, 1980] and the loss of dopaminergic SNc neurons causes Parkinson's disease [Lev et al., 2003]. Furthermore, the SNc is involved in temporal processing, learned responses to stimuli (conditioning), temporal learning and the pathophysiology of schizophrenia.
Immunocytochemistry of midbrain sections with the anti-TASK-3 antibody shows that TASK-3 is

differentially expressed in neurons of the VTA and SNc and in individual types of VTA neurons. Neurons of the SNc are only very weakly labeled, while most VTA neurons display medium staining intensity with some neurons showing very strong TASK-3 expression (see Fig. 3.26). This is in accordance with ISH studies of Talley and Bayliss [2002] detecting only very low levels of TASK-3 mRNA in the SNc and moderate levels in the VTA. Karschin et al. [2001] reported that only a few neurons of the VTA express moderate levels of TASK-3 mRNA. Granted that immunocytochemistry with the anti-TASK-3 antibody provides a higher sensitivity compared to the *in situ* hybridization studies, those few labeled neurons could be identical with the few strongly TASK-3 immunoreactive neurons seen in our experiments. Given the low expression levels in the SNc, an important role of TASK-3 channels in these neurons seems unlikely. In contrast, the differences in staining intensity between individual VTA neurons are possibly reflective for a stronger expression in a certain subtype of neurons. VTA neurons are classified by the neurotransmitter they contain. Although the VTA is described as an important dopaminergic region, less than 60% of its neurons produce this transmitter [Margolis et al., 2006]. About 35% of VTA neurons are GABAergic and 2-3% are glutamatergic [Nair-Roberts et al., 2008]. A considerably stronger TASK-3 expression in one of these populations could indicate a role of these channels in behaviors or mechanisms associated with this region like the reward system. Immunfluorescence double-labeling experiments with TASK-3 and appropriate marker enzymes could reveal possible differences in TASK-3 expression between dopaminergic, GABAergic and gluthamatergic VTA neurons.

4.3.5 TASK-3 expression in cholinergic neurons of the basal nucleus of Meynert

The basal nucleus of Meynert (NBM) is a group of cholinergic neurons located in the substantia innominata of the basal forebrain and is the main source of acetylcholine for the cerebral cortex. This nucleus is best known from its implication in the pathogenesis of Alzheimer's and also Parkinson's disease. A degeneration of the nucleus leads to a decrease in cholinergic (telencephalic) brain levels causing symptoms like a profound loss of cognitive functions [Ezrin-Waters and Resch, 1986]. A role in learning and memory formation is also under discussion.

Immunocytochemistry of forebrain sections with the anti-TASK-3 antibody displays strong TASK-3 expression in the region of the NBM (see Fig. 3.21). Immunofluorescence double-labeling with anti-TASK-3 and anti-vAChT confirmed the presence of TASK-3 in cholinergic neurons of the basal nucleus of Meynert. Additionally, TASK-3 mRNA was also detected in these neurons. The expression of TASK-3 mRNA in neurons of the NBM had already been described by Karschin et al. [2001], but there are no reports about a TASK-3 expression on the protein level.

TASK-3 expression in neurons of the NBM might be of interest in the treatment of diseases such as Alzheimer's disease. Drugs specific targeting TASK-3 could be helpful in restoring the cell excitability of degenerating cholinergic neurons and thus ameliorate clinical disease symptoms. The same can be proposed for the treatment of diseases such as Parkinson's disease, Huntington's disease, schizophrenia or progressive supranuclear palsy, where a dysfunction or loss of cholinergic striatal interneurons is implicated [Calabresi et al., 2000, Warren et al., 2005, Holt et al., 2005, Picconi et al., 2006].

In the striatum, the giant cholinergic aspiny interneurons provide the sole source of acetylcholine. Therefore, the regulation of their cell excitability is important for many functions of the striatum. They

are involved in the processing of motivationally relevant events [Apicella, 2002], learning [Aosaki et al., 1994] and synaptic plasticity [Wang et al., 2006]. The expression of TASK-3 has been shown on the mRNA [Karschin et al., 2001] and protein level [Berg and Bayliss, 2007]. Immunocytochemical and electrophysiological experiments indicate that TASK-3 is functionally expressed in striatal, cholinergic interneurons and contribute to the membrane potential of these neurons [Berg and Bayliss, 2007]. These results are supported by the detection of TASK-3 mRNA and by immunocytochemical labeling with the new anti-TASK-3 antibody.

4.3.6 TASK-3 expression in motoneurons

Motoneurons mediate the output of the central nervous system, they are the efferent neurons that innervate the muscles of the body, including smooth muscles of the viscera (visceral motoneurons). All vertebrate motoneurons are cholinergic.
The new anti-TASK-3 antibody detected strong TASK-3 expression in all motoneurons examined so far. These include somatic and visceral motoneurons of cranial nerves and also somatic motoneurons of the spinal cord. There are only marginal difference in staining intensity between visceral and somatic motoneurons. TASK-3 expression in the parasympathetic Edinger-Westphal and dorsal vagal nucleus seems to be slightly weaker. Besides dorsal raphe neurons and neurons of the locus coeruleus, motoneurons display the strongest TASK-3 immunoreactivity among all brain neurons. This is in accordance with previous studies reporting about a strong expression of TASK-3 mRNA in cranial and spinal cord motoneurons [Karschin et al., 2001, Talley et al., 2001]. TASK-like currents were detected in somatic motoneurons before the cloning of TASK-3 and had been attributed to TASK-1, which is also strongly expressed in these neurons [Talley et al., 2000, Sirois et al., 2000]. Hypoglossal motoneurons express a background current with characteristic properties best described by TASK-1/TASK-3 heterodimers (e.g. intermediate pH-and isoflurane sensitivity). TASK-like currents in cranial and spinal motoneurons are inhibited by the application of several neurotransmitters such as serotonin, noradrenaline or TRH [Talley et al., 2001]. State-dependent differences in motor activity may be mediated through the inhibition of TASK channels by the action of transmitters associated with behavioral arousal. Furthermore, TASK channels expressed in respiratory motoneurons can directly contribute to their respiratory response, as they are inhibited by acidification following inadequate ventilation [Talley et al., 2001]. The strong TASK channel expression in motoneurons and the fact that they are activated following application of clinical concentrations of volatile anesthetics propose a role in the mediation of the immobilizing effects of anesthetics. TASK knockout mice are less sensitive to the hyperpolarizing effects of halothane and isoflurane and higher concentration of both anesthetics are needed to immobilize the animals [Lazarenko et al., 2010]. The same results were observed when conditional knockout mice were tested that do not express TASK-1 and TASK-3 channels in cholinergic neurons. These results suggest TASK channels as the molecular substrates for the effects of volatile anesthetics at least in spinal motoneurons, because the immobilizing effects of anesthetics are spinally mediated [Lazarenko et al., 2010]. Concluding, TASK-3 and TASK-1 channels in motoneurons are a target for many regulatory mechanisms. Their activation or inhibition by acidification, neurotransmitters or anesthetics leads to an altered cell excitability and therefore an increased or decreased activation of the associated muscles.

4.4 TASK-3 expression in the adrenal gland

The adrenal glands, consisting of a medulla and a surrounding cortex, serve entirely different functions in these two compartments. The adrenal medulla is a part of the autonomic nervous system. Its cells produce adrenaline and noradrenaline that are stored in vesicles and released into the blood stream, especially upon stressful stimuli. The adrenal cortex, by contrast, is organized in three zones. Cells of the outer zona glomerulosa produce mineralcorticoids, the most important being aldosterone regulating the balance of water and electrolytes. Cells of the zona fasciculata predominantly produce glucocorticoids like cortisol in humans or corticosterone in rats. In the zona reticularis glucocorticoids and androgens like androsterone are produced.

A typical feature of glomerulosa cells is their negative resting membrane potenial, conditional on the expression of certain K^+ channels. Among all K^+ channels only a few were found in the adrenal glands. Strong TASK-3 expression in rat adrenal glomerulosa cells was demonstrated in a northern blot study [Czirják and Enyedi, 2002a]. In addition, ISH studies detected high levels of TASK-3 mRNA in zona glomerulosa cells and also in cells of the zona fasciculata and the adrenal medulla [Bayliss et al., 2003]. Immunocytochemistry with our anti-TASK-3 antibody showed that the TASK-3 protein is most prominently expressed ins zona glomerulosa cells (see Fig. 3.28). Inner medullary cells were also strongly labeled, while TASK-3 was not detected in the zona fasciculata and reticularis. This specific expression pattern is in accordance with the previous mentioned reports and confirms the specificity of the anti-TASK-3 antibody. Glomerulosa cells have a very high conductance for K^+ ions. Consequently, their membrane potential closely follows the K^+ equilibrium potential, enabling the cells to react even to small changes in the external K^+ concentrations [Spät and Hunyady, 2004]. An increase of external K^+ leads to a K^+ influx and hence depolarization. This depolarization is the initial stimulus in a chain of events that finally lead to the transcription of aldosterone synthase [Spät and Hunyady, 2004]. Likewise, the inhibition of K^+ channels and the resulting blockade of K^+ efflux can cause depolarization of glomerulosa cells. As a background channel that even remains open at very negative membrane potentials, TASK-3 is a good candidate to mediate the high K^+ conductance of glomerulosa cells. Indeed, there is strong evidence that TASK-3 currents are a major component of the negative resting potassium conductance of these cells. Injection of TASK-3 cDNA and mRNA of zona glomerulosa cells into *Xenopus laevis* oocytes elicited currents with a very similar pharmacological profile [Czirják and Enyedi, 2002a]. An inhibition of TASK-3 channels could depolarize glomerulosa cells leading to the activation of the transcription of aldosterone synthase. A role for TASK-3 channels in the regulation of aldosterone secretion seems likely, because the channels are inhibited by angiotensin II receptor activation and acidification [Czirják and Enyedi, 2002a]. Angiotensin as well as extracellular acidification are known to promote aldosterone secretion [Giacchetti et al., 1996, Radke et al., 1986]. Besides TASK-3, TREK-1 [Enyeart et al., 2004, Brenner and O'Shaughnessy, 2008] and TASK-1 [Czirják et al., 2000, Heitzmann and Warth, 2008] also are strongly expressed in adrenal glomerulosa cells, also inhibited by angiotensin II recpetor activation (TASK-1, TREK-1) and by acidification (TASK-1).

A putative involvement of K_{2P} channels, especially TASK-1 and TASK-3, with disturbed aldosterone homeostasis is currently under investigation. Zona glomerulosa cells of TASK-1/TASK-3 double knockout mice exhibited a notably depolarized membrane potential and an overproduction of aldosterone

[Davies et al., 2008]. These mice show all symptoms typical for primary hyperaldosteronism, therefore serving as an appropriate model to study the mechanisms underlying autonomous aldosterone production. Furthermore, a reduced conductance or expression of TASK channels may underlie some forms of primary hyperaldosteronism.
The expression of TASK-3 in cells of the adrenal medulla suggests an additional role in the regulation of adrenaline and noradrenaline secretion. An increase of the pH in medullary cells induces the release of catecholamines [Fujiwara et al., 1994]. An inhibition of TASK-3 channels by acidification and the resulting depolarization of the membrane potential could be involved with this mechanism. Moreover, the secretion of adrenaline from medullary cells is increased by the activation of muscarinic receptors [Kayaalp and Neff, 1979] and H1 histamine receptors [Borges, 1994]. These receptors are $G_{\alpha q}$-coupled and activation of $G_{\alpha q}$-coupled receptors is known to mediate TASK-3 channel inhibition.

4.5 TASK-3 homodimers or TASK-1/TASK-3 heterodimeric channels

It is well known that the co-assembly of closely related potassium channel subunits provides a mechanism for a increased functional diversity. The resulting heterodimeric channels have characteristics distinct from the homodimers and often intermediary properties, for example a conductance between that of the homodimeric channels. As TASK-1 and TASK-3 channels show a substantial overlap in expression, the co-assembly of these subunits has been discussed for several cell types and brain regions. The formation of heterodimeric TASK-1/TASK-3 channels has first been described in heterologous expression systems. The pH-sensitivity as well as inhibition following AT1a angiotensin II receptor activation I of heterodimers expressed in *Xenopus laevis* oocytes is between that of the individually expressed channels. These heterodimers are insensitive to ruthenium red [Czirják and Enyedi, 2002a]. A contribution of TASK-1/TASK-3 heterodimeric channels to native currents was reported for cultured cerebellar granule neurons [Kang et al., 2004]. In rat carotid body glomus cells TASK-1/TASK-3 heterodimers are the major oxygen-sensitive background channels [Kim et al., 2009].
An overlapping expression of TASK-1 and TASK-3 channels can also be observed in monoaminergic and especially cholinergic neurons. Some of the highest mRNA levels for both channels were found in somatic motoneurons [Karschin et al., 2001, Talley et al., 2001]. Berg et al. [2004] detected high levels of the TASK-3 protein in hypoglossal motoneurons. The pH- and isoflurane sensitivity of TASK-like currents in these neurons could best be described by TASK-1/TASK-3 heterodimers, strongly arguing for a contribution of the co-associated channel subunits to native currents. Immunocytochemical analysis with our TASK-3 antibody show high TASK-3 expression levels in several somatic and visceral motoneurons. All of these neurons also express high levels of TASK-1 mRNA [Karschin et al., 2001]. It is most likely that TASK-1/TASK-3 heterodimeric channels substantially contribute to native background currents of all these motoneurons.
High levels of TASK-1 mRNA were also detected in neurons of the locus coeruleus [Karschin et al., 2001, Talley et al., 2001, Wang et al., 2008] and currents measured in LC neurons displayed kinetic and pharmacological properties identical to cloned TASK-1 channels [Bayliss et al., 2001]. LC neurons also express high levels of TASK-3. Hence, the formation of functional TASK-1/TASK-3 heterodimeric channels in those neurons could be guessed. In raphe neurons only minor TASK-1 mRNA levels were

detected. Regarding the very strong expression of TASK-3 in these neurons, a predominant contribution of TASK-3 homodimeric channels to native currents is likely. Nevertheless, Washburn et al. [2002] isolated TASK-like potassium currents from raphe neurons with a pH-sensitivity intermediate between TASK-1 and TASK-3 channels. This argues for a contribution of heterodimeric channels besides TASK-3 homodimers, giving additional functional properties to raphe neurons. The same can be assumed for neurons of the SNc were only minor TASK-1 mRNA levels were detected [Karschin et al., 2001], but which also demonstrate only weak TASK-3 expression. TASK-1 mRNA was not detected in neurons of the basal nucleus of Meynert. In these neurons TASK-3 activity may predominantly or solely be related to TASK-3 homodimeric channels.

4.6 GPCR-coupling of TASK-3

A particular feature of K_{2P} channels is their regulation by a variety of G protein-coupled receptor (GPCR) pathways. Homo- and heterodimeric TASK channels are inhibited following activation of $G_{\alpha q}$ proteins [Mathie and Veale, 2007]. There are competing hypothesis on the mechanisms of TASK channel inhibition by GPCR activation. The inhibition by the PKC pathway is under discussion. In addition an inhibition by the depletion of PIP_2 from the membrane or a direct regulation of TASK channels by $G_{\alpha q}$ proteins were proposed [Mathie and Veale, 2007].
Among the $G_{\alpha q}$-coupled receptors are the serotoninergic 5-HT2 receptors, cholinergic M1, M3, and M5 receptors, noradrenergic a1 receptors and histaminergic H1 receptors. The inhibition of TASK-3 channels following activation of these receptors has been described in several cell types. In adrenal glomerulosa cells TASK-3 inhibition is mediated by activation of angiotensin II receptors [Czirják and Enyedi, 2002a]. Another example is the inhibition of thalamocortical relay neurons by the activation of muscarinic M3 receptors [Meuth et al., 2003] or the inhibitory action of 5-HT on TASK channels in dorsal vagal motoneurons [Hopwood and Trapp, 2005].
The excitability of cells expressing TASK-3 channels can be modulated by a variety of neurotransmitters such as 5-HT, noradrenaline or acetylcholine. The activation of $G_{\alpha q}$-coupled receptors by neurotransmitter binding inhibits TASK-3 channels. This results in enhanced excitability and a depolarization of the membrane. A multitude of $G_{\alpha q}$-coupled receptors can be found on all analyzed cholinergic and monoaminergic neurons. Activation of all these receptors may result in the inactivation of TASK-3 channels (or TASK-1/TASK-3 heterodimers) to promote cellular activation and increased excitability. This could be of special interest in pathological conditions, when cellular excitability or neurotransmitter release is affected. In the last 20 years a plethora of studies examined the implication of changes in neurotransmitter systems in neuropathological conditions. One of the most discussed examples is the deterioration of the cholinergic system in ageing and neuropsychiatric disorders, especially Alzheimer's disease [Terry and Buccafusco, 2003]. A pharmacological inhibition of TASK-3 could enhance cellular excitability, presumably promoting transmitter release.
On the other hand, the differential localization of TASK-3 channels in monoaminergic and cholinergic cell groups suggests that their expression might be affected in certain pathological conditions. TASK-3 channels are involved in the K^+-dependent apoptosis of cerebellar granule cells [Lauritzen et al., 2003] and their inhibition by ruthenium red or acidification prevents the neuronal death of cultured

granule cells. Furthermore, cell death and cell survival in autoimmune CNS inflammation partly depend on the regulated expression of TASK-1 and TASK-3 [Meuth et al., 2008b]. It can be guessed that an overexpression of TASK-3 channels activates apoptotic pathways, causing neuronal cell death. Pharmacological inhibition of TASK-3 channels might be a possibility to prevent apoptosis of those neurons.

4.7 A role for TASK-3 in the regulation of the sleep-wake-cycle?

Highest TASK-3 levels can be found in monoaminergic and cholinergic neurons. The aforementioned neurons or brain areas are implicated in the regulation of the sleep-wake-cycle. Wakefulness can be characterized by cortical activation as observed in electroencephalograms of the cortex-surface, and by behavioral arousal as seen in electromyograms by enhanced activity of postural muscles. Based on the observation that patient suffering under excessive sleepiness (Economo's encephalitis lethargica) had lesions at the junction of the midbrain and diencephalon, the concept of an ascending arousal system was introduced [Starzl et al., 1951, Moruzzi and Magoun, 1995]. Later, several neuronal cell groups were revealed that promote arousal by the action of specific neurotransmitters [Saper et al., 2001]. There are two major ascending pathways. One pathway mainly arises from cholinergic neurons of the pedunculopontine and laterodorsal tegmental nucleus that activate the cortex by innervating the thalamic relay neurons [Saper et al., 2005]. The second pathway originates from monoaminergic neurons of the brainstem and the caudal hypothalamus and activates neurons of the lateral hypothalamus, the basal forebrain and the cerebral cortex [Jones, 2003]. These monoaminergic cell groups include the LC, the dorsal and median raphe nuclei, the TM and dopaminergic neurons of the ventral periaqueductal grey matter. All these neurons show highest activity during wakefulness, decrease firing during NREM sleep (non-rapid-eye-movement-sleep) and cease firing during REM sleep (rapid-eye-movement-sleep). Their mutual excitatory influences promote maintainance of the waking-state. TASK-3 is strongly expressed in all of these neurons and inhibited by the action of many neurotransmitters, including serotonin, noradrenaline and histamine. In that way, inhibiton of TASK-3 channels may, at least partly, be implicated in the mutual activation of wake-active neurons. Likewise, a disinhibition of TASK-3 channels due to a reduced monoaminergic input could hyperpolarize these neurons, promoting enhanced activity as seen in NREM and REM sleep.
Furthermore, TASK-3 channels might have a special role in the orexinergic control of the sleep-wake-cycle. Orexinergic neurons located in the posterior half of the lateral hypothalamus have an important role in the stabilization of the waking and sleeping state. The transition from sleeping to waking is provided by a mutual inhibition of sleep-active and wake-active neurons. During wakefulness monoaminergic neurons in the raphe, LC and TM are active and inhibit neurons in the ventrolateral preoptic nucleus (VLPO). These neurons become activated at sleep and inhibit the monoaminergic neurons. The stabilization of both states, for example to maintain long awake periods, requires a further control that is provided by the orexinergic system. In the waking state orexinergic neurons are active and innervate monoaminergic neurons, thereby reinforcing their tone. This also results in a strengthened inhibition of VLPO neurons by monoaminergic neurons. On the other hand, the orexinergic neurons receive afferent input from VLPO neurons. If VLPO neurons are activated during

sleeping, they inhibit orexinergic neurons [Saper et al., 2005]. Therefore, in the sleeping state a direct inhibition of monoaminergic neurons and their missing activiation by orexinergic neurons prevents the transition into the waking state.

Orexin mediates its action by the activation of two receptors, orexin 1 receptors and orexin 2 receptors. Both are coupled to $G_{\alpha q}$ proteins. TASK-3 is strongly expressed in DR, LC and TM neurons an inhibited by the activation of $G_{\alpha q}$-coupled receptors. Thus, orexin may exerts its activating effect on the monoaminergic neurons by the inhibition of TASK-3 channels. This seems likely, because orexin also induces activation of paraventricular thalamic neurons by the closure of TASK-3 channels [Doroshenko and Renaud, 2009].

Further support for the hypothesis that TASK-3 channels play a role in the regulation of sleep-wake-cycle and the stabilization of the waking state is given by oberservations on TASK-3 knockout mice. These mice displayed altered natural sleep behavior, with a slower progression from waking to sleeping states and fragmented sleeping episodes [Pang et al., 2009]. Furthermore, Linden et al. [2007] observed altered sleep-wake-behavior of TASK-3 knockout mice with increased nocturnal activity. Although, he proposed that the absence of TASK-3 channels in orexinergic neurons underlies this behavioral change. Another study on TASK-3 knockout mice showed that TASK-3 channels are important for excitability and high-frequency firing of orexinergic neurons [González et al., 2009]. Thus, besides mediating the orexinergic inhibition of monoaminergic neurons, TASK-3 might have a direct role in the orexinergic system by regulating excitability of orexinergic neurons.

The inhibition of TASK-3 channels might also be implicated in the mediation of basal forebrain activation by orexinergic neurons. The basal forebrain is the major source of acetylcholine to the cortex and many of these neurons fire most rapidly during wakefulness and REM sleep. Orexinergic neurons of the hypothalamus project to cholinergic basal forebrain neurons and release orexin during waking. The resulting activation of the cholinergic neurons is thought to play a key role in promoting behavioral arousal [Arrigoni et al., 2010]. TASK-3 channels are strongly expressed in cholinergic neurons of the basal nucleus of Meynert and striatal cholinergic interneurons. Furthermore, scattered neurons in the basal forebrain expose strong TASK-3 immunoreactivity. Immunfluorescence double-labeling experiments with anti-TASK-3 and anti-vAChT revealed the expression of TASK-3 channels in cholinergic neurons of the ventral pallidum, the region of the diagonal band and the medial septum. Though, more detailed analyses are needed to confirm that the strongly TASK-3 immunoreactive neurons of the basal forebrain are cholinergic. Orexinergic inhibition of TASK-3 channels in cholinergic basal forebrain neurons may be implicated in the activation of these neurons during waking and resulting behavioral arousal.

Furthermore, TASK-3 channels expressed in cholinergic neurons are likely candidates for mediating anesthetic actions. TASK-3 channels are activated by clinically relevant doses of volatile anesthetics [Talley and Bayliss, 2002] and TASK-1/TASK-3 double-knockout mice are less sensitive to halothane. A decreased halothane sensitivity to the same extend was observed in conditional knockout mice, lacking TASK channels only in cholinergic neurons [Lazarenko et al., 2010]. Therefore, cholinergic neurons seem to be one of the molecular targets of volatile anesthetics. Activation of TASK-3 channels in cholinergic basal forebrain neurons by anesthetics could hyperpolarize the cells and therefore counteract their activation leading to reduced cortical activation.

An inhibition of TASK-3 channels might also mediate state-dependent modulation of motoneuron activity. In REM-sleep pharyngeal muscle tone is modulated, leading to airway narrowing, increased resistance to breathing and hence sleep induced hypoventilation [Orem et al., 2002]. These effects are caused by the inhibition of the corresponding (hypoglossal) motoneurons during sleep. Reduced hypoglossal motoneuron activity during REM-sleep is at least partially caused by a reduction in the excitatory serotoninergic input from wake-active medullary raphe neurons [Kubin et al., 1998]. TASK - 3 channels are strongly expressed in hypoglossal motoneurons (see Fig. 3.19) and are inhibited by 5-HT. Therefore, a decreased serotoninergic input during sleep might lead to release of inhibition of TASK-3 channels, K^+ efflux, and hence reduced neuronal activity. Inhibition of TASK-3 channels may also mediate the state-dependent-input of noradrenaline, histamine and several other neurotransmitters on respiratory motoneurons.

In conclusion, TASK-3 channels are strongly expressed in neurons of the raphe, locus coeruleus, tuberomammillary and several cholinergic neurons and are sensitive to orexin and many other neurotransmitters. These data are in line with the idea that TASK-3 channels have a role in the regulation of the sleep-wake-cycle, making them potential candidates for the pharmacological treatment of sleep disorders. Drugs specific targeting TASK-3 channels might be used as hypnotics.

Bibliography

L.F. Agnati, D. Guidolin, M. Guescini, S. Genedani, and K. Fuxe. Understanding wiring and volume transmission. *Brain Res Rev*, 64(1):137–59, Sep 2010.

T. Aosaki, H. Tsubokawa, K. Watanabe, A.M. Graybiel, and M. Kimura. Responses of tonically active neurons in the primate's striatum undergo systematic changes during behavioral sensorimotor conditioning. *J. Neurosci.*, 14:3969–3984, 1994.

P. Apicella. Tonically active neurons in the primate striatum and their role in the processing of information about motivationally relevant events. *Eur J Neurosci*, 16(11):2017–26, Dec 2002.

E. Arrigoni, T. Mochizuki, and T. E. Scammell. Activation of the basal forebrain by the orexin/hypocretin neurones. *Acta Physiol (Oxf)*, 198(3):223–35, Mar 2010.

D.A. Bayliss, E.M. Talley, J.E. Sirois, and Q. Lei. TASK-1 is a highly modulated ph-sensitive 'leak' K(+) channel expressed in brainstem respiratory neurons. *Respir Physiol*, 129(1-2):159–74, Dec 2001.

D.A. Bayliss, J.E. Sirois, and E.M. Talley. The TASK family: two-pore domain background K+ channels. *Mol Interv*, 3(4):205–19, 2003.

A.P. Berg and D.A. Bayliss. Striatal cholinergic interneurons express a receptor-insensitive homomeric TASK-3-like background K+ current. *J Neurophysiol*, 97(2):1546–52, 2007.

A.P. Berg, E.M. Talley, J.P. Manger, and D.A. Bayliss. Motoneurons express heteromeric TWIK-related acid-sensitive K+ (TASK) channels containing TASK-1 (KCNK3) and TASK-3 (KCNK9) subunits. *J Neurosci*, 24(30):6693–702, 2004.

C.W. Berridge and B.D. Waterhouse. The locus coeruleus-noradrenergic system: modulation of behavioral state and state-dependent cognitive processes. *Brain Res Brain Res Rev*, 42(1):33–84, Apr 2003.

A. Besana, A. Barbuti, M.A Tateyama, A.J Symes, R.B. Robinson, and S.J.J Feinmark. Activation of protein kinase c epsilon inhibits the two-pore domain K+ channel, TASK-1, inducing repolarization abnormalities in cardiac ventricular myocytes. *J Biol Chem*, 279(32):33154–60, Aug 2004.

R. Borges. Histamine H1 receptor activation mediates the preferential release of adrenaline in the rat adrenal gland. *Life Sci*, 54(9):631–40, 1994.

T. Brenner and K.M. O'Shaughnessy. Both TASK-3 and TREK-1 two-pore loop K channels are expressed in H295R cells and modulate their membrane potential and aldosterone secretion. *Am J Physiol Endocrinol Metab*, 295(6):1480–6, 2008.

S. G. Brickley, M. I. Aller, C. Sandu, E. L. Veale, F. G. Alder, H. Sambi, A. Mathie, and W. Wisden. TASK-3 two-pore domain potassium channels enable sustained high-frequency firing in cerebellar granule neurons. *J Neurosci*, 27(35):9329–40, 2007.

K. J. Buckler, B. A. Williams, and E. Honore. An oxygen-, acid- and anaesthetic-sensitive TASK-like background potassium channel in rat arterial chemoreceptor cells. *J Physiol*, 525 Pt 1:135–42, 2000.

J. A. Büttner-Ennever and U. Büttner. Neuroanatomy of the ocular motor pathways. *Baillieres Clin Neurol*, 1(2):263–87, Aug 1992.

P. Calabresi, D. Centonze, P. Gubellini, A. Pisani, and G. Bernardi. Acetylcholine-mediated modulation of striatal function. *Trends Neurosci*, 23(3):120–6, Mar 2000.

R. Callahan, D.A. Labunskiy, A. Logvinova, M. Abdallah, C. Liu, J.F. Cotten, and C.S. Yost. Immunolocalization of TASK-3 (KCNK9) to a subset of cortical neurons in the rat cns. *Biochem Biophys Res Commun*, 319(2):525–30, Jun 2004.

A.C. Camproux, F. Saunier, G. Chouvet, J.C. Thalabard, and G. Thomas. A hidden markov model approach to neuron firing patterns. *Biophys J*, 71(5):2404–12, Nov 1996.

A. Carlsson. The current status of the dopamine hypothesis of schizophrenia. *Neuropsychopharmacology*, 1(3):179–86, Sep 1988.

K.G. Chandy and G.A. Gutman. Nomenclature for mammalian potassium channel genes. *Trends Pharmacol Sci*, 14(12):434, Dec 1993.

J. Chemin, C. Girard, F. Duprat, F. Lesage, G. Romey, and M. Lazdunski. Mechanisms underlying excitatory effects of group i metabotropic glutamate receptors via inhibition of 2P domain K+ channels. *EMBO J*, 22(20):54035411, October 2003.

X. Chen, E.M. Talley, N. Patel, A. Gomis, W.E. McIntire, B. Dong, F. Viana, J.C. Garrison, and D.A. Bayliss. Inhibition of a background potassium channel by gq protein α-subunits. *Proceedings of the National Academy of Sciences of the United States of America*, 103(9):34223427, February 2006.

S. J. Chinta and J. K. Andersen. Dopaminergic neurons. *Int J Biochem Cell Biol*, 37(5):942–6, May 2005.

A. H. Coons, H. J. Creech, R.N. Jones, and E. Berliner. The demonstration of pneumococcal antigen in tissues by the use of fluorescent antibody. *J. Immunol.*, 45(159-170), 1942.

I. Creese, D.R. Burt, and S.H. Snyder. Dopamine receptor binding predicts clinical and pharmacological potencies of antischizophrenic drugs. *Science*, 192(4238):481–3, Apr 1976.

G. Czirják and P. Enyedi. Formation of functional heterodimers between the TASK-1 and TASK-3 two-pore domain potassium channel subunits. *J Biol Chem*, 277(7):5426–32, 2002a.

G. Czirják and P. Enyedi. TASK-3 dominates the background potassium conductance in rat adrenal glomerulosa cells. *Mol Endocrinol*, 16(3):621–9, 2002b.

G. Czirják and P. Enyedi. Ruthenium red inhibits TASK-3 potassium channel by interconnecting glutamate 70 of the two subunits. *Mol Pharmacol*, 63(3):646–52, 2003.

G. Czirják, T. Fischer, A. Spat, F. Lesage, and P. Enyedi. TASK (TWIK-related acid-sensitive K+ channel) is expressed in glomerulosa cells of rat adrenal cortex and inhibited by angiotensin ii. *Mol Endocrinol*, 14(6):863–74, 2000.

G. Czirják, G. L. Petheo, A. Spat, and P. Enyedi. Inhibition of TASK-1 potassium channel by phospholipase C. *Am J Physiol Cell Physiol*, 281(2):C700–8, 2001.

A. Dahlstroem and K. Fuxe. Evidence for the existence of monoamine-containing neurons in the central nervous system. I. Demonstration of monoamines in the cell bodies of brain stem neurons. *Acta Physiol Scand Suppl*, pages SUPPL 232:1–55, 1964.

L.A. Davies, C. Hu, N.A. Guagliardo, N. Sen, X. Chen, E.M. Talley, R.M. Carey, D.A. Bayliss, and P.Q. Barrett. TASK channel deletion in mice causes primary hyperaldosteronism. *Proc Natl Acad Sci U S A*, 105(6):2203–8, 2008.

N. Decher, M. Maier, W. Dittrich, J. Gassenhuber, A. Bruggemann, A. E. Busch, and K. Steinmeyer. Characterization of TASK-4, a novel member of the ph-sensitive, two-pore domain potassium channel family. *FEBS Lett*, 492(1-2):84–9, 2001.

P. Doroshenko and L. P. Renaud. Acid-sensitive TASK-like K(+) conductances contribute to resting membrane potential and to orexin-induced membrane depolarization in rat thalamic paraventricular nucleus neurons. *Neuroscience*, 158(4):1560–70, 2009.

F. Duprat, F. Lesage, M. Fink, R. Reyes, C. Heurteaux, and M. Lazdunski. Task, a human background K+ channel to sense external pH variations near physiological pH. *EMBO J*, 16(17):54645471, September 1997.

M. Ennis and G. Aston-Jones. Activation of locus coeruleus from nucleus paragigantocellularis: a new excitatory amino acid pathway in brain. *J Neurosci*, 8(10):3644–57, Oct 1988.

J.A. Enyeart, S.J. Danthi, and J.J. Enyeart. TREK-1 K+ channels couple angiotensin II receptors to membrane depolarization and aldosterone secretion in bovine adrenal glomerulosa cells. *Am J Physiol Endocrinol Metab*, 287(6):E1154–65, 2004.

P. Enyedi and G. Czirják. Molecular background of leak K+ currents: two-pore domain potassium channels. *Physiol Rev*, 90(2):559–605, Apr 2010.

H. Ericson, A. Blomquist, and C. Kohler. Brainstem merents to the tuberornammillary nucleus in the rat brain with special reference to brainstem afferents to the tuberomammillary nucleus in the rat brain with special reference to monoaminergic innervation. *J. Comp. Neurol.*, 281(169-192), 1989.

K.S. Eriksson, O. Sergeeva, R.E. Brown, and H.L. Haas. Orexin/hypocretin excites the histaminergic neurons of the tuberomammillary nucleus. *J Neurosci*, 21(23):9273–9, Dec 2001.

Dirk Eulitz, Harald Prüss, Christian Derst, and Rüdiger W Veh. Heterogeneous distribution of Kir3 potassium channel proteins within dopaminergic neurons in the mesencephalon of the rat brain. *Cell Mol Neurobiol*, 27(3):285–302, May 2007.

C. Ezrin-Waters and L. Resch. The nucleus basalis of meynert. *Can J Neurol Sci*, 13(1):8–14, Feb 1986.

J.L. Feldman and C.A. Del Negro. Looking for inspiration: new perspectives on respiratory rhythm. *Nat Rev Neurosci*, 7(3):232–42, Mar 2006.

N. Fujiwara, A. Warashina, and K. Shimoji. Characterization of low pH-induced catecholamine secretion in the rat adrenal medulla. *J Neurochem*, 62(5):1809–15, May 1994.

K. Fuxe. Evidence for the existence of monoamine neurons in the central nervous system. iv. distribution of monoamine nerve terminals in the central nervous system. *Acta Physiol Scand Suppl*, pages SUPPL 247:37+, 1965.

G. Gárdián and L. Vécsei. Medical treatment of Parkinson's disease: today and the future. *Int J Clin Pharmacol Ther*, 48(10):633–642, 2010.

G. Giacchetti, G. Opocher, R. Sarzani, A. Rappelli, and F. Mantero. Angiotensin II and the adrenal. *Clin Exp Pharmacol Physiol*, 23 Suppl 3:S119–24, Sep 1996.

S.A. Goldstein, D. Bockenhauer, I. O'Kelly, and N. Zilberberg. Potassium leak channels and the KCNK family of two-p-domain subunits. *Nat Rev Neurosci*, 2(3):175–84, 2001.

J. A. González, L. T. Jensen, S. E. Doyle, M. Miranda-Anaya, M. Menaker, L. Fugger, D. A. Bayliss, and D. Burdakov. Deletion of task1 and task3 channels disrupts intrinsic excitability but does not abolish glucose or ph responses of orexin/hypocretin neurons. *Eur J Neurosci*, 30(1):57–64, Jul 2009.

G. A. Gutman, J. P. Chandy, K. G.and Adelman, D. A. Aiyar, J.and Bayliss, D. E. Clapham, M. Covarriubias, G. V. Desir, B. Furuichi, K. andGanetzky, M. L. Garcia, S. Grissmer, L. Y. Jan, A. Karschin, D. Kim, S. Kuperschmidt, Y. Kurachi, M. Lazdunski, F. Lesage, H. A. Lester, D. McKinnon, C. G. Nichols, I. O'Kelly, J. Robbins, G. A. Robertson, B. Rudy, M. Sanguinetti, S. Seino, W. Stuehmer, M. M. Tamkun, C. A. Vandenberg, A. Wei, Wulff H., and R. S. Wymore. International Union of Pharmacology. XLI. compendium of voltage-gated ion channels: potassium channels. *Pharmacol Rev*, 55(4):583–6, 2003.

H. Haas and P. Panula. The role of histamine and the tuberomamillary nucleus in the nervous system. *Nat Rev Neurosci*, 4(2):121–30, Feb 2003.

M.E. Hartness, A. Lewis, G.J. Searle, I. O'Kelly, C. Peers, and P.J. Kemp. Combined antisense and pharmacological approaches implicate hTASK as an airway O(2) sensing K(+) channel. *J Biol Chem*, 276(28):26499–508, 2001.

M.A. Haxhiu, F. Tolentino-Silva, G. Pete, P. Kc, and S.O. Mack. Monoaminergic neurons, chemosensation and arousal. *Respir Physiol*, 129(1-2):191–209, Dec 2001.

D. Heitzmann and R. Warth. Physiology and pathophysiology of potassium channels in gastrointestinal epithelia. *Physiol Rev*, 88(3):1119–82, Jul 2008.

H. Hibino, A. Inanobe, K. Furutani, S. Murakami, I. Findlay, and Y. Kurachi. Inwardly Rectifying Potassium Channels: Their Structure, Function, and Physiological Roles. *Physiol. Rev.*, 90(1): 291–366, 2010.

C. F. Hinrichsen and C. D. Watson. The facial nucleus of the rat: representation of facial muscles revealed by retrograde transport of horseradish peroxidase. *Anat Rec*, 209(3):407–15, Jul 1984.

G.K. Hodge and L.L. Butcher. Pars compacta of the substantia nigra modulates motor activity but is not involved importantly in regulating food and water intake. *Naunyn Schmiedebergs Arch Pharmacol*, 313(1):51–67, 1980.

D.J. Holt, S.E. Bachus, T.M. Hyde, M. Wittie, M.M. Herman, M. Vangel, C.B. Saper, and J. Kleinman. Reduced density of cholinergic interneurons in the ventral striatum in schizophrenia: an in situ hybridization study. *Biol Psychiatry*, 58(5):408–16, Sep 2005.

S.E. Hopwood and S. Trapp. TASK-like K+ channels mediate effects of 5-HT and extracellular pH in rat dorsal vagal neurones in vitro. *J Physiol*, 568(Pt 1):145–54, 2005.

J.-P. Hornung. The human raphe nuclei and the serotonergic system. *J Chem Neuroanat*, 26(4): 331–43, Dec 2003.

M. Inoue, K. Harada, H. Matsuoka, T. Sata, and A. Warashina. Inhibition of TASK1-like channels by muscarinic receptor stimulation in rat adrenal medullary cells. *J Neurochem*, 106(4):1804–14, 2008.

K. Itoi and N. Sugimoto. The brainstem noradrenergic systems in stress, anxiety and depression. *J Neuroendocrinol*, 22(5):355–61, May 2010.

W Jänig. Neurobiology of visceral afferent neurons: neuroanatomy, functions, organ regulations and sensations. *Biol Psychol*, 42(1-2):29–51, Jan 1996.

M. Jenke, A. Sánchez, F. Monje, W. Stühmer, R. M. Weseloh, and L. A. Pardo. C-terminal domains implicated in the functional surface expression of potassium channels. *EMBO J*, 22(3):395–403, Feb 2003.

Barbara E. Jones. Arousal systems. *Front Biosci*, 8:s438–51, May 2003.

D. Kang, J. Han, E.M. Talley, D.A. Bayliss, and D. Kim. Functional expression of TASK-1/TASK-3 heteromers in cerebellar granule cells. *J Physiol*, 554(Pt 1):64–77, 2004.

A.G. Karczmar. Brief presentation of the story and present status of studies of the vertebrate cholinergic system. *Neuropsychopharmacology*, 9(3):181–99, Nov 1993.

C. Karschin, E. Wischmeyer, R. Preisig-Müller, S. Rajan, C. Derst, K.H. Grzeschik, J. Daut, and A. Karschin. Expression pattern in brain of TASK-1, TASK-3, and a tandem pore domain K(+) channel subunit, TASK-5, associated with the central auditory nervous system. *Mol Cell Neurosci*, 18(6):632–48, 2001.

S. O. Kayaalp and N. H. Neff. Muscarinic receptor binding in the rat adrenal medulla. *Eur J Pharmacol*, 57(2-3):255–7, Aug 1979.

K.A. Ketchum, W.J. Joiner, A.J. Sellers, L.K. Kaczmarek, and S.A. Goldstein. A new family of outwardly rectifying potassium channel proteins with two pore domains in tandem. *Nature*, 376 (6542):690695, Aug 1995.

D. Kim and C. Gnatenco. TASK-5, a new member of the tandem-pore K(+) channel family. *Biochem Biophys Res Commun*, 284(4):923–30, 2001.

J.E. Kim, S.E. Kwak, and T.C. Kang. Upregulated TWIK-related acid-sensitive K+ channel-2 in neurons and perivascular astrocytes in the hippocampus of experimental temporal lobe epilepsy. *Epilepsia*, 50(4):654–63, 2009.

Y. Kim, H. Bang, and D. Kim. TASK-3, a new member of the tandem pore K(+) channel family. *J Biol Chem*, 275(13):9340–7, 2000.

G. F. Koob and E. J. Nestler. The neurobiology of drug addiction. *J Neuropsychiatry Clin Neurosci*, 9(3):482–97, 1997.

L. Kubin, R. O. Davies, and A. I. Pack. Control of upper airway motoneurons during rem sleep. *News Physiol Sci*, 13:91–97, Apr 1998.

M. Lader. The peripheral and central role of the catecholamines in the mechanisms of anxiety. *Int Pharmacopsychiatry*, 9(3):125–37, 1974.

P.M. Larkman and E.M. Perkins. A TASK-like pH- and amine-sensitive 'leak' K+ conductance regulates neonatal rat facial motoneuron excitability in vitro. *Eur J Neurosci*, 21(3):679–91, 2005.

I. Lauritzen, M. Zanzouri, E. Honore, F. Duprat, M.U. Ehrengruber, M. Lazdunski, and A.J. Patel. K+-dependent cerebellar granule neuron apoptosis. role of TASK leak K+ channels. *J Biol Chem*, 278(34):32068–76, 2003.

R.M. Lazarenko, S.C. Willcox, S. Shu, A.P. Berg, V. Jevtovic-Todorovic, E.M. Talley, X. Chen, and D.A. Bayliss. Motoneuronal TASK channels contribute to immobilizing effects of inhalational general anesthetics. *J Neurosci*, 30(22):7691–704, Jun 2010.

F. Lesage and M. Lazdunski. Molecular and functional properties of two-pore-domain potassium channels. *Am J Physiol Renal Physiol*, 279(5):F793–801, 2000.

F. Lesage, E. Guillemare, M. Fink, F. Duprat, M. Lazdunski, G. Romey, and J. Barhanin. TWIK-1, a ubiquitous human weakly inward rectifying K+ channel with a novel structure. *Embo J*, 15(5): 1004–11, 1996.

N. Lev, E. Melamed, and D. Offen. Apoptosis and parkinson's disease. *Prog Neuropsychopharmacol Biol Psychiatry*, 27(2):245–50, Apr 2003.

A.M. Linden, C. Sandu, M.I. Aller, O.Y. Vekovischeva, P.H. Rosenberg, W. Wisden, and E.R. Korpi. TASK-3 knockout mice exhibit exaggerated nocturnal activity, impairments in cognitive functions, and reduced sensitivity to inhalation anesthetics. *J Pharmacol Exp Ther*, 323(3):924–34, 2007.

C. Liu, J.F. Cotten, J.A. Schuyler, C.S. Fahlman, J.D. Au, P.E. Bickler, and C.S. Yost. Protective effects of TASK-3 (KCNK9) and related 2P K channels during cellular stress. *Brain Res*, 1031(2): 164–73, 2005.

C.M.B. Lopes, P.G. Gallagher, M.E. Buck, M.H. Butler, and S.A.N. Goldstein. Proton block and voltage gating are potassium-dependent in the cardiac leak channel KCNK3. *Journal of Biological Chemistry*, 275(22):1696916978, June 2000.

C.M.B. Lopes, T. Rohács, G. Czirják, T. Balla, P. Enyedi, and D.E. Logothetis. PIP2 hydrolysis underlies agonist-induced inhibition and regulates voltage gating of two-pore domain K+ channels. *The Journal of Physiology*, 564(1):117129, April 2005.

D.P. Lotshaw. Biophysical and pharmacological characteristics of native two-pore domain TASK channels in rat adrenal glomerulosa cells. *J Membr Biol*, 210(1):51–70, 2006.

I. Lucki. The spectrum of behaviors influenced by serotonin. *Biol Psychiatry*, 44(3):151–62, Aug 1998.

A. Lupas. Coiled coils: new structures and new functions. *Trends Biochem Sci*, 21(10):375–82, Oct 1996.

F. Maingret, A.J. Patel, M. Lazdunski, and E. Honoré. The endocannabinoid anandamide is a direct and selective blocker of the background K(+) channel TASK-1. *EMBO J*, 20(1-2):47–54, Jan 2001.

E. B. Margolis, H. Lock, G. O. Hjelmstad, and H. L. Fields. The ventral tegmental area revisited: is there an electrophysiological marker for dopaminergic neurons? *J Physiol*, 577(Pt 3):907–24, Dec 2006.

A. Martorana, Z. Esposito, and G. Koch. Beyond the cholinergic hypothesis: do current drugs work in alzheimer's disease? *CNS Neurosci Ther*, 16(4):235–45, Aug 2010.

A. Mathie and E.L. Veale. Therapeutic potential of neuronal two-pore domain potassium-channel modulators. *Curr Opin Investig Drugs*, 8(7):555–62, 2007.

H.J. Meadows and A.D. Randall. Functional characterisation of human TASK-3, an acid-sensitive two-pore domain potassium channel. *Neuropharmacology*, 40(4):551–9, 2001.

M.M. Mesulam, E. J. Mufson, B.H. Wainer, and A.I. Levey. Central cholinergic pathways in the rat: an overview based on an alternative nomenclature (Ch1-Ch6). *Neuroscience*, 10(4):1185–201, Dec 1983.

S.G. Meuth, T. Budde, T. Kanyshkova, T. Broicher, T. Munsch, and H.C. Pape. Contribution of TWIK-related acid-sensitive K+ channel 1 (TASK1) and TASK3 channels to the control of activity modes in thalamocortical neurons. *J Neurosci*, 23(16):6460–9, 2003.

S.G. Meuth, T. Kanyshkova, P. Meuth, P. Landgraf, T. Munsch, A. Ludwig, F. Hofmann, H.C. Pape, and T. Budde. Membrane resting potential of thalamocortical relay neurons is shaped by the interaction among TASK3 and HCN2 channels. *J Neurophysiol*, 96(3):1517–29, 2006.

S.G. Meuth, A.M. Herrmann, C.W. Ip, T. Kanyshkova, S. Bittner, A. Weishaupt, T. Budde, and H. Wiendl. The two-pore domain potassium channel TASK3 functionally impacts glioma cell death. *J Neurooncol*, 87(3):263–70, 2008a.

S.G. Meuth, T. Kanyshkov, N. Melzer, S. Bittner, B.C. Kieseier, T. Budde, and H. Wiendl. Altered neuronal expression of TASK1 and TASK3 potassium channels in rodent and human autoimmune CNS inflammation. *Neurosci Lett*, 446(2-3):133–8, 2008b.

S.G. Meuth, C. Kleinschnitz, T. Broicher, M. Austinat, S. Braeuninger, S. Bittner, S. Fischer, D.A. Bayliss, T. Budde, G. Stoll, and H. Wiendl. The neuroprotective impact of the leak potassium channel TASK1 on stroke development in mice. *Neurobiol Dis*, 33(1):1–11, Jan 2009.

J.A. Millar, L. Barratt, A.P. Southan, K.M. Page, R.E. Fyffe, B. Robertson, and A. Mathie. A functional role for the two-pore domain potassium channel TASK-1 in cerebellar granule neurons. *Proc Natl Acad Sci U S A*, 97(7):3614–8, 2000.

M. Morton, A. O'Connell, A. Sivaprasadarao, and M. Hunter. Determinants of ph sensing in the two-pore domain K+ channels TASK-1 and -2. *Pflügers Archiv European Journal of Physiology*, 445(5):577583, February 2003.

G. Moruzzi and H. W. Magoun. Brain stem reticular formation and activation of the EEG. 1949. *J Neuropsychiatry Clin Neurosci*, 7(2):251–67, 1995.

D. Mu, L. Chen, X. Zhang, L.H. See, C.M. Koch, C. Yen, J.J. Tong, L. Spiegel, K.C. Nguyen, A. Servoss, Y. Peng, L. Pei, J.R. Marks, S. Lowe, T. Hoey, L.Y. Jan, W.R. McCombie, M. Wigler, and S. Powers. Genomic amplification and oncogenic properties of the KCNK9 potassium channel gene. *Cancer Cell*, 3(3):297–302, 2003.

D.K. Mulkey, E.M. Talley, R.L. Stornetta, A. R. Siegel, G.H. West, X. Chen, N. Sen, A. M. Mistry, P.G. Guyenet, and D.A. Bayliss. TASK channels determine pH sensitivity in select respiratory neurons but do not contribute to central respiratory chemosensitivity. *J Neurosci*, 27(51):14049–58, 2007.

R. G. Nair-Roberts, S. D. Chatelain-Badie, E. Benson, H. White-Cooper, J. P. Bolam, and M. A. Ungless. Stereological estimates of dopaminergic, gabaergic and glutamatergic neurons in the ventral tegmental area, substantia nigra and retrorubral field in the rat. *Neuroscience*, 152(4):1024–31, Apr 2008.

E. Nattie. CO2, brainstem chemoreceptors and breathing. *Prog Neurobiol*, 59(4):299–331, Nov 1999.

M.I. Niemeyer, F.D. Gonzalez-Nilo, L. Zuniga, W. Gonzalez, L.P. Cid, and F.V. Sepulveda. Gating of two-pore domain K+ channels by extracellular ph. *Biochem Soc Trans*, 34(Pt 5):899–902, 2006.

J. Orem, A. T. Lovering, W. Dunin-Barkowski, and E. H. Vidruk. Tonic activity in the respiratory system in wakefulness, NREM and REM sleep. *Sleep*, 25(5):488–96, Aug 2002.

D. S. J. Pang, C. J. Robledo, D. R. Carr, T. C. Gent, A. L. Vyssotski, A. Caley, A. Y. Zecharia, W. Wisden, S. G. G Brickley, and N. P. Franks. An unexpected role for TASK-3 potassium channels in network oscillations with implications for sleep mechanisms and anesthetic action. *Proc Natl Acad Sci U S A*, 106(41):17546–51, Oct 2009.

P. Panula, H.Y. Yang, and E. Costa. Histamine-containing neurons in the rat hypothalamus. *Proc Natl Acad Sci U S A*, 81(8):2572–6, Apr 1984.

D.M. Papazian, T.L. Schwarz, B.L. Tempel, Jan. Y.N., and L.Y. Jan. Cloning of genomic and complementary DNA from shaker, a putative potassium channel gene from drosophila. *Science*, 237 (4816):749753, Aug 1987.

A. Parent. Functional anatomy and evolution of monoaminergic systems. *Am Zool*, 24(3):738–790, 1984.

A.J. Patel and E. Honoré. Molecular physiology of oxygen-sensitive potassium channels. *Eur Respir J*, 18(1):221–7, Jul 2001.

A.J. Patel, E. Honoré, F. Lesage, M. Fink, G. Romey, and M. Lazdunski. Inhalational anesthetics activate two-pore-domain background K+ channels. *Nat Neurosci*, 2(5):422–6, 1999.

L. Pei, O. Wiser, A. Slavin, D. Mu, S. Powers, L.Y. Jan, and T. Hoey. Oncogenic potential of TASK3 (KCNK9) depends on K+ channel function. *Proc Natl Acad Sci U S A*, 100(13):7803–7, 2003.

B. Pettmann and C.E. Henderson. Neuronal cell death. *Neuron*, 20(4):633–47, Apr 1998.

B. Picconi, E. Passino, C. Sgobio, P. Bonsi, I. Barone, V. Ghiglieri, A. Pisani, G. Bernardi, M. Ammassari-Teule, and P. Calabresi. Plastic and behavioral abnormalities in experimental huntington's disease: a crucial role for cholinergic interneurons. *Neurobiol Dis*, 22(1):143–52, Apr 2006.

V.M. Pickel, T.H. Joh, and D.J. Reis. A serotonergic innervation of noradrenergic neurons in nucleus locus coeruleus: demonstration by immunocytochemical localization of the transmitter specific enzymes tyrosine and tryptophan hydroxylase. *Brain Res*, 131(2):197–214, Aug 1977.

K. Pocsai, L. Kosztka, G. Bakondi, M. Gonczi, J. Fodor, B. Dienes, P. Szentesi, I. Kovacs, R. Feniger-Barish, E. Kopf, D. Zharhary, G. Szucs, L. Csernoch, and Z. Rusznak. Melanoma cells exhibit strong intracellular TASK-3-specific immunopositivity in both tissue sections and cell culture. *Cell Mol Life Sci*, 63(19-20):2364–76, 2006.

W. Pradidarcheep, W.T. Labruyere, N.F. Dabhoiwala, and W.H. Lamers. Lack of specificity of commercially available antisera: Better specifications needed. *J Histochem Cytochem*, 56(12):1099–1111, 2008.

H. Prüss, C. Derst, R. Lommel, and R.W. Veh. Differential distribution of individual subunits of strongly inwardly rectifying potassium channels (Kir2 family) in rat brain. *Brain Res Mol Brain Res*, 139(1):63–79, Sep 2005.

K. J. Radke, E. G. Schneider, R. E. Taylor, Jr, and R. E. Kramer. Effect of hydrogen ion concentration on corticosteroid secretion. *Am J Physiol*, 250(3 Pt 1):E259–64, Mar 1986.

S. Rajan, E. Wischmeyer, G. Xin Liu, R. Preisig-Müller, J. Daut, A. Karschin, and C. Derst. TASK-3, a novel tandem pore domain acid-sensitive K+ channel. an extracellular histiding as pH sensor. *J Biol Chem*, 275(22):16650–7, 2000.

S. Rajan, R. Preisig-Müller, E. Wischmeyer, R. Nehring, P. J. Hanley, V. Renigunta, B. Musset, G. Schlichthorl, C. Derst, A. Karschin, and J. Daut. Interaction with 14-3-3 proteins promotes functional expression of the potassium channels TASK-1 and TASK-3. *J Physiol*, 545(Pt 1):13–26, 2002.

R. Reyes, F. Duprat, F. Lesage, M. Fink, M. Salinas, N. Farman, and M. Lazdunski. Cloning and expression of a novel ph-sensitive two pore domain K+ channel from human kidney. *J Biol Chem*, 273(47):30863–9, 1998.

G.B. Richerson. Response to co2 of neurons in the rostral ventral medulla in vitro. *J Neurophysiol*, 73(3):933–44, Mar 1995.

Z. Rusznak, K. Pocsai, I. Kovacs, A. Por, B. Pal, T. Biro, and G. Szucs. Differential distribution of TASK-1, TASK-2 and TASK-3 immunoreactivities in the rat and human cerebellum. *Cell Mol Life Sci*, 61(12):1532–42, 2004.

C. B. Saper, T. C. Chou, and T. E. Scammell. The sleep switch: hypothalamic control of sleep and wakefulness. *Trends Neurosci*, 24(12):726–31, Dec 2001.

C. B. Saper, T. E. Scammell, and J. Lu. Hypothalamic regulation of sleep and circadian rhythms. *Nature*, 437(7063):1257–63, Oct 2005.

C.B. Saper. A guide to the perplexed on the specificity of antibodies. *J Histochem Cytochem*, 57(1): 1–5, 2009.

S. J. Sara. The locus coeruleus and noradrenergic modulation of cognition. *Nat Rev Neurosci*, 10(3): 211–23, Mar 2009.

A. Sawczuk and K. M. Mosier. Neural control of tongue movement with respect to respiration and swallowing. *Crit Rev Oral Biol Med*, 12(1):18–37, 2001.

M. Schwake, D. Athanasiadu, C. Beimgraben, J. Blanz, C. Beck, T. J Jentsch, P. Saftig, and T. Friedrich. Structural determinants of M-type KCNQ (Kv7) K+ channel assembly. *J Neurosci*, 26(14):3757–66, Apr 2006.

J.C. Schwartz, J.M. Arrang, M. Garbarg, H. Pollard, and M. Ruat. Histaminergic transmission in the mammalian brain. *Physiol Rev*, 71(1):1–51, Jan 1991.

J.E. Sirois, Q. Lei, E.M. Talley, C. Lynch, and D.A. Bayliss. The TASK-1 two-pore domain K+ channel is a molecular substrate for neuronal effects of inhalation anesthetics. *J Neurosci*, 20(17): 6347–54, 2000.

A. Spät and L. Hunyady. Control of aldosterone secretion: a model for convergence in cellular signaling pathways. *Physiol Rev*, 84(2):489–539, Apr 2004.

T. E. Starzl, C. W. Taylor, and H. W. Magoun. Ascending conduction in reticular activating system, with special reference to the diencephalon. *J Neurophysiol*, 14(6):461–77, Nov 1951.

H. H. Subramanian and G. Holstege. The nucleus retroambiguus control of respiration. *J Neurosci*, 29(12):3824–32, Mar 2009.

E.M. Talley and D.A. Bayliss. Modulation of TASK-1 (KCNK3) and TASK-3 (KCNK9) potassium channels: volatile anesthetics and neurotransmitters share a molecular site of action. *J Biol Chem*, 277(20):17733–42, 2002.

E.M. Talley, Q. Lei, J.E. Sirois, and D.A. Bayliss. TASK-1, a two-pore domain K+ channel, is modulated by multiple neurotransmitters in motoneurons. *Neuron*, 25(2):399–410, 2000.

E.M. Talley, G. Solorzano, Q. Lei, D. Kim, and D.A. Bayliss. CNS distribution of members of the two-pore-domain (KCNK) potassium channel family. *J Neurosci*, 21(19):7491–505, 2001.

Z.Y. Tan, Y. Lu, C.A. Whiteis, C.J. Benson, M.W. Chapleau, and F.M. Abboud. Acid-sensing ion channels contribute to transduction of extracellular acidosis in rat carotid body glomus cells. *Circ Res*, 101(10):1009–19, 2007.

A. V. Terry, Jr and J. J. Buccafusco. The cholinergic hypothesis of age and alzheimer's disease-related cognitive deficits: recent challenges and their implications for novel drug development. *J Pharmacol Exp Ther*, 306(3):821–7, Sep 2003.

F. Theilig, I. Goranova, J.R. Hirsch, M. Wieske, S. Unsal, S. Bachmann, R.W. Veh, and C. Derst. Cellular localization of thik-1 (K(2P)13.1) and THIK-2 (K(2P)12.1) K channels in the mammalian kidney. *Cell Physiol Biochem*, 21(1-3):63–74, 2008.

C.L. Torborg, A.P. Berg, B.W. Jeffries, D.A. Bayliss, and C.J. McBain. TASK-like conductances are present within hippocampal ca1 stratum oriens interneuron subpopulations. *J Neurosci*, 26(28): 7362–7, 2006.

G. Vanni-Mercier, K. Sakai, and M. Jouvet. Specific neurons for wakefulness in the posterior hypothalamus in the cat. *C R Acad Sci III*, 298:195–200, 1984.

E.L. Veale, L.E. Kennard, G.L. Sutton, G. MacKenzie, C. Sandu, and A. Mathie. G(alpha)q-mediated regulation of TASK3 two-pore domain potassium channels: the role of protein kinase c. *Mol Pharmacol*, 71(6):1666–75, 2007.

E. Vega-Saenz de Miera, D.H. Lau, M. Zhadina, D. Pountney, W.A. Coetzee, and B. Rudy. KT3.2 and KT3.3, two novel human two-pore K(+) channels closely related to TASK-1. *J Neurophysiol*, 86(1):130–42, 2001.

R.W. Veh, R. Lichtinghagen, S. Sewing, F. Wunder, I.M. Grumbach, and O. Pongs. Immunohistochemical localization of five members of the Kv1 channel subunits: contrasting subcellular locations and neuron-specific co-localizations in rat brain. *Eur J Neurosci*, 7(11):2189–205, Nov 1995.

J. Wang, C. Zhang, N. Li, Su L., and G. Wang. Expression of TASK-1 in brainstem and the occurrence of central sleep apnea in rats. *Respir Physiol Neurobiol*, 161(1):23–8, 2008.

W. Wang, J.K. Tiwari, S.R. Bradley, R.V. Zaykin, and G..B Richerson. Acidosis-stimulated neurons of the medullary raphe are serotonergic. *J Neurophysiol*, 85(5):2224–35, May 2001.

Z. Wang, L. Kai, M. Day, J. Ronesi, H.H. Yin, J. Ding, T. Tkatch, D.M. Lovinger, and D.J. Surmeier. Dopaminergic control of corticostriatal long-term synaptic depression in medium spiny neurons is mediated by cholinergic interneurons. *Neuron*, 50(3):443–52, May 2006.

N.M. Warren, M.A. Piggott, E.K. Perry, and D.J. Burn. Cholinergic systems in progressive supranuclear palsy. *Brain*, 128(Pt 2):239–49, Feb 2005.

C.P. Washburn, J.E. Sirois, E.M. Talley, P.G. Guyenet, and D.A. Bayliss. Serotonergic raphe neurons express TASK channel transcripts and a TASK-like pH- and halothane-sensitive K+ conductance. *J Neurosci*, 22(4):1256–65, 2002.

C.P. Washburn, D.A. Bayliss, and P.G. Guyenet. Cardiorespiratory neurons of the rat ventrolateral medulla contain TASK-1 and TASK-3 channel mrna. *Respir Physiol Neurobiol*, 138(1):19–35, Oct 2003.

Y. Yamamoto, W. Kummer, Y. Atoji, and Y. Suzuki. TASK-1, TASK-2, TASK-3 and traak immunoreactivities in the rat carotid body. *Brain Res*, 950(1-2):304–7, 2002.

G. Yellen. The voltage-gated potassium channels and their relatives. *Nature*, 419(6902):35–42, Sep 2002.

List of Figures

List of Tables

Publications

- Rose, U., Derst, C., Wanischeck, M., Marinc, C. and Walther C.: Properties and possible function of a hyperpolarization-activate,d chloride current in Drosophila. J Exp Biol. 2007 Jul;210(Pt 14):2489-500.
- Marinc, C. and Rose, U.: Origin and Development of unusual insect muscle tension receptors. Cell Tissue Res. 2007 Dec;330(3):557-66.
- Prüss, H., Ders,t C., Marinc, C., Wenze,l M. and Veh RW.: Expression of Kir3.3 potassium channel subunits in supraependymal axons. Neurosci Lett. 2008 Nov 7;445(1):89-93.
- Marinc, C., Preisig-Müller, R., Prüss H., Derst, C. and Veh RW.: Immunocytochemical Localization of TASK-3 (K(2P)9.1) Channels in Monoaminergic and Cholinergic Neurons. Cell Mol Neurobiol.2011 Mar;31(2):323-335.
- Marinc, C., Prüss H., Derst, C. and Veh, RW.: Immunocytochemical localization of TASK-3 channels in motoneurons (in preparation)

Danksagung

Ich möchte mich bei allen Personen bedanken, die mir durch Ihre Unterstützung geholfen haben diese Arbeit zu erstellen.
An erster Stelle danke ich Herrn Prof. Dr. Rüdiger Veh für die Überlassung des interessanten Themas und seine fachkundige Betreuung. Die zahlreichen, inspirierenden Diskussionen mit ihm haben nicht nur die Voranbringung meiner Arbeit sondern auch mein fachliches Wissen sowie mein wissenschaftliches Denken gefördert und gefordert. Für die bereitwillige Übernahme des Zweitgutachtens bedanke ich mich herzlich bei Herrn Prof. Dr. Hans-Joachim Pflüger von der Freien Universität Berlin.

Mein besonderer Dank gilt Herrn Dr. Christian Derst, der mich bei allen molekularbiologischen Arbeiten unterstützt hat und sich immer die Zeit genommen mir zu helfen und meine Fragen zu beantworten. Seine konstruktiven Vorschläge und Ideen haben wesentlich zum Gelingen meiner Arbeit beigetragen.

Frau Heike Heilmann, Frau Semanur Ünsal, Frau Berit Söhl-Kielczynski und Frau Ina Wolter danke ich dafür, dass ich von Ihrem Fachwissen profitieren durfte und für die Unterstützung bei meinen Laborarbeiten.
Herrn Dr. Gregor Laube danke ich für viele gute Ratschläge und die Versorgung mit Kaffee.
Vielen Dank an Frau Annett Kaphan, die stets ein offenes Ohr für mich hatte und mir nicht nur bei allen administrativen Fragen und Problemen geholfen hat.
Desweiteren möchte ich allen Mitarbeitern und Mitarbeiterinnen des Instituts für intergrative Neuroanatomie für die freundliche Arbeitsathmosphäre danken und dafür, dass ich immer gerne dort gearbeitet habe.

Zu guter Letzt gilt mein Dank von ganzem Herzen meiner Familie und meinen Freunden, die mich immer unterstützt, an mich geglaubt und meine Launen ertragen haben. Ihr habt mir den Rückhalt, die Energie und Motivation gegeben meinen Weg zu gehen.

Selbständigkeitserklärung

Ich erkläre, dass ich die vorliegende Arbeit selbständig und nur unter Verwendung der angegebenen Literatur und Hilfsmittel angefertigt habe.

Berlin, den 14.03.2011